

Waltheriones and *Trypanosoma cruzi* – Elucidating Potential Mechanisms of Action

INAUGURALDISSERTATION

zur
Erlangung der Würde eines Doktors der Philosophie

vorgelegt der
Philosophisch-Naturwissenschaftlichen Fakultät
der Universität Basel

von
Sabina Eleonora Beilstein

Basel, 2023

Genehmigt von der Philosophisch-Naturwissenschaftlichen Fakultät
auf Antrag von

Erstbetreuer: Prof. Dr. Pascal Mäser
Zusätzlicher Erstbetreuer: Dr. Marcel Kaiser
Zweitbetreuer: Prof. Dr. Till Voss
Externer Experte: Prof. Dr. Jürg Gertsch

Basel, den 20.06.2023

Prof. Dr. Marcel Mayor
Dekan

Abbreviations	1
Summary	3
1 Waltheriones and <i>Trypanosoma cruzi</i> – general introduction	5
1.1 Phytochemicals and parasites	5
1.2 <i>Trypanosoma cruzi</i> and Chagas disease	6
1.3 Treatment options and drug discovery	11
1.4 <i>Waltheria indica</i> and the waltheriones	13
1.5 Aim and Objectives.....	15
2 Laboratory selection of trypanosomatid pathogens for drug resistance ...	17
2.1 Abstract.....	19
2.2 The TriTryp Parasites	20
2.3 New Tools for Target Deconvolution	21
2.4 Artificial Selection for Drug Resistance.....	23
2.5 Biosafety Considerations and Conclusion	31
2.6 Acknowledgments.....	32
3 Effects of waltheriones on <i>Trypanosoma cruzi</i> metabolism	33
3.1 Abstract	35
3.2 Introduction	36
3.3 Material and Methods	38
3.4 Results	45
3.5 Discussion.....	52
3.6 Acknowledgment	55
3.7 Supplementary material	56
4 Resistance to waltheriones and its effect in <i>Trypanosoma cruzi</i>	57
4.1 Abstract	59
4.2 Introduction	60
4.3 Material and Methods	62
4.4 Results	67
4.5 Discussion.....	80
4.6 Acknowledgment	82
4.7 Supplementary material	83

5	<i>Trypanosoma cruzi</i> STIB980: a new assay strain for imaging and reverse genetics	85
5.1	Abstract	87
5.2	Introduction	88
5.3	Results and discussion.....	90
5.4	Conclusion	98
5.5	Material and Methods	99
5.6	Acknowledgments.....	103
6	Waltheriones and <i>Trypanosoma cruzi</i> – general discussion	105
6.1	Waltheriones are hard-to-resist natural molecules.....	105
6.2	Waltheriones affect <i>T. cruzi</i> fatty acid catabolism	107
6.3	A candidate waltherione resistance mutation in mitoribosomes ...	109
6.4	The mitochondrion as a potential target site of waltheriones	110
6.5	How can we test and confirm our findings?	112
7	Waltheriones and <i>T. cruzi</i> – final conclusion	115
	References	117
	Acknowledgment	142

Abbreviations

ATP	Adenosine triphosphate
BSA	Bovine serum albumin
BSF	Bloodstream form
CACT	Carnitine-acylcarnitine translocase
Cas9	CRISPR associated protein 9
CAT	Carnitine acetyltransferase
CPT1 and 2	Carnitine palmitoyltransferase 1 and 2
CRISPR	Clustered regularly interspaced short palindromic repeats
ctr	Control
DMSO	Dimethyl sulfoxide
DNDi	Drugs for Neglected Diseases Initiative
DTU	Discrete typing unit
EGFP	Enhanced green fluorescent protein
ETO	Etomoxir
G6PI	Glucose-6-phosphate isomerase
GAT1	Glycosomal ATP binding cassette transporter 1
GC-MS	Gas chromatography-mass spectrometry
GFP	Green fluorescent protein
gRNA	Guide ribonucleic acid
HSP60	Heat shock protein 60
IC ₅₀	50% inhibitory concentration
iFCS	Inactivated fetal calf serum
kDNA	Kinetoplast deoxyribonucleic acid
LC-MS	Liquid chromatography-mass spectrometry
LIT	Liver infusion tryptose
LSHTM	London School of Hygiene & Tropical Medicine
LucNeon	Red-shifted luciferase and green fluorescent protein
MEF	Microtus embryonic fibroblast
mRNA	Messenger ribonucleic acid
NMR	Nuclear magnetic resonance
NTR1	Nitroreductase 1
PBS	Phosphate buffered saline

PCR	Polymerase chain reaction
PMM	Peritoneal mouse macrophages
RNAi	Ribonucleic acid interference
RPMI medium	Roswell Park Memorial Institute medium
rRNA	Ribosomal ribonucleic acid
SNP	Single nucleotide polymorphism
STIB	Swiss Tropical Institute Basel
TCA	Tricarboxylic acid cycle
VSG	Variant surface glycoprotein
WF	Waltherione F
WG	Waltherione G
wt	Wildtype

Summary

Natural products, and phytochemicals in particular, constitute a huge potential for drug discovery and medical use against parasitic diseases. Novel drugs and safer and more efficacious treatment options are urgently needed to fight neglected tropical diseases such as Chagas disease, caused by *Trypanosoma cruzi*.

So far, antichagasic drug discovery was marked by the lack of financial resources and restricted by low throughput. Research subsequently fell back on drug repurposing and target-based approaches, which did not translate to new drugs against Chagas disease. Understanding drug action and discovering potential mechanisms of action is vital in finding alternative, safe, and efficacious treatment options.

Waltheriones are a group of natural compounds isolated from the plant *Waltheria indica*, a plant occurring in tropical and subtropical area. Their activity against *T. cruzi* observed in protozoan phenotypic screens and the high selectivity towards the parasitic cells make the waltheriones very attractive for research, potentially leading to a candidate drug or advancing the knowledge about a novel drug target in *T. cruzi*.

In my Ph.D. thesis, I have investigated drug action of the waltheriones against *T. cruzi* by using cell biological and molecular approaches. Untargeted exposure metabolomics of extracellular epimastigote *T. cruzi* with waltherione revealed an accumulation of acylcarnitines, indicating an effect on fatty acid metabolism downstream of carnitine palmitoyltransferase 1 (CPT1). This finding was further investigated using isotopically labelled palmitate and NMR or mass spectrometry. This demonstrated that β -oxidation is functional in the vector form of *T. cruzi*. However, no effect of waltherione on β -oxidation or TCA metabolites was observed.

In vitro drug resistance selection was used as a starting point for finding possible mechanisms of resistance and possible mechanisms of action. Selecting for drug resistance in *T. cruzi* toward waltheriones proved to be difficult. Waltherione-resistant *T. cruzi* were generated and analysed with comparative transcriptomics revealing a candidate resistance mutation in a mitoribosomal protein.

In conclusion, untargeted exposure metabolomics and comparative transcriptomics point to a mitochondrial involvement in waltherione drug action and a possible drug resistance mechanism. Stage-specific waltherione sensitivity profiles in different protozoan parasites further consolidate the hypothesis that the mode of action of waltheriones against *T. cruzi* involves interference with mitochondrial metabolism.

1 *Waltheriones* and *Trypanosoma cruzi* – general introduction

1.1 Phytochemicals and parasites

Nature is an incredibly rich source for pharmacophores. Natural compounds are molecules produced by a biological source such as plants, fungi or bacteria. Phytochemicals have already succeeded as antiparasitic agents. Quinine from the bark of the cinchona tree has been used as an antimalarial for centuries (and yet its mode of action is not fully understood). The discovery of the antimalarial agent artemisinin earned Tu Youyou the Nobel Prize in 2015 (Tu, 2016). The medical use of phytochemicals extends far beyond the field of parasitology, though. The pain reliever aspirin from the willow tree (Fuster and Sweeny, 2011), the most potent narcotic morphine from the poppy plant (Brook et al., 2017), and paclitaxel from the yew tree used in cancer treatment are just a few prominent examples (Wani et al., 1971).

Plants are highly specialised and optimised production sites for biochemically active compounds. Therefore, phytochemical libraries usually yield a high hit rate in screening campaigns. However, the hit-to-lead development of natural products is restricted due to the difficulties to chemically synthesise and modify phytochemical compounds because they are often large and complex molecules with several stereocenters.

Taken together, natural compounds have limitations but also many advantages over synthetic compounds, as summarised in Table 1. Drug discovery can benefit from both fields. Screening for natural products facilitates the identification of bioactive and selective hit molecules, benefitting from a large diversity. Synthetic chemistry helps to overcome the limited product availability and facilitates modification. One way forward could be to first identify hits by screening biochemicals, then identify their target proteins in the pathogen, and finally perform screening campaigns on the purified target with synthetic derivative molecules. Such an approach is long and laborious but profits from the best of both fields, natural and synthetic chemistry.

Table 1. Characteristics of natural and synthetic compounds. Lipinski's rule of five assesses the drug likeness of a chemical compound and determines its likeliness to be an orally available drug (Lipinski, 2004, Lipinski et al., 2001).

	Natural compounds	Synthetic compounds
Diversity and availability	<ul style="list-style-type: none"> · very diverse · limited accessibility 	<ul style="list-style-type: none"> · good accessibility
Bioactivity	<ul style="list-style-type: none"> · optimised for bioactivity by nature · fast metabolised 	<ul style="list-style-type: none"> · requires optimisation for bioactivity · low potency
Specificity	<ul style="list-style-type: none"> · very specific 	<ul style="list-style-type: none"> · low specificity
Chemistry	<ul style="list-style-type: none"> · difficult to synthesise · difficult to modify · less drug like according to Lipinski's rule of five 	<ul style="list-style-type: none"> · easy to synthesise · easy to modify · usually follow Lipinski's rule of five
Hit rate	<ul style="list-style-type: none"> · high hit rate in screens 	<ul style="list-style-type: none"> · low hit rate in screens

In contrast to malaria, natural compounds have so far not been used in the treatment of infections caused by trypanosomatid parasites. However, I believe that this untapped reservoir holds potential for antitrypanosomal agents as well, and that phytochemicals can also play an invaluable role in the treatment of Chagas disease caused by the parasite *Trypanosoma cruzi*. The waltheriones isolated from *Waltheria indica* (Cretton et al., 2014) are a promising starting point and the subject of the present work.

1.2 *Trypanosoma cruzi* and Chagas disease

T. cruzi is a unicellular eukaryote and the causative agent of Chagas disease, one of the neglected tropical diseases (Hotez et al., 2013, WHO, 2023, CDC, 2022). It belongs to the trypanosomatid family, which additionally comprises the human pathogenic parasites *Trypanosoma brucei* and *Leishmania*. Triatomine bugs are the competent vector for transmitting *T. cruzi* to its mammalian hosts. The parasite is

known to infect innumerable genera of mammalian species, making it a zoonotic pathogen (Zingales et al., 2012, WHO, 2002).

T. cruzi originated in Latin America, where the insect vector is prevalent. Due to climate change, the vector is spreading further north, making reports of vector-transmitted Chagas disease also on the North American continent more frequent (Garcia et al., 2015). With increased mobility and migration, the disease has spread also to other continents (Requena-Méndez et al., 2015). Even in vector-free areas Chagas disease is of increasing concern as *T. cruzi* can be transmitted by blood transfusion, organ transplantation, congenitally, or orally by contaminated food (Pérez-Molina and Molina, 2018).

The disease manifests itself in different clinical forms. The majority of the acute infections are asymptomatic and resolve spontaneously in about 90% of cases. Only about 5-10% of all acute infections directly progress to symptomatic and life-threatening conditions. The acute phase is followed by the chronic phase of the disease, which can be marked by either the indeterminate or the determinate form. During the chronic indeterminate form, the parasites persist in host tissues without triggering any symptoms (Sanchez-Valdez et al., 2018). In the determinate form, the disease manifests itself in cardiomyopathy or megacolon and premature death (Rassi et al., 2010). In mice, the intestinal system is the primary site for persisting *T. cruzi* parasites (Lewis et al., 2014). In chronic human Chagas disease patients, reactivation of the persisting parasites could lead to the determinate form of the disease. This might occur under certain conditions, such as immunosuppression (Gray et al., 2018). The chronic form of Chagas disease also complicates the clinical phase of drug development. A novel drug must achieve total parasite clearance, also targeting parasites residing in specific host tissue.

Different clinical manifestations of Chagas disease have been associated with different parasite strains, categorised in discrete typing units (DTU), which follow a geographical distribution as recently systematically reviewed (Velásquez-Ortiz et al., 2022). Drug research and development needs to consider potential influences of strain specificity when interpreting efficacy of novel hits, as well as the fact that artefacts may arise since many experimental strains have experienced laboratory adaptation (Sykes et al., 2023).

In the present work, I exclusively use the strain *T. cruzi* STIB980, which was previously used to design a new live *in vitro* drug assay (Fesser et al., 2020). This

strain has a short history of *in vitro* cultivation and thus is still more natural than other laboratory-adapted strains. *T. cruzi* STIB980 belongs to the DTU TcI as determined by PCR on the glucose-6-phosphate isomerase (G6PI) gene, the large ribosomal subunit (LSU), and the heat-shock protein 60 (HSP60) gene (Fesser, 2021). DTU TcI is widespread throughout the whole South American continent and circulates extensively among humans. Therefore, *T. cruzi* STIB980 is well suited for drug discovery. The best annotated *T. cruzi* reference genome is that of *T. cruzi* CL Brener Esmeraldo-like. However, it is a hybrid of DTU TcII subgroups and had been chosen for the first *T. cruzi* genome to be sequenced as it was experimentally already well characterised (El-Sayed et al., 2005, Zingales et al., 1997). For STIB980, I have used the closely related Dm28c 2018 as reference genome for genetic experiments, which is also a DTU TcI (Berná et al., 2018).

The life cycle of *T. cruzi* alternates between the insect vector and a mammalian host, with morphologically distinguishable forms (Figure 1). The insect vector takes up *T. cruzi* parasites during a blood meal on the mammalian host. The extracellular trypomastigote *T. cruzi* differentiate inside the insect midgut to the epimastigote form upon changing environmental conditions and nutrient supply (Barisón et al., 2017). The epimastigotes proliferate extracellularly in the midgut. Eventually, they differentiate to the infective metacyclic trypomastigote stage in the insect's hindgut triggered by the proline-rich environment (Barrett and Friend, 1975, Contreras et al., 1985, Lucena et al., 2019). During a next blood meal, infective *T. cruzi* are deposited with the bug's faeces onto the host and can enter the bite wound or any mucosal membrane. Parasites then invade nucleated cells where they differentiate into the intracellular replicative amastigote form (de Souza et al., 2010). Inside the host cell, *T. cruzi* differentiate into the trypomastigote form in an asynchronous manner. The trypomastigotes enter the blood circulation or the lymphatic system upon lysis of the host cell (Dvorak and Hyde, 1973, Taylor et al., 2020). The insect vector then again takes up the extracellular trypomastigote form.

The entire lifecycle can be maintained *in vitro* without the need for any animal passage. In the present work, different life cycle stages were used. However, the extracellular and axenically cultured epimastigote *T. cruzi* simplify many experiments and were therefore used preferentially.

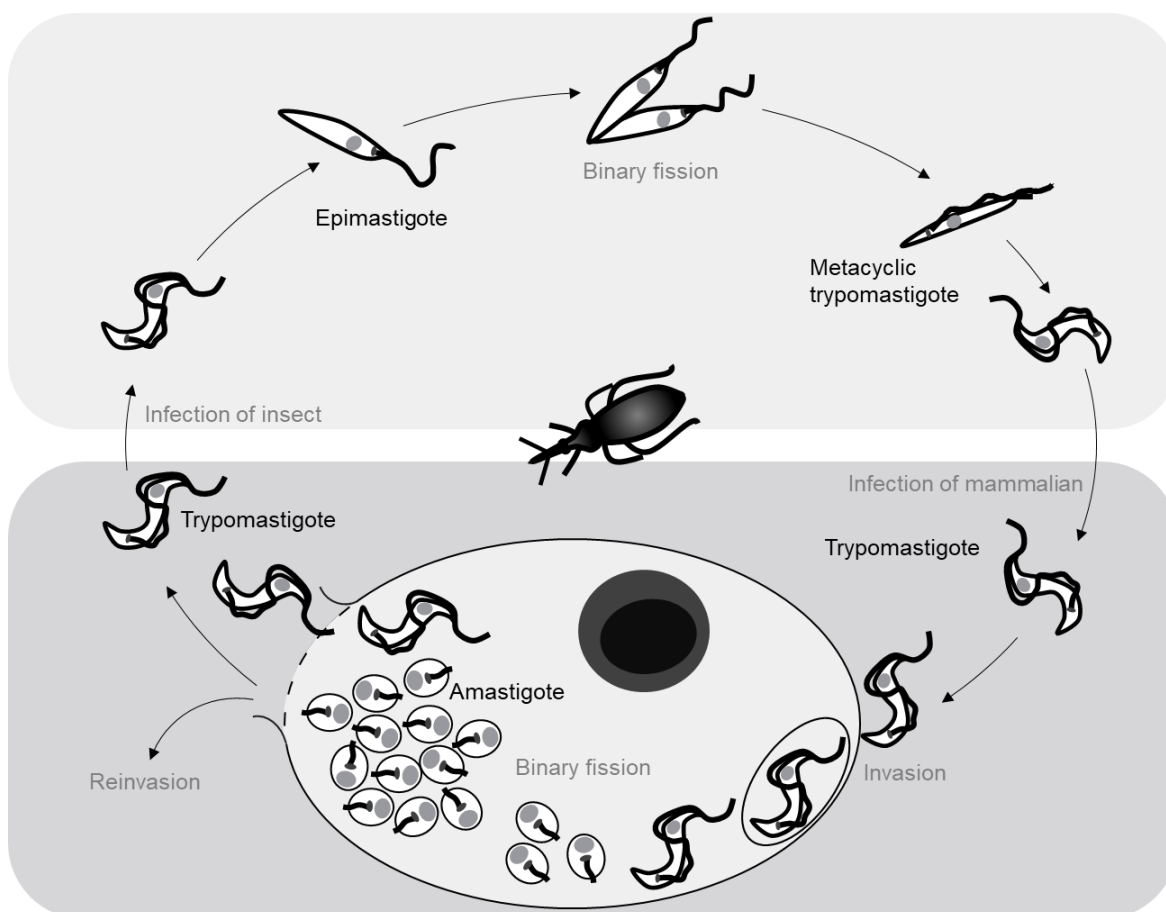


Figure 1. Life cycle of *Trypanosoma cruzi*.

The biology of *T. cruzi* holds some unique features, which are at the same time intriguing for basic science and promising for drug discovery. Some were already suggested as potential antitrypanosomal drug targets.

Trypanosoma parasites possess only one single mitochondrion (Hellemond et al., 2005). The proper function of this singular organelle is vital. The mitochondrion is a site of energy generation comprising the enzymes for fatty acid import, β -oxidation, and the TCA cycle as well as the electron transport chain (Atwood et al., 2005). Maintaining the mitochondrial membrane potential is essential for cell viability. Alterations in the mitochondrial potential upon drug exposure indicate drug targets in energy metabolism within the mitochondrion. These include cytochrome bc1 or F0/F1 ATP synthase, which are part of the electron transport chain and oxidative phosphorylation. Both were discussed as potential antiparasitic drug targets (Khare et al., 2015, Wall et al., 2020, Dean et al., 2013, Muscat et al., 2023).

Trypanosomes belong to the class of kinetoplastea. The name originates from the kinetoplast containing the kinetoplast DNA (kDNA), a multicircular DNA structure encoding for mitochondrial genes as well as guide RNAs involved in the unique trypanosomal RNA editing process (Callejas-Hernández et al., 2021). A single point mutation in the gamma-subunit of the ATP synthase of the bloodstream form *T. brucei* causes tolerance to kDNA loss (Schnauffer et al., 2005). With this compensatory mutation, bloodstream-form *T. brucei* can survive without kDNA (Dean et al., 2013, Schnauffer et al., 2005). kDNA and the ATP synthase have been suggested as antitrypanosomal drug targets as they are important for mitochondrial gene expression and parasite survival (Fidalgo and Gille, 2011).

Mitochondrial ribosomes (mitoribosomes) are responsible for the translation of mitochondrial-encoded genes and feature a conserved ribosomal core formed by ribosomal RNA (rRNA). The trypanosomal mitoribosome is special in two ways. First, it holds the smallest rRNA, and second it has a higher protein but reduced rRNA content compared to other eukaryotic cells (Ramrath et al., 2018). The ribosomal proteins are nuclear-encoded with only one exception, uS12m, which is kinetoplast encoded as are the rRNAs (Aphasizheva et al., 2013, Ramrath et al., 2018). The mitoribosome was suggested as a potential antitrypanosomal drug target due to its evolutionary divergence in trypanosomes and its key mitochondrial functions (Ramrath et al., 2018, Scaltsoyiannes et al., 2022).

The glycosome is a specialised, peroxisome-like organelle found in kinetoplastids. This organelle contains several glycolytic enzymes and it is the site where most steps of glycolysis occur. Only the three last steps, converting 3-phosphoglycerate into pyruvate, occur in the cytosol. In all other eukaryotes, the entire glycolysis happens in the cytosol (Opperdoes and Borst, 1977, Acosta et al., 2019). In contrast to the mitochondrion, glycosomes are present in large quantities (Opperdoes et al., 1984, Quiñones et al., 2020). The glycosomes also contain enzymes for purine salvage and β -oxidation (Acosta et al., 2019, Quiñones et al., 2020). Fatty acid catabolism via β -oxidation is an alternative pathway for energy generation in case of glucose starvation (Barisón et al., 2017). One site of β -oxidation is the mitochondrion. All enzymes of β -oxidation were also identified in the proteomes of *T. cruzi* and *T. brucei* glycosomes (Acosta et al., 2019, Güther et al., 2014).

T. cruzi is more infectious than *T. brucei* and thus requires extra caution in experimental handling. Therefore, work with *T. cruzi* is restricted to biosafety level 3 laboratories in Europe. Working with *T. cruzi* is challenging because, i) there is a higher infection risk compared to other parasitic diseases, ii) there is no safe and efficacious drug treatment available, iii) the disease might manifest in a chronic clinical outcome, where no drug treatment is available, iv) parasites can persist in specific host tissues, and v) the disease-relevant stage is obligate intracellular and requires host cells for cultivation, adding a layer of complexity in drug research.

1.3 Treatment options and drug discovery

Benznidazole and nifurtimox are the two drugs that are approved for the treatment of Chagas disease. Both treatments are accompanied by severe side effects and are indicated for acute or reactivated Chagas disease only (CDC, 2021). For the chronic stage of the disease, no effective drug exists. Fexinidazole is currently in focus as a potential alternative treatment. This compound is the most recently approved drug for the treatment of human African trypanosomiasis, caused by *T. brucei*.

Benznidazole and fexinidazole are both nitroimidazoles, and nifurtimox is a nitrofuran. All three compounds are prodrugs that need activation upon entering the cell. Type I nitroreductase (NTR1) was shown to be the enzyme responsible for the reduction of the nitro group of the molecules (Dattani et al., 2021, Wilkinson et al., 2008, Edwards, 1993). The reaction results in highly reactive products interacting with biological molecules and causing damage to the cell (Hall et al., 2011, Trochine et al., 2014a). Fexinidazole activity against *T. cruzi* was shown in the mouse model (Bahia et al., 2012). The highly promising results from the phase II clinical trial were published only recently, suggesting further investigation of fexinidazole as a treatment option for Chagas disease (Torrìco et al., 2023).

Posaconazole was a promising antichagasic compound, which, however, failed during clinical trials due to limited curative potential (Molina et al., 2014). This underlines the challenge of curing Chagas disease and the significance of finding molecules that can reach also persistent parasites. Posaconazole inhibits sterol 14 α -demethylase (CYP51), an enzyme of the *T. cruzi* essential sterol biosynthesis (Urbina et al., 1998, Lepesheva et al., 2006).

The examples just mentioned are the result of drug repurposing and cell-based screening. Phenotypic screening approaches thus brought the most recent advancements in research and development of new drugs (Chatelain and Ioset, 2018). Identifying the drug target, nevertheless, is the challenging but important next step.

The experimental approaches to elucidate the mode of action of, or resistance mechanism to, an active molecule are manifold. Phenotypic approaches include straightforward techniques that measure the effect of drug exposure on morphology, changes in the mitochondrial potential, or growth. More sophisticated techniques include cell cycle analysis with imaging or flow cytometry (Wheeler et al., 2012, Signorell et al., 2009, Sarkar et al., 2003), isothermal microcalorimetry to monitor growth and metabolism in real time (Gysin et al., 2018, Wenzler et al., 2012), and untargeted exposure metabolomics to investigate the biochemistry of drug action (Trochine et al., 2014b, Wenzler et al., 2012). Untargeted metabolomics investigates the total composition of low molecular weight molecules present in a sample qualitatively (Fillet and Frederich, 2015, Creek et al., 2011). This method was used in *T. cruzi* to compare the entire metabolome of parasites exposed to benznidazole and the non-exposed control. This indicated the thiol binding capacity of reduction products of benznidazole (Trochine et al., 2014a). Targeted metabolomics is the next step to quantitatively investigate the metabolome which requires prior knowledge of the metabolites of interest (Creek et al., 2011). Isotopically labelled molecules are used to quantitatively resolve specific metabolic pathways of interest including energy metabolism (Krishnan et al., 2020, Saunders et al., 2014). Depending on the approach and on the metabolites of interest, metabolite extraction can be adapted followed by liquid or gas chromatography coupled to mass spectrometry or NMR spectroscopy (Creek et al., 2011).

Next to the diverse set of direct exposure -omics approaches, selection strategies to investigate the mechanism of resistance can indirectly inform about the mechanism of action or the actual target (Wiedemar et al., 2018, Bernhard et al., 2007). Drug resistance selection followed by genomic and transcriptomic analysis led to important findings in *T. brucei* and its resistance mechanism against suramin (Wiedemar et al., 2018). Benznidazole drug resistance selection in *T. cruzi* coupled to genomic analysis revealed an accumulation of genome wide mutations associated with possible resistance mechanisms (Campos et al., 2017). Whole

genome sequencing has the advantage of finding mutations also in the intergenic regions and regulatory elements (McKenna et al., 2010). Total RNA sequencing, in contrast, enables the identification of differentially expressed genes and might also disclose alteration in the regulatory region of genes (Love et al., 2014, Anders et al., 2015). A detailed overview on the different protocols to select for drug resistance is provided in the next chapter (Chapter 2). This will form the basis of my approach towards selecting for walterione resistance in *T. cruzi*.

1.4 *Waltheria indica* and the walteriones

Walteriones were isolated and characterised from the malvacea *Waltheria indica* (Cretton et al., 2014). The plant is a yellow flowering shrub common in tropical and subtropical regions (Zongo et al., 2013). *W. indica* is used in traditional medicine in various regions all over the world for different indications. In Hawaii the plant is well recognised in traditional medicine and has been used to treat respiratory disorders and pain. In Central America and Africa the plant is also used as anti-inflammatory decoction (Zongo et al., 2013, Bala et al., 2010). In Nigeria, the plant is used to treat cattle for 'Nagana', the zoonotic form of African sleeping sickness caused by *Trypanosoma brucei brucei* (Bala et al., 2010). The whole plant extract was investigated for its potential antiplasmodial effect due to its traditional use in Burkina Faso (Jansen et al., 2010).

The walteriones were identified upon fractionation of extracts of different parts of the plant. Dichloromethane, methanol, and water were used to extract air-dried and powdered plant material from the root and aerial parts of *Waltheria indica*. The walteriones were found in the apolar dichloromethane extract of the root material, and they are heterocyclic quinoline alkaloid molecules (Figure 2) (Cretton et al., 2014, Cretton et al., 2015).

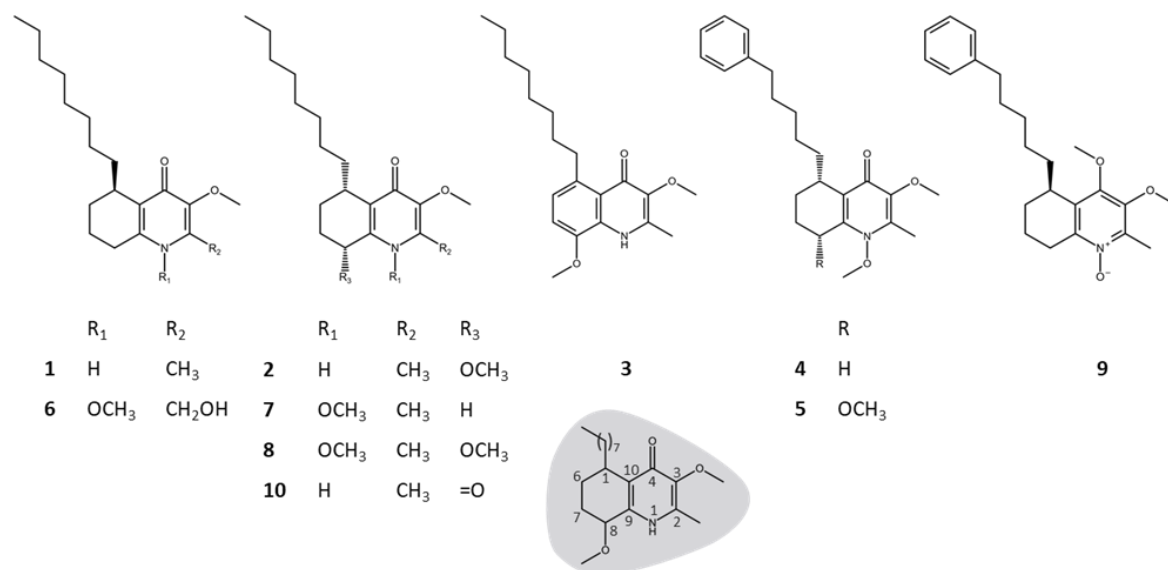


Figure 2. Chemical structures of the walteriones. (1) 8-deoxoantidesmone, (2) walterione E, (3) walterione F, (4) walterione G, (5) walterione H, (6) walterione I, (7) walterione J, (8) walterione K, (9) walterione L, (10) antidesmone. The molecule with grey background is also walterione F with numbered positions. (Cretton et al., 2014)

Walteriones showed activity in protozoan phenotypic screens, especially walterione F and G against *T. cruzi* (Cretton et al., 2014, Cretton et al., 2015). Cytotoxicity on mammalian cells for those two molecules was very low, resulting in very good selectivity towards *T. cruzi* (Cretton et al., 2014). Good transcellular permeation was found for walterione G among other pharmacologically active walteriones by parallel artificial membrane permeability assay (PAMPA) (Petit et al., 2016).

To date, the total chemical synthesis is only known for walterione F, and still in development for the chiral walterione G. The synthesis enabling modifications at positions 2 and 3 can assist in adding different functional groups to the molecule (Zdorichenko et al., 2019). Testing a variety of synthetic walterione analogues against *T. cruzi* will inform about the structure-activity relationship of the molecules.

Walterione F and G are interesting molecules because they are i) natural compounds, ii) highly active against *T. cruzi*, and iii) selective towards the parasites.

1.5 Aim and Objectives

My doctoral thesis aims to further characterise the antitrypanosomal action of the walteriones, in particular to elucidate potential mechanisms of action and identify candidate targets of the walteriones in *T. cruzi*. The presented work is part of a larger collaborative project following an interdisciplinary and comprehensive approach, including molecular and cell biology, different omics techniques, synthetic chemistry and modelling.

The literature review forming the first part of this work (Chapter 2) critically evaluates different approaches to select trypanosomatid parasites for drug resistance and outlines its importance for target deconvolution. This work helped to assess different experimental procedures to select walterione resistant *T. cruzi*, which was decisive for the experimental part outlined in the second part of this work (Chapter 3 and 4).

The experimental part followed the same objective with two different approaches: elucidating potential mechanisms of action using i) a phenotypic and ii) a genetic approach. Untargeted exposure metabolomics revealed effects elicited by walteriones on *T. cruzi* carnitine metabolism. Semi-targeted exposure metabolomics was subsequently used to further explore fatty acid catabolism (Chapter 3). Meanwhile, *in vitro* drug resistance selection had been performed, which is a time-consuming process of unknown duration. Comparative transcriptomic analysis with walterione-resistant and susceptible *T. cruzi* revealed candidate resistance mutations pointing to the mitoribosome as a candidate target of walteriones (Chapter 4). A transgenic line of *T. cruzi* STIB980 was generated that will allow to follow up on the results from the phenotypic and genetic investigation.

2 Laboratory selection of trypanosomatid pathogens for drug resistance

Sabina Beilstein^{1,2}, Radhia El Phil^{3,4}, Suzanne Sherihan Sahraoui^{3,4}, Leonardo Scapozza^{3,4}, Marcel Kaiser^{1,2} and Pascal Mäser^{1,2,*}

¹ Dept. Medical Parasitology and Infection Biology, Swiss Tropical and Public Health Institute, 4051 Basel, Switzerland

² University of Basel, 4002 Basel, Switzerland

³ School of Pharmaceutical Sciences, University of Geneva, 1205 Geneva, Switzerland

⁴ Institute of Pharmaceutical Sciences of Western Switzerland, University of Geneva, 1211 Geneva, Switzerland

* Corresponding author: Pascal Mäser; pascal.maeser@swisstph.ch

2022

Pharmaceuticals (Basel) 15(2) 135

This review was initiated, outlined, and written by me under the supervision of Prof. Dr. Pascal Mäser. Drug sensitivity assays from Supplementary Table 2 were performed by Monica Cal, Romina Rocchetti, Sonja Keller-Märki, and Dennis Hauser. The group under Prof. Dr. Leonardo Scapozza contributed to the topic of new tools for target deconvolution.

2.1 Abstract

The selection of parasites for drug resistance in the laboratory is an approach frequently used to investigate the mode of drug action, estimate the risk of emergence of drug resistance, or develop molecular markers for drug resistance. Here, we focused on the How rather than the Why of laboratory selection, discussing different experimental set-ups based on research examples with *Trypanosoma brucei*, *Trypanosoma cruzi*, and *Leishmania* spp. The trypanosomatids are particularly well-suited to illustrate different strategies of selecting for drug resistance, since it was with African trypanosomes that Paul Ehrlich performed such an experiment for the first time, more than a century ago. While breakthroughs in reverse genetics and genome editing have greatly facilitated the identification and validation of candidate resistance mutations in the trypanosomatids, the forward selection of drug-resistant mutants still relies on standard *in vivo* models and *in vitro* culture systems. Critical questions are: is selection for drug resistance performed *in vivo* or *in vitro*? With the mammalian or with the insect stages of the parasites? Under steady pressure or by sudden shock? Is a mutagen used? While there is no bona fide best approach, we think that a methodical consideration of these questions provides a helpful framework for selection of parasites for drug resistance in the laboratory.

2.2 The TriTryp Parasites

Trypanosoma brucei, *Trypanosoma cruzi* and *Leishmania* comprise the human-pathogenic species in the trypanosomatid family. They cause the neglected tropical diseases sleeping sickness, Chagas disease and leishmaniasis, which have an estimated total prevalence of over 10 million and impose a substantial burden on global health (Murray and Lopez, 2017, Lee et al., 2013). The insect vectors - tsetse flies, triatomine bugs and phlebotomine sandflies, respectively - transmit the parasites to the mammalian host during a blood meal. The parasites thus encounter very different environments in their transmission cycles. Furthermore, the three species are zoonotic and infect various mammals. *Leishmania* and *T. cruzi* are intracellular in the mammalian host and extracellular in the gut of the insect, whereas all life-cycle stages of *T. brucei* are extracellular. This renders *T. brucei* easier to cultivate than *T. cruzi* or *Leishmania*. In addition, *T. brucei* is more readily amenable to reverse genetics than other trypanosomatids (Barnes et al., 2012). Table 1 compares the cellular and molecular characteristics of the TriTryp parasites *T. brucei*, *T. cruzi* and *L. donovani*. The drugs for treating the respective diseases are listed in Table 2, along with the *in vitro* sensitivity of the different life-cycle stages of the parasites. These drugs were developed by phenotypic, cell-based approaches rather than target-based. Consequently, for some of them, even though they have been used for decades, the mechanism of action is still not fully understood.

Table 1. Molecular and cellular characteristics of the three selected trypanosomatids.

	<i>T. brucei</i>	<i>T. cruzi</i>	<i>L. donovani</i>
Genome size ¹	26.1 Mb	60.4 Mb	32.4 Mb
Protein-coding genes ¹	9068	~12,000	>8000
Genes of RNAi pathway ²	present	partially present	absent
RNAi gene silencing ²	functional	non-functional	non-functional
CRISPR/Cas9 editing ³	established	established	established
Mammalian stages	extracell. trypomastigotes	intracell. amastigote, extracell. trypomastigote	intracell. amastigote
Vector stages	procyclic trypomastigote, epimastigote, metacyclic trypomastigote	procyclic epimastigote, metacyclic trypomastigote	procyclic promastigote, metacyclic promastigote

1 (Berriman et al., 2005, El-Sayed et al., 2005, Downing et al., 2011)

2 (Patrick et al., 2009, Garcia Silva et al., 2010, Lye et al., 2010, Batista and Marques, 2011)

3 (Beneke et al., 2017, Lander et al., 2015, Peng et al., 2014, Zhang and Matlashewski, 2015)

Table 2. Standard drugs and sensitivity of mammalian vs. insect stages. All values are *in vitro* IC₅₀ in µg/mL, original data from our trypanosomatid drug screening platform.

Parasite	Drug	Mammalian Stage Intracellular	Mammalian Stage Axenic	Vector Stage
<i>T. brucei</i>	Pentamidine	n.a.	0.001	0.43
	Suramin	n.a.	0.056	>10
	Melarsoprol	n.a.	0.004	0.057
	Eflornithine	n.a.	2.0	>100
	Nifurtimox	n.a.	0.31	1.6
	Fexinidazole	n.a.	0.62	1.2
<i>T. cruzi</i>	Benznidazole	0.47	n.a.	3.1
	Nifurtimox	0.14	n.a.	0.87
<i>L. donovani</i>	Pentostam	92	220	>1000
	Miltefosine	1.4	0.29	3.8
	Amphotericin B	0.33	0.26	0.03
	Paromomycin	28	>30	10

2.3 New Tools for Target Deconvolution

Knowing a drug's target is of great importance for the development of more effective, better tolerated therapies and for the management of drug resistance. However, the genetic mapping of mutations conferring resistance, which in *Caenorhabditis elegans* was key to the identification of anthelmintic drug targets (Sangster et al., 2005), is precluded in trypanosomatids as sexual recombination, if it occurs at all, is not obligate. This lack of forward genetics is to some extent compensated for by the declining costs of next-generation DNA sequencing, which have made it affordable to identify resistance mutations by whole genome sequencing or transcriptome sequencing of drug-resistant mutants (Graf et al., 2016, Leprohon et al., 2015). In addition, reverse genetic tools were developed that have helped to overcome the lack of forward genetics.

Inducible RNA interference (RNAi) libraries were used as a high-throughput method for genome-wide loss-of-function studies in *T. brucei* (Alsford et al., 2012, Alsford et al., 2011). Performing RNAi induction followed by drug selection confirmed the role of the known drug resistance genes *TbAT1*, *AAT6* and *NTR1* as

determinants of susceptibility to melarsoprol, eflornithine and nifurtimox, respectively (Schumann Burkard et al., 2011, Baker et al., 2011). An experimental trypanocide whose target was validated by RNAi is 4-[5-(4-phenoxyphenyl)-2H-pyrazol-3-yl]morpholine, a molecule that turned out to function as a hyperactivator of *T. brucei* adenosine kinase (Kuettel et al., 2011, Kuettel et al., 2009). These approaches obviously require the presence of a functional RNAi system in the target cell (Table 1). This, however, is not the case for *T. cruzi* and most species of *Leishmania*, with the notable exception of *L. braziliensis* (Lye et al., 2010). Parsimony suggests that the common trypanosomatid ancestor had been competent of RNAi and that the genes for Argonaute and Dicer proteins were lost multiple times in the subsequent course of evolution (Matveyev et al., 2017).

Genome editing by CRISPR-Cas9 is more generally applicable. First established for *T. cruzi* (Lander et al., 2015, Peng et al., 2014, Soares Medeiros et al., 2017), it was also successfully applied to *Leishmania* (Sollelis et al., 2015, Zhang and Matlashewski, 2015) and *T. brucei* (Beneke et al., 2017, Rico et al., 2018, Shaw et al., 2020). Further improvements simplified the genetic manipulation of the trypanosomatids, providing a high-throughput system for large-scale genetic knock-out screens (Beneke et al., 2017, Beneke and Gluenz, 2020, Yagoubat et al., 2020). Another high-throughput tool that has helped to understand the molecular genetics of drug action in *Leishmania* are cosmid libraries. Cos-Seq is based on the selection for enriched loci under drug pressure with subsequent sequencing and candidate gene identification (Fernandez-Prada et al., 2018, Gazanion et al., 2016). Targeted overexpression of candidate genes is possible as well; with DNA repair genes, this has provided new insights into the mode of action of benznidazole in *T. cruzi* (Rajão et al., 2014). Inducible gene overexpression libraries have been developed for trypanosomatids that allow identifying drug targets by screening for genes whose overexpression causes drug resistance (Wall et al., 2018).

Proteomic techniques are applicable to trypanosomatid parasites as well (Sioud, 2007, Werbovets, 2000). Chemical proteomics combine chemistry to synthesize a drug-derived probe with biology to search for the target protein. This is achieved either by affinity chromatography, in which the chemical probe is immobilized on a matrix and incubated with a cell lysate to fish for proteins, or in situ, where the probe is added to live cells and cross-linked to target proteins e.g., by means of a photoreactive group (Kubota et al., 2019). The first approach was

used to identify MAP kinases and cdc2-related kinases as putative targets of 2,4-diaminopyrimidines in *T. brucei* (Mercer et al., 2011). The second identified candidate targets of the antiobesity drug orlistat and the antichagasic protease inhibitor K11777 (Yang et al., 2012a, Yang et al., 2012b). Other innovative techniques for target fishing were developed, such as protein chips, phage display, or the yeast three-hybrid system (Chidley et al., 2011, Terstappen et al., 2007), but have to our knowledge not yet been applied to trypanosomatids.

2.4 Artificial Selection for Drug Resistance

Selecting pathogens for drug resistance is a classical experiment in a parasitology laboratory. The first scientist known to have performed it was Paul Ehrlich, the father of chemotherapy. Ehrlich and co-workers infected mice with African trypanosomes and treated the animals with subcurative doses of parafuchsin. They observed that after several passages, the trypanosomes had lost their susceptibility to the drug (Ehrlich, 1907). Decades later, Alexander Fleming observed the same phenomenon when he cultured bacteria on plates with sublethal concentrations of penicillin (Fleming, 1945). Ehrlich's main interest in drug resistance was to learn about the nature of the subcellular drug targets. He proposed to use artificially selected drug-resistant pathogens as a 'therapeutic sieve' based on cross-resistance profiles (Ehrlich, 1908). Thus, by testing a new drug candidate against a panel of resistant strains, he was able to tell whether it had a different mode of action. A hundred years later, this concept was incorporated for the development of antimalarials (Chugh et al., 2015). Today, the selection of drug-resistant mutants in the laboratory mainly serves three purposes: (i) to learn about the mode of drug action, i.e., to identify drug transport pathways and drug targets; (ii) to estimate the risk of emergence of drug resistance in the field based on how quickly resistance evolves in the laboratory; and (iii) to find molecular markers for drug resistance that enable rapid, DNA-based tests. In the following, we focus on the How rather than the Why in the experimental process of laboratory-selection for drug resistance, illustrating different protocols with examples from the 'TriTryp' parasites.

2.4.1 Selection *In Vitro* vs. *In Vivo*

The selection for drug-resistant trypanosomatids by subcurative dosing of a rodent model of infection is the closest situation to what happens in a treated patient. Therefore, the knowledge that will be gained about the genes and mutations involved in drug resistance is likely to be relevant for the situation in the clinics. A second advantage of selecting *in vivo* is the high numbers of parasites that can be reached in an infected animal, increasing the probability of success in obtaining a drug-resistant mutant. The main point against *in vivo* selection is the use of animals *per se*, if it can be replaced by an *in vitro* system. In addition, *in vivo* studies are usually more laborious and expensive than *in vitro* experiments. A further advantage of *in vitro* systems is the better control over parameters such as drug concentration and number of parasites.

Overall, there has been a good correlation between the drug resistance phenotypes obtained *in vivo* and *in vitro* (Kaminsky and Mäser, 2000), except in one case, where bloodstream-form *T. b. brucei*, which had been selected *in vivo* for Cymelarsan resistance, were only weakly resistant to arsenicals in culture (Scott et al., 1996, Scott et al., 1997). A possible explanation is the fast metabolism of melamine-based arsenicals *in vivo* (Keiser et al., 2000). Some mechanisms, such as phenomena involving tissue tropism, will only evolve *in vivo*, whereas others might occur only *in vitro*. The latter is exemplified by the finding that expression of a particular variant surface glycoprotein (VSG) in *T. brucei* causes suramin resistance (Wiedemar et al., 2018). Such a mechanism is hardly sustainable *in vivo*, where the parasites will be eliminated by the adaptive immune response unless they switch to express another VSG.

The first studies on the selection of trypanosomatids for drug resistance were performed *in vivo*, as long-term culture systems were unavailable at the time. Early studies with *T. brucei* mainly focused on arsenical resistance (Yorke and Murgatroyd, 1930, Yorke et al., 1931, Yorke et al., 1933, Lourie and Yorke, 1938, Fulton and Yorke, 1942) and on the phenomenon of cross-resistance between melamine-based arsenicals and diamidines (Rollo and Williamson, 1951). Generally, *T. brucei* spp. were propagated in immunosuppressed mice. The animals were treated with increasing but subcurative concentrations of arsenicals, and the relapsing trypanosomes were passaged to new mice (Frommel and Balber, 1987,

Scott et al., 1996, Pospichal et al., 1994, Fairlamb et al., 1992). In a typical experiment, it took eight rounds of infection to obtain a stable resistance phenotype with a resistance factor of 15 (Pospichal et al., 1994). There are only a few studies where *T. cruzi* or *Leishmania* were selected for drug resistance *in vivo*. Two different approaches were applied, both successfully, to obtain benznidazole-resistant *T. cruzi*. In the first, selection was performed by repeated treatment shocks: an infected mouse at peak parasitemia was treated with a single oral dose of 500 mg/kg benznidazole and after 6 hours, the surviving blood trypomastigotes were inoculated into another mouse. This procedure was repeated about 10 days later, again at the peak of parasitemia. After 25 rounds, the obtained *T. cruzi* were unresponsive to benznidazole and cross-resistant to nifurtimox and other nitroimidazoles (Murta and Romanha, 1998). The second approach used a lower but constant dose: infected mice were given an oral dose of 100 mg/kg benznidazole daily for 20 consecutive days. Thereafter, the animals were immunosuppressed with cyclophosphamide, and the emerging trypomastigotes in the blood were harvested and inoculated into new mice. Four out of five *T. cruzi* isolates became unresponsive to benznidazole after 2 to 9 rounds of selection (Dos Santos et al., 2008). A similar attempt to generate drug-resistant mutants of *L. infantum* and *L. donovani* by repeated subcurative dosing of infected hamsters succeeded remarkably quickly for paromomycin, but not for miltefosine (Hendrickx et al., 2015). A different approach, pre-exposing animals before infection, was used to test a possible link between the presence of arsenic in the drinking water and the emergence of antimonial resistance in *Leishmania*. Mice that had been given drinking water with 10 ppm arsenite for 1 month were infected with *L. donovani*. After 28 days, still with arsenite in the animals' drinking water, the *Leishmania* were passaged to a new group of arsenite pre-exposed mice. After 5 such rounds, the *Leishmania* had become unresponsive to a dose of 500 µg/mL when tested *in vitro* (Perry et al., 2013).

There have been many reports on the successful *in vitro* selection of trypanosomatids for drug resistance (Table 3).

Table 3. Reports of successful *in vitro* selection of trypanosomatids for drug resistance (BSF, bloodstream form; PCF, procyclic form; epi, epimastigotes; pro, promastigotes; trypo, trypomastigotes; RF, resistance factor; n.s., not specified).

Drug	Species	Stage	Mutagen	Pressure	Duration	RF	Ref.
DB75	<i>T. b. brucei</i>	BSF	no	steady	2.5 mth	20	(Lanteri et al., 2006)
Berenil	<i>T. b. brucei</i> Δ at1	BSF	no	steady	5 mth	9.2	(Teká et al., 2011)
Eflornithine	<i>T. b. brucei</i>	BSF	no	steady	2 mth	41	(Vincent et al., 2010)
Eflornithine, pentamidine, 1433	<i>T. b. brucei</i>	BSF	no	steady	50–120 d	32	(Ranade et al., 2013)
Melarsenoxide cysteamine	<i>T. b. brucei</i>	BSF	no	steady	4 mth	15	(Pospichal et al., 1994)
Mycophenolic acid	<i>T. b. gambiense</i>	PCF	no	steady	n.s.	17	(Wilson et al., 1994)
Nifurtimox	<i>T. b. brucei</i>	BSF	no	steady	4.7 mth	8	(Sokolova et al., 2010)
Pentamidine	<i>T. b. brucei</i>	BSF	no	steady	2 mth	26	(Berger et al., 1993)
Pentamidine	<i>T. b. brucei</i> Δ at1	BSF	no	steady	several mth	130	(Bridges et al., 2007)
Pentamidine, melarsoprol	<i>T. b. rhodesiense</i>	BSF	no	steady	21 mth	140, 24	(Bernhard et al., 2007)
Pyrimidine analogs	<i>T. b. brucei</i>	BSF	no	steady	several mth	83–830	(Ali et al., 2013a)
Suramin	<i>T. b. rhodesiense</i>	BSF	no	shock	6 d	96	(Wiedemar et al., 2018)
Benznidazole	<i>T. cruzi</i>	epi	no	steady	n.s.	26	(Nirde et al., 1995)
Benznidazole	<i>T. cruzi</i>	epi	no	intermittent	15 w	\geq 4.7	(Campos et al., 2013)
Benznidazole	<i>T. cruzi</i>	epi	no	steady	n.s.	9–26	(Campos et al., 2014)
Benznidazole	<i>T. cruzi</i>	epi	no	steady	several w	n.s.	(Mejía et al., 2012)
Benznidazole	<i>T. cruzi</i>	epi	no	steady	4 mth	9–26	(Campos et al., 2017)
Benznidazole	<i>T. cruzi</i>	epi	no	steady	n.s.	23	(Nogueira et al., 2006)
Fluconazole	<i>T. cruzi</i>	epi	no	steady	4 mth	100	(Buckner et al., 1998)
Nifurtimox	<i>T. cruzi</i>	epi	no	steady	8 mth	4	(Wilkinson et al., 2008)
Nifurtimox	<i>T. cruzi</i>	epi, trypo	no	steady	60 d	3–10	(Nozaki et al., 1996)
Tubercidin	<i>T. cruzi</i>	epi	yes	shock	1 mth	180–260	(Nozaki and Dvorak, 1993)
CB3717	<i>L. tropica</i>	pro	no	steady	3–12 mth	25000	(Garvey et al., 1985)
Allopurinol	<i>L. infantum</i>	pro	no	steady	23 w	20	(Yasur-Landau et al., 2017)
Amphotericin B, miltefosine paromomycin, Sb ^{III}	<i>L. donovani</i>	pro	no	steady	18 w	11–20	(García-Hernández et al., 2012)
Methotrexate	<i>L. tropica</i>	pro	no	steady	3–11 mth	n.s.	(Beverley et al., 1984)
Arsenite	<i>L. mex.</i> , <i>L. amazon.</i>	pro	no	steady	1 mth	12	(Detke et al., 1989)
Hoechst 33342	<i>L. donovani</i>	pro	no	steady	n.s.	30	(Marquis et al., 2005)

Drug	Species	Stage	Mutagen	Pressure	Duration	RF	Ref.
Daunomycin	<i>L. tropica</i>	pro	no	steady	6 mth	62	(Chiquero et al., 1998)
Methotrexate	<i>L. donovani</i>	pro	no	shock	7-10 gen	n.s.	(Kaur et al., 1988)
Methotrexate	<i>L. major</i>	pro	no	steady	n.s.	n.s.	(Iovannisci and Beverley, 1989)
Miltefosine	<i>L. donovani</i>	pro	no	steady	6 mth	15	(Seifert et al., 2003)
Miltefosine, paromomycin	<i>L. infantum</i>	pro	yes	steady	10 d	2.5-8.5	(Bhattacharya et al., 2019)
Paromomycin	<i>L. donovani</i>	pro	no	steady	3 mth	3	(Jhingran et al., 2009)
Pentostam	<i>L. donovani</i>	pro	no	steady	n.s.	26	(Ullman et al., 1989)
Primaquin, pentamidine, terbinafine, chloroquine	<i>L. major</i>	pro	no	steady	n.s.	2.0-4.4	(Ellenberger and Beverley, 1989)
Pyrimidine analogs	<i>L. mex., L. major</i>	pro	no	steady	12 mth	1->3500	(Alzahrani et al., 2017)
Sinefugin	<i>L. infantum</i>	pro	no	steady	n.s.	n.s.	(Bhattacharya et al., 2019)
Sodium arsenite	<i>L. mex., L. amazon.</i>	pro	no	steady	>1 mth	12	(Detke et al., 1989)
Sb ^{III}	<i>L. major</i>	pro	no	shock	n.s.	30	(Marquis et al., 2005)

Early *in vitro* selection experiments were performed even before it was possible to propagate the parasites in culture: African trypanosomes were isolated from an infected rodent at peak parasitemia, exposed *in vitro* for 1 hour to high concentrations of trypanarsamide, and reinjected into another animal. After 3 to 13 cycles, the trypanosomes had become less sensitive to trypanarsamide (Hawking and Walker, 1966). The first culture systems for trypanosomatids were established for the insect stages, i.e., the procyclic, trypomastigote form of *T. brucei* (Brun and Schönenberger, 1979), the epimastigote form of *T. cruzi* (Berens et al., 1976), and the promastigote form of *Leishmania* (Krassner and Flory, 1972). When maintained in appropriate medium at 27 °C, these forms readily proliferate in axenic culture and reach densities of over 10^7 cells per mL before they enter stationary phase. The cultivation of the mammalian stages is less straightforward. Axenic *in vitro* cultivation is possible for *T. brucei* bloodstream forms (Baltz et al., 1985). Amastigote *Leishmania*, too, can proliferate in axenic culture if they are kept at low pH to simulate the phagolysosome (Balanco et al., 1998). Axenic long-term cultivation of *T. cruzi* amastigotes has been reported (Engel and Dvorak, 1988) but is not a standard procedure. Overall, the insect stages of trypanosomatid parasites do not require host cells, are easier to culture than the mammalian stages, and they reach much higher cell densities favoring the selection of drug-resistant mutants. The obvious drawback is that the insect stages are not clinically relevant.

2.4.2 Selection of Insect Stages vs. Mammalian Stages

The key question regarding the choice of the life cycle-stage is whether the mode of drug action is preserved in the insect stages, including drug transport pathway(s) and intracellular target(s). We would argue that if there is no difference in drug susceptibility between mammalian and insect stages, the mode of drug action is likely to be preserved and hence, *in vitro* selection for drug resistance will be easier and faster with the insect stages even though it is not the stage causing pathogenesis in mammals. However, if the insect stages are clearly less susceptible than the mammalian stages, they might not provide valuable insights on drug resistance (even though the target could be preserved but not essential in the insect stage). Benznidazole for *T. cruzi* is a typical example of a drug that is equally active against either stage, epimastigotes and amastigotes (Revollo et al., 2019) (Table 2). Epimastigote *T. cruzi* selected for benznidazole resistance kept the phenotype

after transformation to amastigotes (Nirde et al., 1995). In contrast, paromomycin resistance that had been selected for *in vivo* was lost after the amastigote *Leishmania* had been transformed to promastigotes (Hendrickx et al., 2015). Regarding *T. brucei*, most drugs used for the treatment of sleeping sickness are much less effective against the procyclic forms in the tsetse fly midgut than against the mammalian bloodstream forms (Table 2). This might be due to the fact that some of the transporters mediating drug uptake are only expressed in the latter (de Koning, 2001, Ziegelbauer and Overath, 1992).

An interesting aspect about the relevance of selecting insect stages of trypanosomatid parasites for drug resistance is the question of whether the insect stages ever come into contact with drugs in nature. With African trypanosomes, a scenario that seems plausible is that of an infected tsetse fly that takes a blood meal on a cow that has received nagana drugs, whereupon the procyclic trypanosomes in the fly midgut will be exposed to sublethal drug concentrations. This was experimentally reproduced: *Glossina morsitans* infected with *T. congolense* were fed over 1 month on rabbits that received weekly prophylactic doses of 2 mg/kg Samorin (isometamidium chloride). The flies were then used to infect mice, which in turn served to infect a new group of teneral flies. After four such cycles, the selected *T. congolense* had a significantly lower susceptibility to Samorin than unselected ones, passaged in untreated animals (Nyeko et al., 1988).

2.4.3 Selection of a Clone vs. a Population

The probability of obtaining a drug-resistant mutant increases with the genetic diversity of the starting population. This might suggest starting with a heterogeneous population of parasites when selecting for drug resistance in order to speed up the process. However, once the desired drug-resistant mutants have been obtained, their molecular genetic analysis is greatly facilitated if they all derive from the same parental, drug-sensitive clone. Otherwise, there are likely to be too many confounding nucleotide polymorphisms that are unrelated to the resistance phenotype. A typical procedure that facilitates downstream genomics, transcriptomics, and proteomics is to start the selection process with a fresh clone and select several lines independently. Thus, a melarsoprol-resistant mutant of *T. b. rhodesiense* was found to express only two genes (other than VSG) at a different level from the parental, melarsoprol-sensitive clone (Graf et al., 2016), even though

it had taken two years of *in vitro* selection to obtain the mutant (Bernhard et al., 2007).

A successful approach towards high-level pentamidine resistance in *T. brucei* was to start with a genetically engineered clone that was already less susceptible to pentamidine since it was homozygously disrupted in the gene *TbAT1*, which encodes an aminopurine permease that also transports diamidine drugs (Mäser et al., 1999). This starting clone was already 2.4-fold resistant (Matovu et al., 2003); after several months of *in vitro* exposure to increasing concentrations of pentamidine, a resistance factor of 130 was obtained (Bridges et al., 2007).

2.4.4 Selection with Mutagens vs. Adaptive Evolution

The use of chemical mutagens poses a similar dilemma as discussed above: it will increase the probability of obtaining a drug-resistant mutant and thus shorten the process of selection. At the same time, it will confront the downstream analyses of the obtained mutants with the challenging task of identifying which of the many mutations are the cause of drug resistance. Since back-crossing to the parental, drug-sensitive line is not feasible with trypanosomatid parasites, resistance selection based on chemical mutagenesis requires a large number of drug-resistant mutants that have been selected in parallel, preferably from the same, freshly cloned parent. Ethyl methanesulfonate (EMS) is frequently used as a mutagen to generate point mutations. It alkylates guanine to ethylguanine, which can form a base pair with thymine, leading to the transition from a G:C pair to A:T. EMS and other mutagens were applied to *L. infantum* promastigotes, followed by plating on media containing either miltefosine or paromomycin, which allowed the isolation of drug-resistant mutants (Bhattacharya et al., 2019). Finally, the drug itself can be mutagenic. This is the case for ethidium bromide (homidium), which is used in veterinary medicine for *T. congolense* infections. Benznidazole, too, is mutagenic to trypanosomes (Campos et al., 2017).

2.4.5 Selection under Constant Pressure vs. Sudden Shock

The intuitive approach to select parasites for drug resistance in culture is to apply a steady selective pressure with a sublethal drug concentration, which can be gradually increased as the parasites lose susceptibility. This has been the most commonly used procedure (Table 3). Such an approach is likely to result in the

accumulation of several mutations over time, and the phenotype of drug resistance that is ultimately obtained might result from a combination of genetic mechanisms. It is, therefore, imperative to freeze away intermediate samples, which will allow one to determine at what time point a given mutation has occurred. A different, potentially much faster approach is to start with a high inoculum of parasites, expose them to a supposedly lethal concentration of drug, and then wait and see whether, eventually, a population of parasites will recover. This worked well to select *T. brucei* for suramin resistance: when bloodstream-form trypanosomes were incubated with suramin at 5- to 25-fold the IC₅₀, all cells seemed to be dead by the following day. However, the cultures were further incubated, and after 6 days a population had regrown that was about 100-fold resistant to suramin (Wiedemar et al., 2018). Obviously, such a shock treatment bears the risk that the culture is not going to recover simply because all the parasites are dead. Nevertheless, we think it is a worthwhile experiment to try, since it quickly delivers a (positive or negative) answer.

2.5 Biosafety Considerations and Conclusion

Parasites that have been selected for drug resistance may require additional biosafety measures or even an upgrade in the biosafety level. *T. cruzi* bears the highest biohazard risk among the trypanosomatids. Highly infectious not only by traumatic inoculation but also via mucous membranes, *T. cruzi* is considered in many countries as a pathogen of biosafety level 3 (Table 4). Only two drugs are available for the treatment of an accidental infection with *T. cruzi*, benznidazole and nifurtimox. Both are nitroimidazoles, and they have the same mechanism of action: activation by electron transfer catalysed by nitroreductase 1 (NTR1), leading to the formation of radicals. Cross-resistance between benznidazole and nifurtimox due to reduced levels of *NTR1* expression is the most frequently observed mechanism (Murta and Romanha, 1998). Thus, when *T. cruzi* is being selected for resistance to nitroimidazoles, this will demand even more stringent biosafety measures than required anyhow. This word of caution also applies to selection experiments with the insect stages, because densely grown cultures of epimastigote *T. cruzi* will contain infective metacyclic forms.

In summary, selecting trypanosomatid parasites for drug-resistant mutants requires special care. Moreover, whatever the experimental approach, it also

requires patience and luck (in German *Geduld* and *Glück*), two of Paul Ehrlich's famous Four Gs (Raju, 1998). With points 3.1 to 3.5, we hope to have provided some guidance about the parameters that need to be considered when planning a drug selection experiment. While there is no bona fide best approach, a methodological consideration of the points outlined above will provide a framework for the successful planning of experiments.

Table 4. Risk group and biosafety level categorisation of *T. brucei*, *T. cruzi* and *L. donovani* (in an infected insect vector, all human-pathogenic trypanosomatids are classified as biosafety level 3).

Countries	<i>T. brucei</i>	<i>T. cruzi</i>	<i>L. donovani</i>
USA	2	2	2
AU/NZ	2	2	n.s.
EU	2 (Tbb), 3 * (Tbr)	3	3 *
UK	2 (Tbb), 3 * (Tbr)	3	3 *
CH	2	3	2

* Limited danger of transmission; usually not transmitted through the respiratory tract (Risk Group Database of the American Biological Safety Association, <https://my.absa.org/Riskgroups>, accessed on 19 July 2021).

2.6 Acknowledgments

We thank Monica Cal, Dennis Hauser, Sonja Keller-Märki and Romina Rocchetti for performing the assays for Table 2. This research was funded by the Swiss National Science Foundation, grant number CRSII5_183536.

3 Effects of walteriones on *Trypanosoma cruzi* metabolism

Sabina Beilstein^{1,2}, Ozlem Sevik Kilicaslan^{3,4}, Sylvian Cretton^{3,4}, Julien Boccard^{3,4},
Frédéric Bringaud^{5,6}, Joachim Kloehn⁷, Marcel Kaiser^{1,2}, Muriel Cuendet^{3,4},
Pascal Mäser^{1,2}

¹ Swiss Tropical and Public Health Institute, 4123 Allschwil, Switzerland

² University of Basel, 4001 Basel, Switzerland

³ School of Pharmaceutical Sciences, University of Geneva, 1205 Geneva,
Switzerland

⁴ Institute of Pharmaceutical Sciences of Western Switzerland, University of
Geneva, 1211 Geneva, Switzerland

⁵ Laboratoire de Microbiologie Fondamentale et Pathogénicité (MFP), Université
de Bordeaux, CNRS, UMR-5234, Bordeaux, France

⁶ Centre de Résonance Magnétique des Systèmes Biologiques (RMSB),
Université de Bordeaux, CNRS, UMR-5536, Bordeaux, France

⁷ Department of Microbiology and Molecular Medicine, Faculty of Medicine,
University of Geneva, Geneva, Switzerland

2023

Working manuscript

All metabolomics experiments were done under my lead. I have performed all experiments for assessing drug sensitivity in epimastigote *T. cruzi*. Drug sensitivity in amastigote *T. cruzi* was assessed by Monica Cal. Parasite culturing and metabolite extractions were done by myself. LC-MS analysis was done by Sylvian Cretton, Ozlem Sevik Kilicaslan, and Julien Boccard. NMR analysis was performed by Frédéric Bringaud and Marc Biran. GC-MS analysis was done by Joachim Kloehn.

3.1 Abstract

Chagas disease is caused by the parasite *Trypanosoma cruzi*. Autochthonous to Latin America and the southern United States, Chagas disease has spread globally due to travel and migration. The options to treat Chagas disease are very limited, with benznidazole and nifurtimox the only available drugs. Treatment is commonly marked with side effects and no treatment success for the chronic form of the disease is guaranteed. Therefore, new drugs are needed urgently. Natural compounds are a rich source of biologically optimised compounds with high potential for new drugs. In particular, the waltheriones are a group of quinoline alkaloids isolated from the medicinal plant *Waltheria indica* that have shown promising activity against *T. cruzi*. Waltheriones are specifically active against *T. cruzi* but not against the related parasite *Trypanosoma brucei* nor against *Leishmania*. Here we investigate the elusive mode of action of the waltheriones. We demonstrate that *T. cruzi* extracellular epimastigote forms are as sensitive to waltheriones as intracellular amastigotes. This offers the possibility to use untargeted exposure metabolomics to study the action of waltheriones. Incubation of epimastigote *T. cruzi* with waltherione G leads to an accumulation of acylcarnitine adducts in the parasite. This indicates an interference with fatty acid metabolism downstream of carnitine palmitoyltransferase 1 (CPT1), e.g. with the carnitine shuttle system or with subsequent β -oxidation. This study provides the first evidence on the mode of antichagasic action of the waltheriones, highlighting the mitochondrion as site of action and informing further (i.e. molecular genetic) studies to support the development of waltheriones as antichagasic agents.

3.2 Introduction

There is an urgent need for drugs to cure Chagas disease. Chagas disease is a vector-borne neglected tropical disease caused by the protozoan parasite *Trypanosoma cruzi*. Originating on the South American continent, infection with *T. cruzi* is more frequently occurring further north and spreading globally due to climate change and human mobility and migration (Pérez-Molina and Molina, 2018). Triatomine bugs are the competent hosts and vectors for *T. cruzi*, but there are alternative routes of transmission such as blood transfusion, organ transplantation, congenital transmission as well as foodborne transmission, all of which are of high epidemiological relevance (Howard et al., 2014, Pinazo et al., 2011, Shikanai-Yasuda and Carvalho, 2012, El Ghouzzi et al., 2010).

To date, the treatment of Chagas disease still relies on benznidazole and nifurtimox only, drugs showing limited efficacy and substantial side effects (Aldasoro et al., 2018, Molina et al., 2015). Efforts to find alternative drugs were unsuccessful so far. Posaconazole was one drug candidate showing initial activity during the chronic phase of the disease, but failed to deliver cure due to relapses in the follow-up period, leaving benznidazole as the first choice for Chagas disease treatment (Molina et al., 2014).

In protozoan screens of natural molecules for novel antichagasic candidates, the waltheriones have emerged as top hits (Cretton et al., 2014). The waltheriones are phytochemical compounds of the plant *Waltheria indica* belonging to the quinoline alkaloids (Cretton et al., 2014). Two out of the ten analogues (waltheriones F and G) exhibited exceptional activity against *T. cruzi* intracellular amastigotes and good selectivity indices as compared to uninfected mammalian cells. Remarkably, there was no activity against bloodstream-form *Trypanosoma brucei*, making this class of phytochemicals even more intriguing.

Quinoline alkaloids are a well-known group of bioactive molecules and still drug candidates for the parasitology field, in particular quinine and related quinoline antimalarials (Foley and Tilley, 1997). The therapeutic potential of the N-based heterocyclic compounds extends beyond the field of parasitology including antitumor, antibacterial, antiviral, or anti-inflammatory activities (Shang et al., 2022). Apart from their promising activity profiles, very little is known about a potential mode of action of quinoline alkaloids against trypanosomatids. 2-n-propylquinoline

from *Galipea longiflora* had shown efficacy in BALB/c mice in the treatment of visceral leishmaniasis (Fournet et al., 1993). Further studies suggested an inhibitory effect on P-glycoprotein as a possible mechanism of action (Belliard et al., 2003).

Untargeted metabolomics upon drug exposure is a powerful tool for deconvolving a compound's mode of action, as it is a hypothesis-free approach, which provides information on the molecular level in an unbiased way. In drug discovery for protozoans, it was successfully used in *Plasmodium falciparum* and *T. brucei* (Ali et al., 2013b, Alkhaldi et al., 2015, Creek et al., 2016). In *T. cruzi* untargeted metabolomics helped to identify the mechanism of action of benznidazole, a prodrug that is reduced and metabolised to several different metabolites that elicit toxic reactions by binding to low molecular weight thiols as well as protein thiols (Trochine et al., 2014b).

The relevant lifecycle-stage for the pathology of Chagas diseases is the amastigote form, which is obligate intracellular and thus not amenable to metabolomics. Here we take advantage of the finding that the waltheriones are active against the vector stage as well as the mammalian forms of *T. cruzi*. We report the results from untargeted exposure metabolomics with extracellular epimastigote *T. cruzi* exposed to waltherione G, and in particular the effects elicited by waltherione G on the parasites' fatty acid metabolism.

3.3 Material and Methods

3.3.1 Parasite strain and culturing

The epimastigote form of *Trypanosoma cruzi* STIB980 clone 1 (DTU Tc1) was cultured in liver infusion tryptose (LIT) medium supplemented with 10% inactivated fetal calf serum (iFCS) and 2 µg/mL hemin at 27 °C (Fernandes and Castellani, 1966). Parasites were diluted once a week to maintain cultures in exponential growth.

3.3.2 Epimastigote drug sensitivity testing

In vitro drug sensitivity was tested on the epimastigote form of *T. cruzi* STIB980. In a 96-well microtiter plate serial drug dilutions from 10 µg/mL to 0.17 ng/mL in 1:3 steps were prepared. Parasites were added to a final starting density of 5×10^6 per mL. The starting concentration for the standard drug benznidazole was 100 µg/mL and 10 µg/mL for waltherione F and G, respectively. Stock solutions were prepared at a concentration of 10 mg/mL and pre-diluted to 1 mg/mL for waltherione F and G. After 69 h, resazurin was added to a final concentration of 0.01 µg/mL (stock solution of 0.125 µg/mL in PBS). After a total assay duration of 72 h, the plate was read in a spectrofluorometer (SpectraMAX GEMINI EM Microplate, Molecular Devices, San Jose, CA). Fluorescence values (excitation and emission wavelength of 536 and 588 nm) were recorded using SoftMax Pro Software (version 5.4.6.005). 50% inhibitory concentration (IC₅₀) values were calculated using nonlinear regression in GraphPad Prism (version 8.2.1).

3.3.3 Metabolite extraction for untargeted metabolomics

Epimastigote *T. cruzi* were cultured over two weeks to a high density of 2.5×10^7 parasites per mL. They were then kept for 2 days in the incubator reaching a density of 10^8 parasites per mL. Parasite density was adjusted to 10^8 parasites per mL before drug was added according to the experimental set up (Supplementary Table 1). Ten times the IC₅₀ (0.5 µg/mL or 1.4 µM) of waltherione G was used for the experiment. The same concentration of 0.5% (v/v) DMSO was added to the control sample as waltherione G was dissolved in 100% DMSO. The cells were incubated for 6 h. To preclude changes in parasite number in the different samples, only a short incubation period was used (Trochine et al., 2014b). After the incubation,

parasites were placed for 3 min on ice to slow down metabolic activity. The same drug concentration and DMSO concentration was then added to the untreated parasites as a control to exclude any immediate effect or stress response on the parasites. Parasites were pelleted by centrifugation (3 min at 2000 g and 4 °C). 100 µL of the supernatant was collected (supernatant fraction). The rest of the supernatant was removed carefully to receive the pellet only. The supernatant fraction, the cell pellet and an additional fresh medium sample were extracted with a monophasic solvent already used by Trochine et al. (Trochine et al., 2014b). The cell pellet was additionally first dissolved in 40 µL water. Methanol was added in a ratio of 3:1. One part chloroform was then added to the sample, resulting in a monophasic extraction solvent (water, methanol, chloroform in the volumetric ratio of 1:3:1). Extraction was done for 1 h in a Thermomixer (VWR Thermal Shake lite, at 1000 rpm and 4 °C). By a second centrifugation step (3 min at 13,000 g and 4 °C) cell debris were separated from the extract. To get an additional quality control, fractions of only the pellet samples, only the supernatant samples, the total pool of all samples, and a sample with only the extraction solvent were prepared. The samples were kept at -80 °C until analysis. The experiment was repeated in biological replicates 5 times on independent time points, each with up to 10 replicates.

3.3.4 LC-HRMS for untargeted metabolomics analysis

Samples from metabolite extraction were analysed on a Q Exactive Focus Hybrid quadrupole-orbitrap mass spectrometer (Thermo Scientific, Waltham, MA, USA) using electrospray ionization in positive-ion mode. The instrument was programmed with spray voltage at 3.5 kV; sheath gas flow rate (N₂) at 50 units; capillary temperature at 320 °C; S lens RF level at 50 and probe heater temperature at 425 °C.

The separation was performed with a mobile phase, (A) acetonitrile with 0.1% formic acid; (B) water with 20 mM of ammonium formate and 0.1% formic acid; flow rate, 400 µL/min; injection volume, 2 µL; gradient, 95% A during 2 min, linear gradient of 95–60% A over 6 min, and then reconditioning at 95% A during 4 min.

3.3.5 Untargeted metabolomics data treatment

The raw files were converted to .mzXML (mass spectrometry data format) using MSConvert software (version 0.30), part of the ProteoWizard package (ProteoWizard, Palo Alto, CA, USA) (Chambers et al., 2012). The converted files were then processed using MZmine software suite (version 2.53) (Pluskal et al., 2010). For mass detection at MS¹ level, the noise level was set to 10⁵. For MS² detection, the noise level was set to 0.00. The ADAP chromatogram builder parameters were set as follows: minimum group size of scans of 5, minimum group intensity threshold of 10⁵, minimum highest intensity of 10⁵, and *m/z* tolerance of 8.0 ppm. The ADAP algorithm (wavelets) was used for chromatogram deconvolution with the following parameters: signal-to-noise tolerance of 50, minimum feature height of 5×10⁶, coefficient area threshold of 110, peak duration range between 0.02 and 1.5 min and RT wavelet range between 0.02 and 0.05 min. Isotopes were detected using the isotope peak grouper with a *m/z* tolerance of 8.0 ppm, an RT tolerance of 0.05 min (absolute), a maximum charge set at 2, while in isotope grouping the determining peak in case of several isotopes was the lowest *m/z*. The peak alignment was done with the join-aligner method with an *m/z* tolerance of 8.0 ppm, an RT absolute tolerance of 0.05 min, and a weight for *m/z* and RT at 30. The peak list was then gap-filled using the same RT and *m/z* gap filler with an *m/z* tolerance of 10.0 ppm. Each file was filtered by retention time within a range from 0.70 to 10.0 min, and only the ions with an associated MS² spectrum were kept. Peaks of the last batch of analysis of 10 replicates were removed using duplicate peak filtering with *m/z* tolerance of 7.0 ppm and an RT tolerance of 0.2 min. Peaks were filtered using a relative mean standard deviation threshold of 0.5 in pooled QC samples. Intensity drift along the analytical sequence was then corrected for each individual feature based on LOESS regression (Dunn et al., 2011). Samples were then treated using Probabilistic Quotient Normalization (PQN) based on median QC values to guarantee their comparability (Dieterle et al., 2006).

The resulting aligned peak list was exported for further analysis as an .mgf file. The MassBank of North America (MONA) library was used for compound annotation by accurate mass and MS/MS spectral similarity (Horai et al., 2010). The MZmine files were exported in .mgf format to SIRIUS 5.6 (version 5.6) (Lehrstuhl für Bioinformatik, Jena, Germany) for the feature annotation (calculating the feature raw formula, predicting the fragmentation pattern with CSI, inferring the chemical

class with the CANOPUS module) (Dührkop et al., 2019, Dührkop et al., 2021, Dührkop et al., 2015). Statistical analysis was done with GraphPad Prism (version 8.2.1).

3.3.6 Sample preparation of U-¹³C₁₆-palmitate assay and NMR analysis of the medium

A uniformly labelled U-¹³C₁₆-palmitate-BSA conjugate (final concentration of 5 mM in 7% BSA) was prepared for incubation of epimastigote *T. cruzi*. Conjugation was done according to the protocol used in Huynh et al. (Huynh et al., 2014). Fatty acid-free BSA (Sigma, A9205) was dissolved in water to 7.5% and heated to 42 °C under continuous stirring. 77 mM solution of sodium palmitate uniformly labelled with ¹³C (Sigma, 700258) in water was prepared and dissolved under continuous heating at 70 °C until the fatty acids were dissolved. The BSA (7.5%) was added to the solubilised sodium palmitate and kept at 42 °C for 30 min under continuous stirring to get the final palmitate-BSA conjugate of 5 mM in 7% BSA. The BSA control solution without sodium palmitate was prepared with the same procedure in parallel.

Epimastigote *T. cruzi* were cultured and adjusted to a density of 2.5×10^7 parasites per mL. Over the succeeding 72 h the parasites were kept in the incubator to reach a density of 10^8 parasites per mL without providing any fresh medium to enhance the depletion of glucose and force the parasites to starvation. For each condition and replicate, 1 mL of roughly 1.5×10^8 parasites per mL were pelleted (10 min at 1400 g and room temperature) and washed twice with PBS. Parasites were incubated for 6 h at 27 °C in 1.5 mL of PBS supplemented with 2 g/L NaHCO₃ (pH 7.4) together with the treatment according to the experimental set up. The sodium bicarbonate favours carboxylation steps in the subsequent NMR analysis. According to the experimental set up samples were supplemented with 0.3 μM U-¹³C₁₆-palmitate and drug. For walterione F and G the concentrations were ten times the IC₅₀ (3.0 μg/mL = 9.0 μM and 0.5 μg/mL = 1.4 μM, respectively). For etomoxir (ETO) the concentration was 500 μM (Souza et al., 2021). For a second experiment cells were pre-incubated for 18 h to reach a final incubation time of 24 h with drug. After the incubation time, cells were centrifuged for 10 min at 7500 g at room temperature. To get parasite-free samples, the supernatant was collected, filtered with a Spin-XTM filter (Corning™ 8161), and centrifuged for 5 min at 2000 g

at room temperature. Samples were stored at -20 °C until NMR analysis. For later GC-MS analysis, pellets were kept at -80 °C (Supplementary Table 2).

The collected and filtered supernatant samples were supplemented with 10 mM maleate solution in D₂O as an internal reference. ¹H-NMR spectra were collected according to the previously published protocol (Souza et al., 2021). Statistical analysis was done with GraphPad Prism (version 8.2.1).

3.3.7 Metabolite extraction of pellets from U-¹³C₁₆-palmitate assay for GC-MS analysis

T. cruzi pellets isolated from the U-¹³C₁₆-palmitate assay were thawed for 10 min on ice. Metabolite extraction was performed according to Krishnan et al. and Saunders et al. (Krishnan et al., 2020, Saunders et al., 2014). Parasites were lysed and metabolites extracted by adding 50 µL chloroform followed by thorough vortexing. 200 µL methanol/water solvent were added at a ratio of 3:1 (v/v), resulting in a monophasic mixture. All solvents used were of analytical grade. After thorough vortexing, the samples were centrifuged (10 min at 20,000 g and 4 °C) to separate the insoluble material from the soluble phase. The supernatant was transferred to a new vial containing 100 µL water, resulting in a biphasic chloroform/methanol/water mixture at a ratio of 1:3:3, and vortexed thoroughly. The upper polar phase of about 300 µL was separated from the lower apolar phase of about 50 µL by centrifugation (10 min at 20,000 g and 4 °C). The extracts were stored at -80 °C until derivatisation.

Both, the polar and the apolar phase, were transferred to a mass spectrometry glass vial insert and dried by centrifugal evaporation (Speed Vac). The polar phase was dried sequentially, adding 50 µL at a time. Free aldehyde groups of the polar phase metabolites were protected by reacting with 20 µL methoxyamine hydrochloride in pyridine (Sigma, 20 mg/mL) over night at room temperature. The next day, silylation was performed by adding 20 µL N,O-Bis-(trimethylsilyl)-trifluoroacetamide (BSTFA with 1% trimethylchlorosilane, Cerilliant) to mask hydroxyl and amino groups (Krishnan et al., 2020, Saunders et al., 2014). Fatty acids contained in the apolar phase were resuspended in 40 µL chloroform/methanol (2:1, v/v) supplemented with 3% (v/v) of 3-(trifluoromethyl)-phenyltrimethylammonium hydroxide (TCl) to hydrolyse fatty acids from lipids and convert them to their respective fatty acid methyl ester (FAME) (Krishnan et al., 2020, Saunders et al., 2014, Saunders et al., 2011).

3.3.8 GC-MS on pellet extracts from U-¹³C₁₆-palmitate assay

The extracted pellet samples from the labelled U-¹³C₁₆-palmitate assay were analysed by GC-MS using a 6890N Network GC system (Agilent Technologies, Santa Clara, CA, USA), equipped with a VF-5ms capillary column with a 10 m EZ guard (Agilent Technologies, Santa Clara, CA, USA) and connected to a 5973 Network Mass Selective Detector (MSD, Agilent Technologies, Santa Clara, CA, USA). The GC system was operated using helium as carrier gas at a flow rate of 1 mL/min.

Per run, 3 µL of derivatised polar metabolites were injected and analysed in splitless mode using the following GC oven temperature gradient, lasting a total of 24 min: 70 °C hold for 2 min, ramp to 295 °C at 12.5 °C/min, ramp to 320 °C at 25 °C/min, and hold 320 °C for 3 min. Samples were analysed twice, once with the MSD operating in scan mode, scanning all ions between m/z 70-700, and once in selected ion monitoring (SIM) mode detecting specifically the parental ion and mass isotopologues of succinate-TMS (m/z 247-251), malate-TMS (m/z 335 -339), and citrate-TMS (m/z 465-471).

As for the polar metabolites, 3 µL of derivatised apolar metabolites were injected per run and analysed in splitless mode. Samples were analysed using the following GC oven temperature gradient, lasting a total of 37 min: 80 °C hold for 2 min, ramp to 140 °C at 30 °C/min, ramp to 250 °C at 5 °C/min, ramp to 265 °C at 15 °C/min, and hold at 265 °C for 10 min. As above, the samples were analysed twice, once in scan mode, scanning all ions between m/z 70-700, and once in a selected ion monitoring method detecting specifically the parental ion of the palmitate-methyl ester and its mass isotopologues (i.e., m/z 270-286), with m/z 286 corresponding to the fully U-¹³C₁₆-palmitate labelled sample, which was introduced as labelled precursor.

Polar metabolites and FAMES were identified using authentic standards. Citrate-TMS and the palmitate-methyl ester eluted at 14.500 and 18.657 minutes, respectively, using the column and temperature gradients described above. Abundance of the citrate-TMS (m/z 465-471) and palmitate-methyl ester mass isotopologues (m/z 270-286) were inferred using Mass Hunter Workstation Software (Agilent Technologies, Quantitative Analysis, version B07.00). The extent of ¹³C-labelling was calculated using Excel (Microsoft) software following correction

for the occurrence of natural isotopes as described by Zamboni et al. (Zamboni et al., 2009). Statistical analysis was done with GraphPad Prism (version 8.2.1).

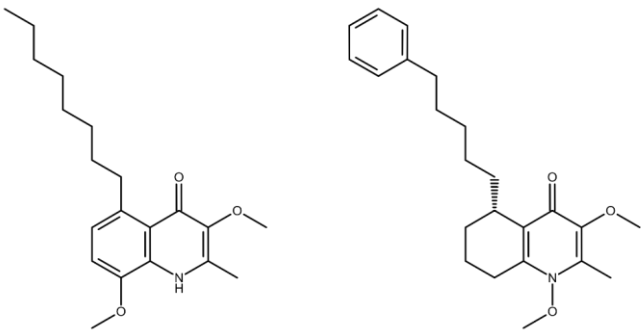
3.3.9 Bioinformatics: Translocase search

The carnitine-acyl carrier from rat, annotated in UniProt as TB 2.A.29.8.1 was used as starting point to build a HMM library and as reference sequence. A blastp search was performed with this sequence against the SwissProt and RefSeq protein databases. In the search, eutheria (taxid:9347) and metazoa were excluded and instead alveolata and oomycetes as well as some specific additional sequences were included. A diverse sequence set of eleven hits annotated as carnitine-acyl carrier were downloaded. With the help of the MegaX software (version 10.0.5) a phylogenetic tree with the neighbour joining method and a distance table were created to detect almost identical sequences. No sequences were removed, though. The multiple alignment was done using ClustalW in Biolinux. The multiple alignment was converted to a HMM profile with hmmbuild of the HMMer3 package (Eddy, 2009). The profile was used to search the proteomes of *T. cruzi* and *T. brucei* with hmmscan of the HMMer3 package (Eddy, 2009).

3.4 Results

3.4.1 Waltheriones are active against amastigote and epimastigote *T. cruzi*

Waltherione F and G are highly active against *T. cruzi* amastigotes (Cretton et al., 2014). Waltherione G shows higher activity against *T. cruzi* compared to waltherione F and has a higher selectivity index of more than 200 (Figure 1). Amastigotes are the relevant lifecycle-stage for the treatment of Chagas disease. However, the amastigotes are not readily amenable to metabolomics as they only proliferate inside host cells. Remarkably, waltherione F and G are active also against *T. cruzi* epimastigotes, with IC₅₀ values in the same, submicromolar range (Figure 1). Thus, we concluded that the epimastigotes are a valid and convenient substitution for the amastigotes to perform metabolomics without having to deal with host cell metabolites.



	Waltherione F	Waltherione G
<i>T. cruzi</i> amastigotes	0.48 ± 0.45	0.11 ± 0.10
<i>T. cruzi</i> epimastigotes	0.27 ± 0.13	0.10 ± 0.03
Rat L6 myoblasts	39.4 ± 34.2	26.3 ± 22.6
Selectivity index	82	231

Figure 1. Chemical structure and *in vitro* activity of waltherione F and G. The 50% inhibitory concentration (IC₅₀) is shown in μM ± standard deviation (n≥3). SI, selectivity index = IC₅₀ L6/IC₅₀ *T. cruzi* amastigote.

3.4.2 Untargeted exposure metabolomics

Untargeted exposure metabolomics was performed to obtain a general insight into the effect of walterione G on *T. cruzi* metabolism. With a monophasic solvent of water, methanol, and chloroform (ratio 1:3:1, v/v/v), metabolites were extracted for LC-MS analysis (Figure 2). The procedure for drug incubation and metabolite extraction was done according to Trochine et al. (Trochine et al., 2014b), where untargeted metabolomics on epimastigote *T. cruzi* had been used to investigate benzimidazole drug action. The protocol was optimised to *T. cruzi* strain STIB980 and to our biosafety facility, complying with biosafety and chemical safety guidelines. This explains the stepwise addition of extraction components. Walterione G-treated epimastigotes were compared to non-treated epimastigotes separating the supernatant and cell pellet fractions. Walterione G was dissolved in 100% DMSO. To exclude any cytotoxic effect elicited by the drug solvent a concentration of 0.5% of DMSO was added as control. In total 5 independent experiments with at least 3 replicates were performed (n1=3, n2=5, n3=5, n4=5, n5=10).

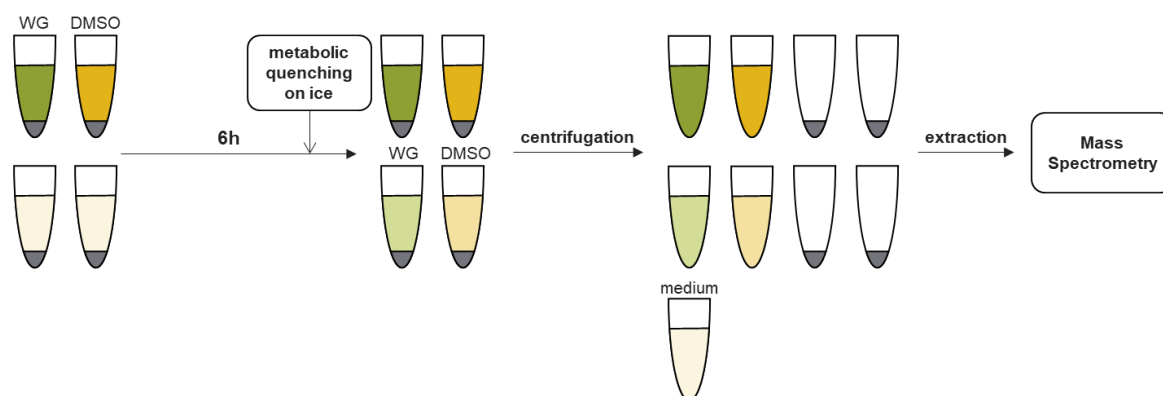


Figure 2. Drug incubation and metabolite extraction. Epimastigote *T. cruzi* were incubated with 10x the IC_{50} of walterione G (WG). Drug and DMSO was first only added to the treated samples. After 6 h of drug incubation, all samples were metabolically quenched on ice. Drug and DMSO was instantly added to the untreated control samples accordingly. An additional medium sample was taken along as control. Centrifugation and metabolite extraction was performed on the pellet and supernatant fraction separately.

The first two experiments served as pilot experiments without including any metabolite standards. Throughout all the biological replicates, walterione G

treatment resulted in an overabundance of acylcarnitines in the pellet fraction and a lower abundance of acetylcarnitine (Table 1 and Figure 3A, B, and C). Strikingly several different acylcarnitine analogues were detected in the same experiment including isovalerylcarnitine, oleoylcarnitine, and palmitoylcarnitine. This pointed to an interference of waltherione G with fatty acid catabolism. Hypoxanthine and inosine were two other metabolites which showed an altered abundance in the waltherione treated pellet fraction.

Table 1. Metabolites identified in the WG-treated epimastigote *T. cruzi*. Acylcarnitines, hypoxanthine, and inosine were identified in all 5 experiments. m/z, mass-to-charge ratio; level of identification, 5 levels with different data requirements (MS/MS, confidence level 4; Standard, confidence level 5) (Xue et al., 2019).

	Identification	m/z	Level of identification
Experiment 1	Carnitine	162.1125	MS/MS
	Oleoyl-L-carnitine	426.357	MS/MS
	Palmitoylcarnitine	400.3418	MS/MS
	Isovalerylcarnitine	246.1698	MS/MS
	Inosine	269.088	MS/MS
	Hypoxanthine	137.0458	MS/MS
	Sphinganine 1-phosphate	382.2719	MS/MS
	Phe-Pro-Leu	376.223	MS/MS
	Glu-Ala	219.0976	MS/MS
Experiment 2	Carnitine	162.1125	MS/MS
	Oleoyl-L-carnitine	426.357	MS/MS
	Isovalerylcarnitine	246.1698	MS/MS
	Propionylcarnitine	218.1388	MS/MS
	Acetylcarnitine	204.1231	MS/MS
	Inosine	269.088	MS/MS
	Hypoxanthine	137.0458	MS/MS
	Sphinganine 1-phosphate	382.2719	MS/MS
Experiment 3	Carnitine	162.1125	Standard
	Oleoyl-L-carnitine	426.357	MS/MS
	Palmitoylcarnitine	400.3418	standard
	Isovalerylcarnitine	246.1698	Standard
	Acetylcarnitine	204.1231	MS/MS
	Inosine	269.088	MS/MS
	Hypoxanthine	137.0458	MS/MS
	Sphinganine 1-phosphate	382.2719	MS/MS
Experiment 4	Carnitine	162.1125	Standard
	Oleoyl-L-carnitine	426.357	MS/MS
	Palmitoylcarnitine	400.3418	standard
	Isovalerylcarnitine	246.1698	Standard
	Acetylcarnitine	204.1231	MS/MS
	Inosine	269.088	MS/MS
	Hypoxanthine	137.0458	MS/MS

	Identification	m/z	Level of identification
	Sphinganine 1-phosphate	382.2719	MS/MS
Experiment 5	Carnitine	162.1125	Standard
	Oleoyl-L-carnitine	426.357	MS/MS
	Palmitoylcarnitine	400.3418	standard
	Isovalerylcarnitine	246.1698	Standard
	Propionylcarnitine	218.1388	MS/MS
	Acetylcarnitine	204.1231	MS/MS
	Inosine	269.088	MS/MS
	Hypoxanthine	137.0458	MS/MS
	Sphinganine 1-phosphate	382.2719	MS/MS
	Phe-Pro-Leu	376.223	MS/MS
	Glu-Ala	219.0976	MS/MS

A	Log ₂ fold change WG/ctr					mean	sd
	1	2	3	4	5		
Experiment							
Isovalerylcarnitine	1.17	1.67	2.10	0.01	1.42	1.27	0.70
Oleoylcarnitine	2.82		2.18	0.27	1.70	1.74	0.94
Palmitoylcarnitine	3.55		3.44	0.06	1.84	2.22	1.42
Acetylcarnitine	-0.18	-1.17	-1.13	0.15	-0.73	-0.61	0.52
Carnitine	-0.24	-0.80	0.14	-0.22	0.64	-0.10	0.48

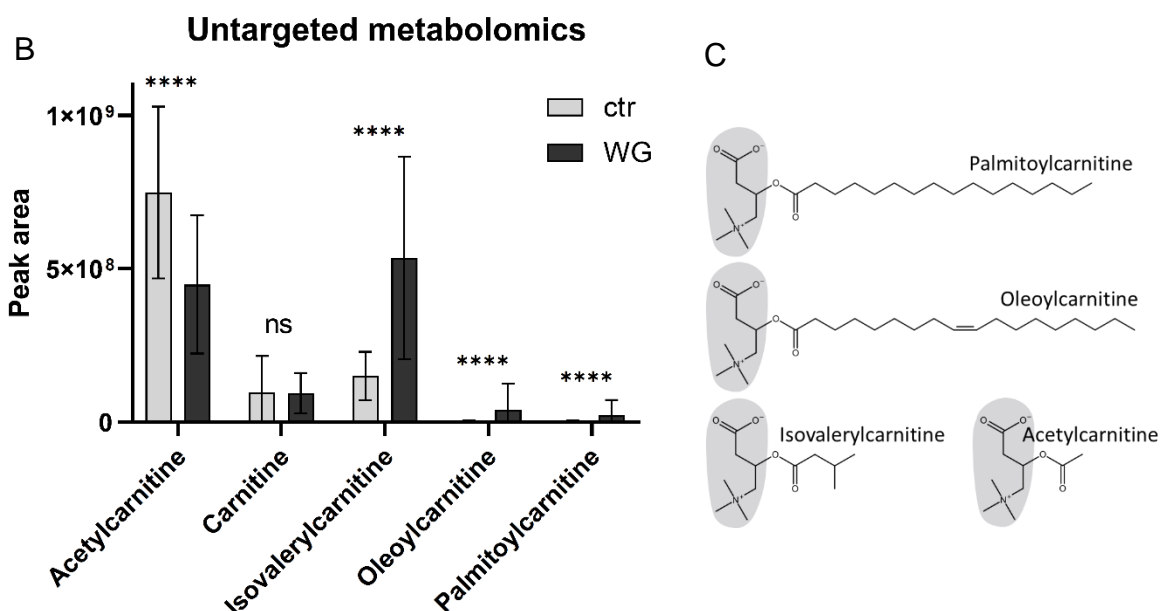


Figure 3. (A) Accumulation and depletion of metabolites identified in the pellet samples of waltherione G treated and control samples in all 5 experiments. The log₂ fold change values were calculated based on the peak area ($n \geq 3$). (B) Accumulation and depletion of carnitine analogues calculated across all replicates ($n \geq 20$). P-values were assessed by unpaired t-test (****= $p < 0.0001$, ns= $p > 0.05$). (C) Structure of palmitoylcarnitine, oleoylcarnitine, isovalerylcarnitine, and acetylcarnitine. The carnitine moiety is marked in grey.

3.4.3 U-¹³C₁₆-palmitate uptake and metabolism

To investigate fatty acid uptake and metabolism in more detail, a semi-targeted approach using isotopically labelled fatty acid was followed. *T. cruzi* epimastigotes were cultured to the very late exponential growth phase whereby pushing them to glucose starvation. 6 h prior to harvesting, the cells were transferred to PBS, depleting them of the remaining nutrients. During those 6 h PBS was supplemented with U-¹³C₁₆-palmitate. The samples were treated with walterione F, walterione G, or ETO. ETO inhibits CPT1 in *T. cruzi* (Kiorpes et al., 1984) and was used as a control. It had been shown that ETO is only effective against *T. cruzi* at the very high concentration of 500 µM, and only in late exponential growth (Souza et al., 2021).

Starved epimastigotes excrete acetate as primary end product of carbon consumption through fatty acid catabolism (Souza et al., 2021). Therefore, the supernatant of the U-¹³C₁₆-palmitate-fed epimastigotes was analysed with NMR focusing on acetate, hypothesizing walteriones to affect the carnitine-mediated fatty acid shuttling or downstream catabolism. ¹³C-labelling was detected in the acetate identified in the supernatant. No clear difference was seen between the different treatments (adjusted p-value for all samples >0.3, assessed by One Way ANOVA followed by Tukey's post-test) (Figure 4A). Preincubating the cells for 18 more hours led to the same result. The signal for unlabelled acetate in the second experiment was in general higher, likely reflecting the higher degree of starvation.

To gain more detailed insights into palmitate catabolism, the pellets of the U-¹³C₁₆-palmitate fed *T. cruzi* were analysed with GC-MS with the focus on fatty acids and TCA metabolites. In both experiments, the ETO-treated parasites showed, as expected, an accumulation of U-¹³C₁₆-palmitate (adjusted p-value <0.0001, assessed by One Way ANOVA with Tukey's post-test) (Figure 4B). However, contrary to the expectation, this did not result in a depletion of ¹³C incorporated into citric acid (Figure 4B). No clear differences were seen in the walterione-treated cells compared to the non-treated control (adjusted p-value for all walterione treatments >0.5, assessed by One Way ANOVA with Tukey's post-test).

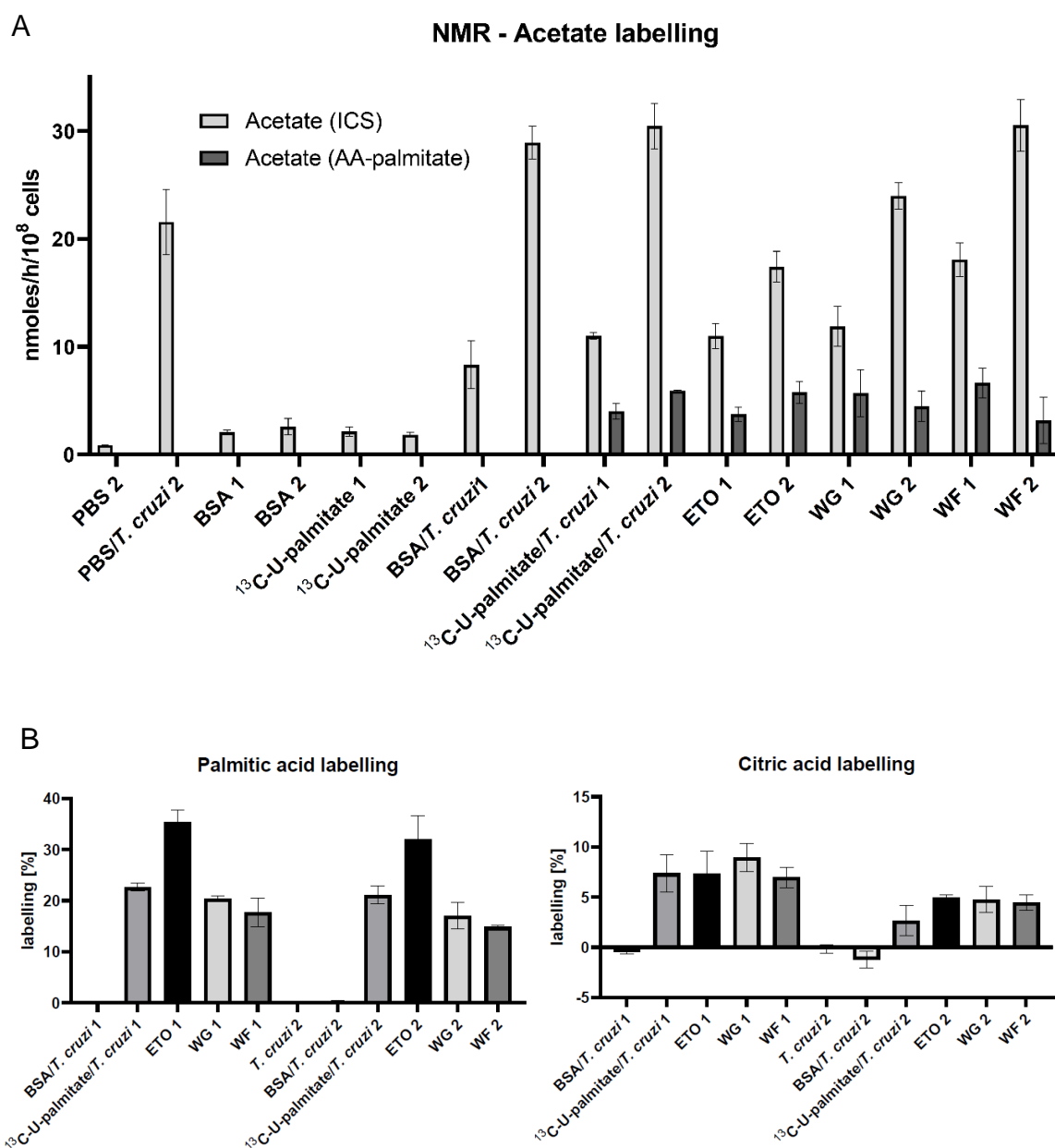


Figure 4. (A) NMR results of analysing the medium fraction of experiment 1 and 2. Experiment 2 was a repetition of experiment 1 including 18 h additional drug incubation prior to PBS starvation, and PBS and PBS/*T. cruzi* as additional controls. Acetate is the primary end product of β -oxidation. ^{13}C labelling was traced in this metabolite. (B) GS-MS results of extracted pellets of experiment 1 and 2. ^{13}C labelling was determined in citric acid representing a TCA metabolite. ICS, internal carbon source; AA-palmitate, acetate from labelled palmitate; BSA, bovine serum albumin; ETO, etomoxir; WG, waltherione G; WF, waltherione F.

3.4.4 Profile-based search - carnitine-acylcarnitine translocase and fatty acid metabolism

The carnitine-acylcarnitine antiporter (carnitine-acylcarnitine translocase, CACT) appeared as a potential target of walterione G based on the untargeted metabolomics experiment. However, it was not conclusive from the literature (Quiñones et al., 2020, Güther et al., 2014) whether that gene was actually present in *T. cruzi*. Therefore, a search was performed on the predicted proteome of *T. cruzi* Dm28c 2018 (version TriTrypDB-57). Starting from the known carnitine-acylcarnitine carrier from rat, a hidden Markov model-based profile (Eddy, 2009) was built that included diverse species. This identified C4B63_28g89 as the candidate carnitine-acylcarnitine antiporter of *T. cruzi*.

3.5 Discussion

Waltheriones have a potential for further development to a new drug for Chagas disease. However, their mode of action against *T. cruzi* is unknown. Here we aimed to reveal which metabolic pathways are targeted by metabolomic approaches, profiting from the fact that the waltheriones are active not only against *T. cruzi* intracellular amastigotes but also against extracellular epimastigotes. Waltherione G was slightly more potent than waltherione F (Figure 1) and was therefore chosen to investigate drug action. The most consistently observed effect of waltherione G exposure on the metabolome of *T. cruzi* was an accumulation of acylcarnitines in the cellular fraction (i.e. pellet), which occurred over five independent consecutive experiments, each carried out in multiple replicates. Carnitine is involved in long-chain fatty acid shuttling across the inner mitochondrial membrane (Kerner and Hoppel, 2000). In *T. cruzi* a putative carnitine O-acyltransferase (CPT) had been found in the glycosomal proteome, but no carnitine-acylcarnitine translocase (CACT) (Güther et al., 2014, Acosta et al., 2019, Quiñones et al., 2020). A profile-based search on carnitine-acylcarnitine antiporter confirmed the general presence of a putative carnitine-acylcarnitine antiporter gene in *T. cruzi* and *T. brucei*, which makes the mitochondrion a plausible site of drug action.

Inside the insect vector of *T. cruzi*, the extracellular epimastigote form switches from glucose as their primary carbon source to amino acids under poor nutrient availability (Barisón et al., 2017). It was shown that fatty acids are used as an alternative carbon source upon glucose starvation (Souza et al., 2021). An operational fatty acid catabolism in *T. cruzi* epimastigotes, even in standard medium that contained glucose, was confirmed by our results. Furthermore, the accumulation of acylcarnitines observed in untargeted metabolomics suggested that waltherione G interfered with fatty acid catabolism downstream of CPT1, the enzyme that links fatty acids to carnitine, implicating mitochondrial acylcarnitine import or β -oxidation as potential targets (Figure 5). To further investigate fatty acid metabolism, the fate of U- $^{13}\text{C}_{16}$ -palmitate was traced after having depleted the parasite cells of nutrients and providing them only uniformly isotopically labelled palmitate as a C-source. The GC-MS data from extracted *T. cruzi* STIB980 cells showed that U- $^{13}\text{C}_{16}$ -palmitate was taken up and metabolised, as indicated by the

presence of isotopically labelled C atoms in citrate. This confirmed that β -oxidation and the TCA cycle are functional in these cells.

Epimastigote *T. cruzi* excrete acetate as the primary end-product when relying on fatty acids as a carbon source (Souza et al., 2021). The presence of a large fraction of unlabelled acetate in the medium fraction questions whether the U- $^{13}\text{C}_{16}$ -palmitate really was the only available C-source and indicates an internal reservoir of carbon sources. The presence of internal lipid storage, which is known for epimastigote *T. cruzi*, might be visualised using BODIPY staining and fluorescence imaging (Pereira et al., 2018). The glucose and triglyceride content of the medium could additionally be measured to ensure total glucose depletion (Souza et al., 2021).

ETO inhibits CPT1, which leads to a block of fatty acid uptake into the mitochondrion (Lopaschuk et al., 1988). The effect of ETO was apparent in the cellular fraction, where an accumulation of labelled palmitate was indicative of inhibition of CPT1. However, contrary to expectations, ETO treatment did not reduce the amount of ^{13}C incorporated into citrate (Figure 4B) or secreted acetate (Figure 4A). So either 500 μM ETO did not sufficiently block CPT1 activity, or there is an alternative, carnitine-independent pathway for β -oxidation. The glycosome might provide such an alternative path. In procyclic *T. brucei*, the glycosomal ABC (ATP-binding cassette) transporter 1 (GAT1) had been demonstrated to import long-chain fatty acids into the glycosome (Igoillo-Esteve et al., 2011). Enzymes involved in fatty acid catabolism were shown to be present in the *T. cruzi* glycosomal proteome (Quiñones et al., 2020)). What we can conclude at present is that ETO indeed inhibited CPT1, but that this did not impair the incorporation of C-atoms from palmitate into citrate and acetate. The reverse conclusion is that the observed lack of inhibition of the walteriones on ^{13}C incorporation into citrate and acetate does refute the hypothesis that the walteriones inhibit carnitine shuttling or β -oxidation.

The target of walteriones is connected with mitochondrial fatty acid metabolism, as indicated by the striking accumulation of acylcarnitines upon walterione treatment. What exactly kills the parasite remains to be elucidated. We confirm here that β -oxidation is functional in epimastigote *T. cruzi*. However, β -oxidation is unlikely to be essential when the parasites are grown in standard medium, and yet the walteriones are highly active also against epimastigotes (Figure 1). Acylcarnitines and fatty acids in excess are toxic to cells (Kerner and

Hoppel, 2000). Thus, either an inhibition and subsequent internal nutrient depletion or a toxic effect from accumulation of carnitine derivatives might be responsible for cell death.

The observed difference in the abundance of hypoxanthine and inosine in *T. cruzi* upon walterione exposure might be of interest as well. Like all trypanosomatids, *T. cruzi* cannot synthesise purines *de novo* and rely on purine salvage from their host to build nucleic acids (Berens et al., 1981). An accumulation of purine bases and nucleosides, but not nucleotides, could indicate a block in purine interconversion, e.g. affecting hypoxanthine/guanine phosphoribosyl-transferase (Glockzin et al., 2022). Purine salvage *per se* is essential for proliferation of the parasites (Berens et al., 1981). However, given the high degree of redundancy in trypanosomatid purine salvage pathways, no single enzyme is likely to be essential.

To conclude, untargeted exposure metabolomics consistently and most strikingly showed an accumulation of acylcarnitines in *T. cruzi* epimastigotes. Fatty acid uptake, β -oxidation, and the TCA cycle were functional in the epimastigote *T. cruzi* STIB980 independent of treatment. Thus, the walteriones are likely to interfere with mitochondrial fatty acid metabolism downstream of CPT1, highlighting the mitochondrion to be involved in the mechanism of action of walteriones.

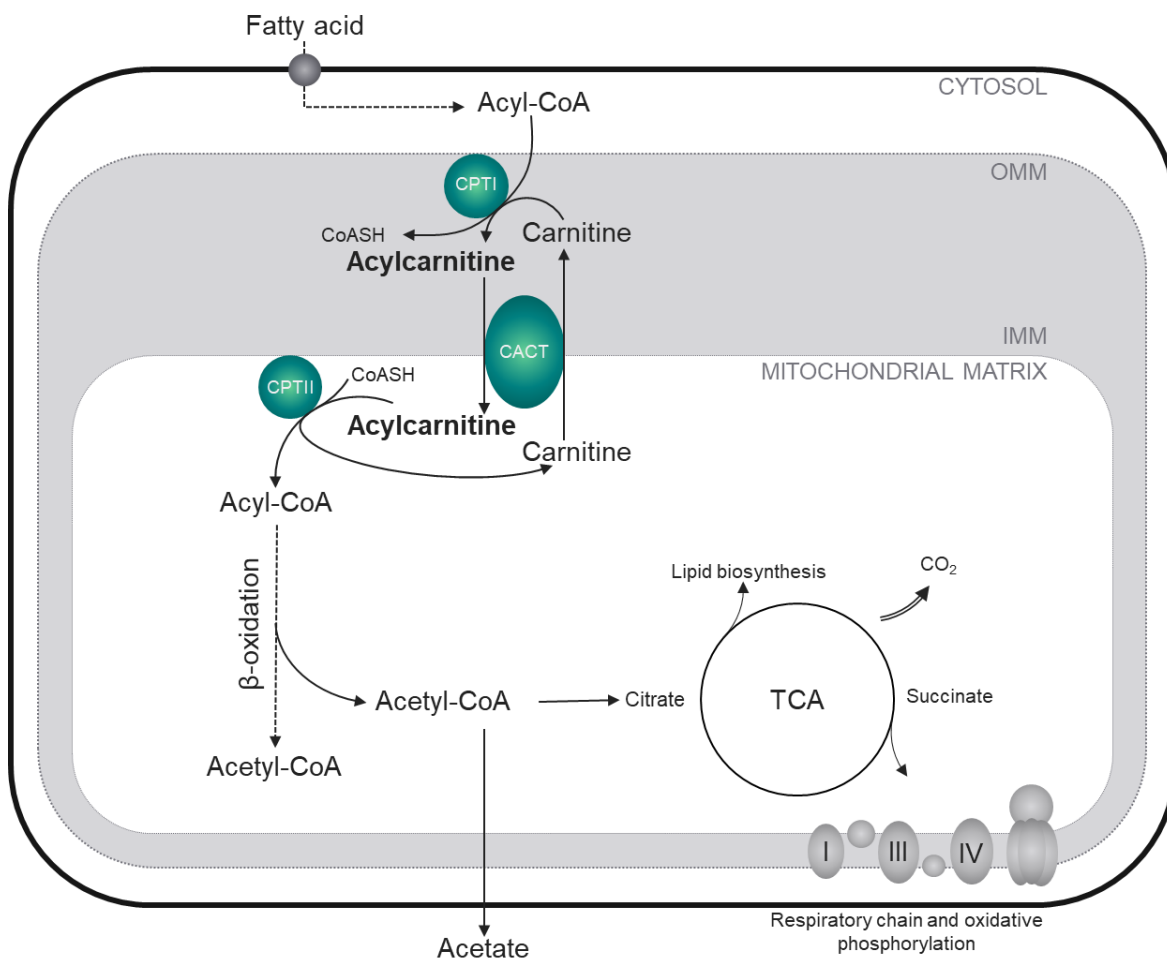


Figure 5. *T. cruzi* mitochondrion showing fatty acid shuttling and catabolism. TCA, tricarboxylic acid cycle; OMM, outer mitochondrial membrane; IMM, inner mitochondrial membrane; CoA, coenzyme A; CPTI, carnitine palmitoyltransferase 1; CPTII, carnitine palmitoyltransferase 2; CACT, carnitine-acylcarnitine translocase.

3.6 Acknowledgment

We are grateful to Monica Cal for performing drug sensitivity assays, to Marc Biran for performing NMR analysis and to Rodolpho Ornitz O. Souza giving input and advice on interpreting *T. cruzi* metabolism. This research was funded by the Swiss National Science Foundation, grant number CRSII5_183536.

3.7 Supplementary material

Supplementary Table 1. Experimental set up of untargeted exposure metabolomics analysis.

Sample	Treatment	Aim
10WG	Drug treated parasites	Drug effect
10WGnt	Non-treated, drug added after metabolic quenching	Immediate drug reaction
10D	DMSO treated parasites	General stress response
10Dnt	Non-treated, DMSO added after metabolic quenching	Negative control
m10WG	Medium fraction from 10WG samples	Drug effect
m10WGnt	Medium fraction from 10WGnt samples	Immediate reaction
m10D	Medium fraction from 10D samples	General stress response
m10Dnt	Medium fraction from 10Dnt samples	Negative control
Med	Fresh medium	Control
Sol	Extraction solvent	Control
QC	Quality control, pool of all extraction derived samples	Control
QC P	Quality control, pool of all pellet samples	Control
QC SN	Quality control, pool of all supernatant samples	Control

Supplementary Table 2. Experimental set up of U-¹³C₁₆-palmitate uptake and metabolism experiment.

Experiment 1	
condition	Treatment
PBS + BSA	
PBS + palmitate	
PBS + cells + BSA	
PBS + cells + palmitate	
PBS + cells + palmitate + ETO (500 μM)	ETO (500 μM)
PBS + cells + palmitate + WG (10× IC50)	WG (10× IC50)
PBS + cells + palmitate + WF (10× IC50)	WF (10× IC50)

Experiment 2/18 h preincubation of treatment	
condition	Treatment
PBS	
PBS + cells	
PBS + BSA	
PBS + palmitate	
PBS + cells + BSA	
PBS + cells + palmitate	
PBS + cells + palmitate + ETO (500 μM)	ETO (500 μM)
PBS + cells + palmitate + WG (10× IC50)	WG (10× IC50)
PBS + cells + palmitate + WF (10× IC50)	WF (10× IC50)

4 Resistance to walteriones and its effect in *Trypanosoma cruzi*

Sabina Beilstein^{1,2}, Monica Cal^{1,2}, Romina Rocchetti^{1,2}, Sonja Keller-Märki^{1,2},
Dennis Hauser^{1,2}, Marcel Kaiser^{1,2}, Pascal Mäser^{1,2}

¹ Swiss Tropical and Public Health Institute, 4123 Allschwil, Switzerland

² University of Basel, 4001 Basel, Switzerland

2023

Working manuscript

I have performed all experiments and analysis of drug sensitivity assays on epimastigote *T. cruzi*, isothermal microcalorimetry, drug resistance selection, and transcriptomics. Monica Cal, Romina Rocchetti, Sonja Keller-Märki, and Dennis Hauser performed drug sensitivity assays on all other protozoan parasites. I performed the time-lapse/washout assays with the assistance of Monica Cal and Marcel Kaiser. With the assistance of Prof. Dr. Pascal Mäser I performed phylogenetic analysis.

4.1 Abstract

Chagas disease is a neglected tropical disease caused by the parasite *Trypanosoma cruzi*. The treatment options of Chagas disease are limited to two drugs only, benznidazole and nifurtimox, which require long treatment and cause adverse effects. Finding alternative drugs that are safe and efficacious in all stages of the infection is key in fighting Chagas disease. The waltheriones are a group of natural compounds isolated from the plant *Waltheria indica*. These phytochemicals show exceptional activity and selectivity against *T. cruzi*. However, nothing is known on their mode of action. Here we combine isothermal microcalorimetry, drug resistance selection, and transcriptomics to investigate the mechanisms of drug resistance and drug action. *In vitro* drug resistance selection not only helps to inform about potential threats of resistance *in vivo* but is also a good starting point for target deconvolution. Moreover, this approach coupled to omics techniques has already been applied successfully in other protozoan parasites. This study aims at elucidating the mode of resistance and the mode of action of waltheriones. Our results indicate an effect on mitochondria, specifically on mitochondrial ribosomal proteins.

4.2 Introduction

Natural products still serve as an attractive starting point for drug discovery. The diversity of pharmacophores synthesised by plants is a vast source for potential drug candidates. One of the most successful examples in parasitology is quinine from the cinchona tree and the related quinolines in malaria treatment (Foley and Tilley, 1997, Schmidt et al., 2012). Phytochemicals have been optimised for their bioactivity during the evolution of the plant, be it for protection against herbivores or pathogens, making them highly attractive for drug discovery. In return, herbivores including humans have developed defence mechanisms against those phytochemicals during coevolution. This makes translation from *in vitro* to *in vivo* more complex (Schmidt et al., 2012).

Trypanosoma cruzi is the causative agent of Chagas disease, a neglected tropical disease that is autochthonous to Latin America and the southern United States but has spread globally due to travel and migration (Requena-Méndez et al., 2015, Bern and Montgomery, 2009). The disease progresses slowly, with an asymptomatic phase that can last for decades, but eventually produces life-threatening pathology, in particular of the heart and the digestive tract (Rassi et al., 2010). There is an urgent need for new and better drugs for the treatment of Chagas disease (Pérez-Molina et al., 2021). However, drug discovery for Chagas disease is hampered by the difficulty to work with *T. cruzi* in the laboratory. It is a biosafety level 3 organism in Europe and the replicative stages in the human host, the amastigotes, are strictly intracellular.

Target-based approaches have so far not yielded new drugs for *T. cruzi* (Chatelain, 2015), in spite of the fact that the parasite possesses many biochemical peculiarities as potential drug targets, such as the ergosterol synthesis pathway (Urbina and Docampo, 2003, Urbina et al., 1998), the glycosome, a peroxisome-like organelle found in trypanosomatids only (Dawidowski et al., 2017), or the mitoribosomes (Ramrath et al., 2018). Mitoribosomes were already suggested as promising drug targets in trypanosomatids because of their peculiar protein-based architecture differing from other eukaryotic cells (Ramrath et al., 2018). Posaconazole, which inhibits sterol 14 α -demethylase (CYP51), (Lepesheva et al., 2006) was one of the most promising drug candidates. However, it failed in clinical

trials due to relapse in the follow-up after treatment (Molina et al., 2014). This example underscores the importance for a compound to kill all the parasites.

The waltheriones are a group of natural quinoline alkaloids isolated from the plant *Waltheria indica* (Cretton et al., 2014). The waltheriones were tested against different protozoan parasites, including *Trypanosoma cruzi*, *Trypanosoma brucei*, *Leishmania donovani*, and *Plasmodium falciparum*. *T. cruzi* showed high sensitivity towards waltherione G and waltherione F with promising selectivity indices (Cretton et al., 2014) (Figure 1). It is exceptional that *T. cruzi* alone shows susceptibility in phenotypic drug screening against trypanosomatid parasites, where *T. brucei* is usually the most sensitive species (Mahmoud et al., 2020). This distinct activity pattern is intriguing as it points to targets that might be specific to *T. cruzi* and absent in *T. brucei*, or targets that are conserved between the two species but essential only in *T. cruzi*. As the waltheriones are a rather recent discovery, nothing is known about their mode of action and their target(s) in *T. cruzi*. Here we aim to identify potential targets of waltheriones and mechanisms of resistance by combining cellular and molecular approaches.

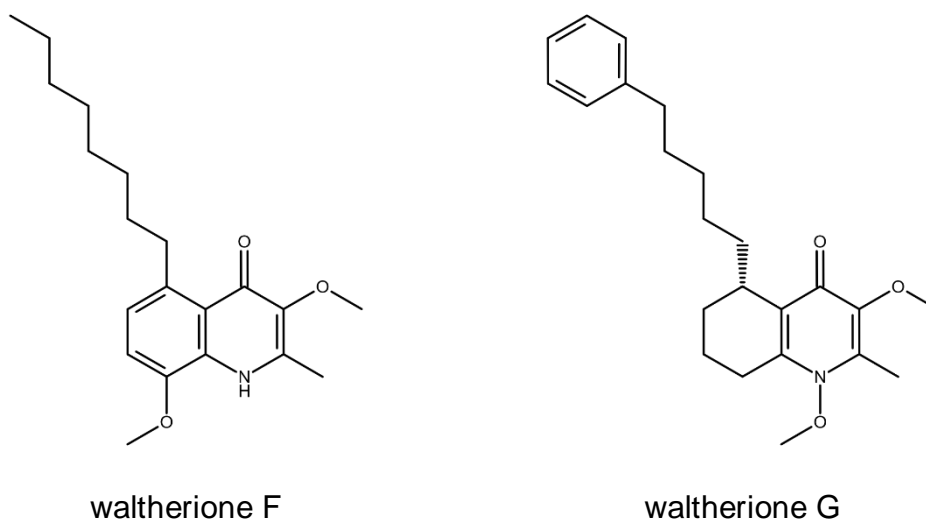


Figure 1. Chemical structures. Waltherione F and G show anti-parasitic activity.

4.3 Material and Methods

4.3.1 *T. cruzi* parasite strain and culturing

T. cruzi STIB980 clone 1 (DTU TcI) (Fesser et al., 2020) extracellular epimastigotes were maintained in liver infusion tryptose (LIT) medium supplemented with 10% inactivated fetal calf serum (iFCS) and 2 µg/mL hemin (complete LIT) at 27 °C (Fernandes and Castellani, 1966). The parasites were kept in exponential growth by diluting the culture once or twice a week.

The intracellular amastigote form was cultured in RPMI-1640 medium supplemented with 10% iFCS and 1.7 µM L-glutamine (complete RPMI medium) and kept at 37 °C and 5% CO₂ (Dumoulin and Burleigh, 2018). Microtus embryonic fibroblast (MEF) cells were used as host cells for infection with *T. cruzi*. Host cells were sub-cultured once a week in complete RPMI medium using 0.05% trypsin in 0.02% EDTA treatment to detach the cells from the culture flask. Freshly egressed trypomastigotes were passaged weekly onto an uninfected MEF culture.

4.3.2 Differentiation of the epimastigote culture to amastigote/trypomastigote culture

The extracellular epimastigote form of *T. cruzi* was differentiated to the trypomastigote and intracellular amastigote form. Parasites were cultured to a high density of about 10⁸ parasites per mL. About 0.5 mL of this dense culture, which already contained metacyclic trypomastigotes, was passaged onto freshly seeded MEF cells. The intracellular parasites were subsequently maintained as described above.

4.3.3 Epimastigote drug sensitivity testing

In vitro drug sensitivity on the extracellular epimastigote form of *T. cruzi* was tested in complete LIT medium. Stepwise 1:3 serial drug dilution were performed in a 96-well microtiter plate starting with 100 µg/mL for benznidazole and 10 µg/mL for walthersones F and G. Parasites were added at a concentration of 5×10⁶ per mL in complete LIT medium. After 69 h resazurin was added to a final concentration of 0.01 µg/mL (stock solution at 0.125 µg/mL in PBS). After a total assay duration of 72 h, the plate was read in a spectrofluorometer (SpectraMAX GEMINI EM Microplate, Molecular Devices, San Jose, CA). Fluorescence values at excitation

and emission wavelength of 536 and 588 nm, respectively, were recorded using SoftMax Pro Software (version 5.4.6.005). 50% inhibitory concentration (IC₅₀) values were calculated by nonlinear regression using GraphPad Prism (version 8.2.1).

4.3.4 Amastigote drug sensitivity testing

In vitro drug sensitivity of intracellular amastigotes was determined using the *T. cruzi* infected macrophage assay. 10,000 peritoneal mouse macrophages (PMM) in 100 µL complete RPMI medium per well were seeded into a 96-well microtiter plate (PS µClear, Chimney well Greiner Bio-One PN 655090). After 48 h incubation at 37 °C and 5% CO₂, the medium was replaced with 100 µL *T. cruzi* suspension to reach a macrophage to parasite ratio of 1:3. After 24 h, the supernatant was removed and the infected adherent cells were washed twice with 200 µL PBS before adding 100 µL of fresh complete RPMI medium. A 1:3 stepwise serial drug dilution was performed with a drug starting concentration of 100 µg/mL. The plates were incubated for 96 h before fixation with 10% formalin solution, and stained with a 5 µM DRAQ5™ (BioStatus, Leicestershire, UK) solution in PBS. Image acquisition was done with the high-content analyser Operetta® CLS™ (PerkinElmer, Waltham MA, USA) and analysis was performed with the corresponding Harmony™ software (version 4.9). IC₅₀ values were calculated by nonlinear regression using GraphPad Prism (version 8.2.1).

4.3.5 Amastigote time-laps/washout assay with *T. cruzi* STIB980-LucNeonGreen

To assess the time-to-kill of a given compound and to monitor eventual recrudescence of the parasites, an assay using PMM as host cells was designed. 10,000 PMM per well were seeded into a 96-well microtiter plate (PS µClear, Chimney well Greiner Bio-One PN 655090) in complete RPMI medium. After 48 h of incubation at 37 °C and 5% CO₂, the PMM were infected with fluorescent trypomastigote *T. cruzi* STIB980 reporter line LucNeonGreen. STIB980 was transfected with the plasmid pTRIX2-Luc::Neon-HYG providing the red shifted luciferase and green fluorescent protein domains according to the protocol previously published (Costa et al., 2018, Fesser et al., 2020) in a ratio of 1:3. After 72 h, a washing step with 200 µL complete RPMI medium was done and the plate

was imaged with the high-content analyser Operetta® CLS™ (PerkinElmer, Waltham MA, USA) for mNeonGreen (emission and excitation at 460-490 and 500-550 nm, respectively). Drugs were then added in a stepwise 1:3 serial dilution with a starting concentration of 100 µg/mL prepared on a separate 96-well plate. After 24, 48, 72, and 96 h drug incubation the plates were imaged again. After the last imaging, the wells were washed twice with 200 µL complete RPMI medium, 100 µL complete RPMI medium were added, and the plate was imaged again (100 h). Further image acquisition of the plates followed after 168, 264, 360, and 432 h. The plate was fixed after the last image acquisition with 10% formalin, stained with 5 µM DRAQ5™, and imaged again with the high-content analyser Operetta® CLS™ (PerkinElmer, Waltham MA, USA) for EGFP and DRAQ5™ (emission and excitation at 615-645 and 655-760 nm, respectively).

4.3.6 Isothermal microcalorimetry with epimastigote *T. cruzi*

Isothermal microcalorimetry was performed to monitor drug action in real time. Extracellular epimastigote *T. cruzi* parasites in exponential growth were diluted in complete LIT medium to a density of 5×10^5 parasites per mL. Each ampoule was prepared with 2 mL of parasite culture and supplemented with waltherrone F or G in concentrations of 3x, 10x, or 30x IC₅₀. Waltherrone G was also tested at 100x IC₅₀. The positive controls were untreated parasites and parasites treated with 0.15% (v/v) DMSO, the negative control was complete LIT medium. Over a period of 6 to 8 weeks, the heat flow was measured at 27 °C in a TAM III isothermal microcalorimeter (thermal activity monitor, model 249; TA instruments, New Castle DE, USA). Data acquisition was done with the TAM Assistant software (version 2.0.175.1) and data analysis was performed in Microsoft Excel (version 16.0) and R (version 4.1.3).

4.3.7 Drug resistance selection with epimastigote *T. cruzi*

Extracellular epimastigote *T. cruzi* STIB980 cultured in the exponential growth phase of about 5×10^7 parasites per mL were diluted to a density of 10^7 parasites per mL in 10 mL complete LIT medium and supplemented with 10x IC₅₀ of waltherrone F or G. As a control, the parental cell line was cultured in parallel without drug but with normal regular sub-culturing. The culture was kept in a non-vented 75 cm² Sarstedt® Tissue Culture Flasks at 27 °C. After 10, 20, and 30 d, 1 mL fresh

medium supplemented with the respective drug concentration was added to the culture to prevent death by nutrient shortage. Parasites were regularly monitored for their viability. After 40 d, there were still very few parasites alive. 1 mL of the culture was transferred to 4 mL fresh LIT medium without drug. After about 10 d, the culture had recovered to usual growth. Epimastigote drug sensitivity testing was performed to check for a shift in the IC₅₀. Cryopreservation in LIT medium containing 0.08% DMSO (v/v) was done from the recovered cultures.

4.3.8 Cloning of epimastigote *T. cruzi*

Cloning was done with the gilded paperclip method already used for *T. brucei* (Wiedemar et al., 2018). In a 96-well plate, 15 µL of standard LIT medium were given to one side of the well. A parasite suspension of 10⁵ parasites per mL was prepared. With a gilded paperclip a micro-drop of this cell suspension was placed next to the medium droplet and inspected under an inverted microscope to confirm the presence of a single parasite in one droplet. 35 µL medium were supplemented to the wells. After 3 days 50 µL medium were added to ensure that the wells did not dry out. The wells were regularly checked for parasite growth. After one week, 200 µL medium were added to the wells with growing clonal culture before transferring them to the standard culture procedure as described earlier.

4.3.9 RNA isolation, mRNA-sequencing and comparative transcriptomics analysis

10⁷ parasites were centrifuged and washed once with PBS. Total RNA was isolated using the QIAGEN RNeasy® Mini Kit including an on-column DNA digestion with the QIAGEN RNase-Free DNase Set. RNA was stored at -80 °C after quick-freezing in liquid nitrogen. 1 µg of RNA from the three independently cultivated cultures per strain was used for library preparation with the Illumina Truseq Stranded mRNA kit. Single-end sequencing of 120 nucleotides was done on an Illumina NovaSeq 6000 (Illumina San Diego, USA). All data analysis performed on sciCORE (<http://scicore.unibas.ch/>), the scientific computing centre at University of Basel as described (Hitz et al., 2021, Wiedemar et al., 2018). Sequencing read quality control was performed with FastQC (version 0.11.9) (Babraham Bioinformatics, 2022). The reads were mapped to the genome of *T. cruzi* Dm28c 2018 (version TriTrypDB-57) using Burrows-Wheeler Aligner (version 0.7.17) with the default parameters (Li and

Durbin, 2009). Samtools (version 1.15) was used to convert the alignment files from the SAM format to binary files in BAM format (Li and Durbin, 2009). The binary files were coordinate-sorted and read groups were added with Picard tools (version 2.26.10) (Broad Institute, 2022). The Genome Analysis Toolkit's (GATK, version 4.2.6.1) HaplotypeCaller in GVCF mode with a minimal mapping quality of 10 was used for variant calling (McKenna et al., 2010). GATK was then used to combine the g.vcf files and for subsequent genotyping (McKenna et al., 2010). For variant annotation, SnpEff (version 5.0e) was used after manually supplementing the SnpEff database with the genome of Dm28c 2018 (version TriTrypDB-57) (Cingolani et al., 2012). Read counts per transcript were determined using the Python package HTSeq (version 0.11.2) (Anders et al., 2015) and raw counts were analysed with the R package DESeq2 with independent filtering disabled (version 1.30.18) (Love et al., 2014).

4.3.10 DNA isolation, PCR amplification, and confirmation of candidate variants

Epimastigotes or trypomastigotes from *T. cruzi* STIB980_wt, STIB980_ctr, and STIB980_WF were cultured to reach the exponential phase. 10^7 parasites were collected by centrifugation. Genomic DNA was isolated using the QIAGEN DNeasy Blood & Tissue Kit. 1-2 μ g of isolated DNA was used to PCR amplify the genes of interest. PCR was performed with Taq polymerase (New England Biolabs, Ipswich MA, USA) and forward and reverse primers designed 300 base pairs adjacent to the suspected mutation (Supplementary Table 1). PCR amplified fragments were Sanger sequenced (Microsynth AG, Switzerland) to confirm the presence on the genomic level of the variants identified in the transcriptomics analysis.

4.3.11 Phylogeny of the mitochondrial small subunit ribosomal protein

Blastp searches were performed on-line at NCBI, and sequences downloaded in fasta format. Multiple alignments performed with Muscle and phylogenetic trees were calculated with the MegaX software (version 10.0.5), using the neighbour joining algorithm and bootstrap resampling of 1000 times. The non-parasitic kinetoplastid *Bodo saltans* served as an outgroup species.

4.4 Results

4.4.1 Waltherione G and F show activity on different protozoa depending on the parasite stage

Waltherione G and F are both highly active against *T. cruzi*, on both the extracellular epimastigote form as well as the intracellular and disease-relevant amastigote form. Investigating drug sensitivity and testing the compounds against different stages of other protozoan parasites revealed specific sensitivity profiles. As shown in Table 1, both waltheriones were active against the procyclic form but not against the bloodstream form of *T. brucei rhodesiense*. In *L. donovani*, WG was again active against the procyclic and axenic amastigote form. However, when tested against the intracellular amastigote form cultured in peritoneal mouse macrophages, the obtained IC₅₀ value was 10-times higher and the selectivity over mammalian cells was lost. Neither of the waltheriones was active against *P. falciparum*. A selectivity index value above 80 calculated for the intracellular *T. cruzi* is very high and makes waltheriones promising compounds to further investigate.

Table 1. *In vitro* sensitivity of protozoans to walthेरiones and standard drugs. The 50% inhibitory concentration (IC₅₀) is shown in $\mu\text{M} \pm$ standard deviation ($n \geq 3$). Bsf, blood stream form; proc., procyclic form; intracel. amast., intracellular amastigote; extrac. epimast., extracellular epimastigote; ax. amast., axenic amastigote; in macr., in macrophages; promast., promastigote; *T. b. rhod.*, *Trypanosoma brucei rhodesiense*; *T. cruzi*, *Trypanosoma cruzi*; *L. don.*, *Leishmania donovani*; *P. falc.*, *Plasmodium falciparum*; Cytotox. L6, mammalian cytotoxicity on rat skeletal myoblasts; SI, selectivity index = IC₅₀ cytotoxicity/IC₅₀ *T. cruzi* intracellular amastigote activity. Values given for *T. cruzi* and Cytotoxicity were previously reported (Chapter 3).

	<i>T. cruzi</i>		<i>T. b. rhod.</i>			<i>L. don.</i>			<i>P. falc.</i>	Cytotox.	SI <i>T. cruzi</i>
	intracel. amast.	extrac. epimast.	bsf	proc.	ax. amast.	in macr.	promast.		L6		
Walthेरione F	0.48 \pm 0.45	0.27 \pm 0.13	40.7 \pm 4.3	5.14 \pm 3.2	1.42 \pm 1.1	10.2 \pm 4.7	1.30 \pm 0.15	14.4 \pm 0.9	39.4 \pm 34.2	82	
Walthेरione G	0.11 \pm 0.10	0.10 \pm 0.03	26.9 \pm 13.3	0.58 \pm 0.30	1.40 \pm 0.91	15.1 \pm 5.5	1.10 \pm 0.12	11.2 \pm 2.6	26.34 \pm 22.6	231	
Benznidazole	2.82 \pm 0.96	4.78 \pm 0.99									
Melarsoprol			0.009 \pm 0.005	0.117 \pm 0.013							
Miltefosine					0.86 \pm 0.24	3.13 \pm 0.72	3.51 \pm 0.52				
Chloroquine								0.005 \pm 0.002			
Podophyllotoxin									0.015 \pm 0.002		

4.4.2 First attempts to select for walterione resistance were unsuccessful

Drug resistance selection of epimastigote and amastigote *T. cruzi* STIB980 was attempted using different approaches listed in the following: i) a constant subcurative dose was applied to epimastigote and amastigote *T. cruzi* over a long period of time and sub-culturing whenever the culture reached high enough density, ii) a single but high drug dose was applied to epimastigote *T. cruzi* repeatedly for 48 h followed by a washing step and recovery phase until sub-culturing was possible, iii) a single but constant high drug dose was applied to epimastigote *T. cruzi* just once with subsequent monitoring for surviving and viable parasites. Selecting parasites at a subcurative dose over several months did not result in resistance to walterione F and G. Even a very high dosage of $10\times IC_{50}$ on 10^6 parasites per mL in 10 mL did not lead to resistant parasites after four weeks of incubation. From these results we concluded that (i) the walteriones are not prone to drug resistance, underscoring their potential as novel antichagasic agents; and (ii) that a more rational approach is needed for the selection of drug-resistant *T. cruzi* mutants. For this purpose, we monitored the *in vitro* pharmacodynamics of the walteriones against epimastigote trypanosomes.

4.4.3 Isothermal microcalorimetry shows decelerated and diminished growth

Isothermal microcalorimetry can be used to monitor cell growth by measuring the heat produced by the cells' metabolism (Wenzler et al., 2012). This method was used to observe drug action and potential emerging resistance in African trypanosomes (Gysin et al., 2018, Wenzler et al., 2012, Wiedemar et al., 2018). It cannot be used for intracellular pathogens though, due to the heat produced by the host cell. However, the fact that the walteriones are active not only against intracellular amastigote *T. cruzi* but also against extracellular epimastigotes, meant that the latter can be used as a model for the former, disease-relevant form. In pilot experiments, the suitable parasite starting density was assessed to be 5×10^5 epimastigote *T. cruzi* per mL. Independent of the concentration, the onset of action of the walteriones was extremely fast, as apparent from the divergent heat flow right from the beginning (Figure 2). The action itself, however, was rather slow. The curves of the treated samples were shifted towards the right indicating a delayed

growth. The overall heat flow of the samples treated with concentrations above 3× IC₅₀ was reduced compared to the untreated control. Treatment with 30× IC₅₀ waltherrone F or 100× IC₅₀ waltherrone G was necessary to completely abolish growth. Treatments with 10× IC₅₀ waltherrone F and 30× IC₅₀ waltherrone G still enabled growth, though decelerated and diminished. This observation formed the basis for setting the conditions for drug resistance selection.

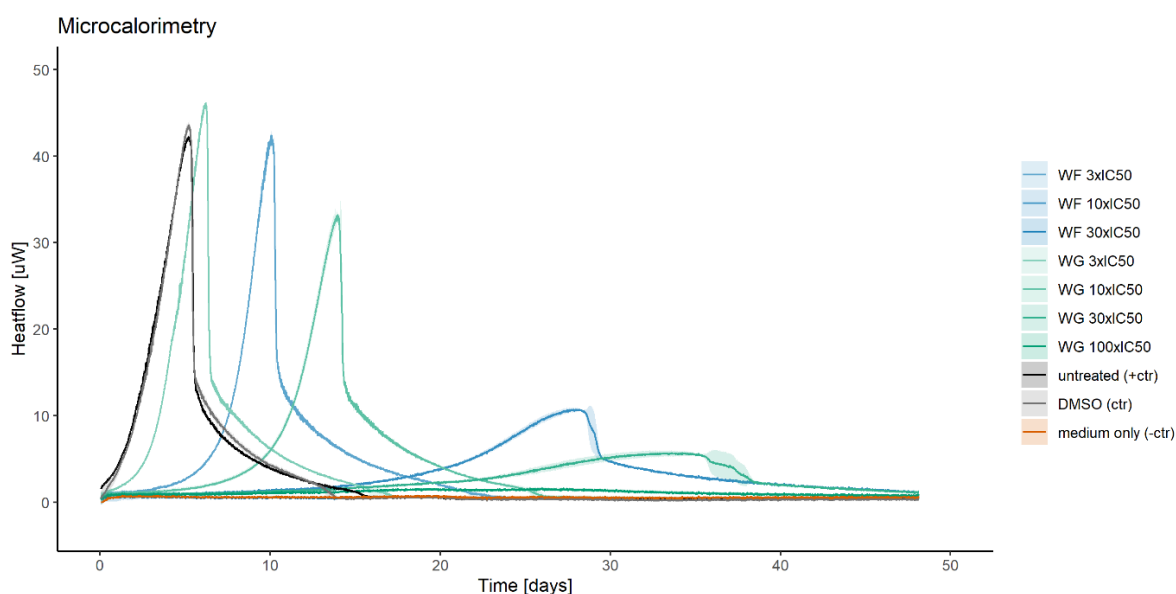


Figure 2. Isothermal micro-calorimetry with *T. cruzi* STIB980. The curves show the mean (line) and standard deviation (coloured band) of three technical replicates. The heat flow in μW produced by the parasites is displayed against time. Colours refer to the different drugs and drug concentration imposed on the *T. cruzi* STIB980. In a pilot experiment, 30-fold the IC₅₀ of waltherrone G was not sufficient to kill all parasites. Therefore, a fourth concentration of 100-fold the IC₅₀ was included for waltherrone G. The positive control included parasites in standard medium, the negative control only included standard medium without parasites and the DMSO control included the highest used drug solvent concentration of 0.15% DMSO, which is much below the toxic limit of 1%.

4.4.4 *T. cruzi* recovers from a high dose of waltherrone treatment

The amastigote time-laps/washout assay newly designed in our laboratory based on previous work from Anna Fesser (Fesser et al., 2020) measures pharmacodynamics parameters, including the concentration-dependent time-to-kill, the drug concentration reaching total kill, the number of parasites and viability over

time, and eventual re-growth after drug washout at 96 h, revealing potential reversibility (Figure 3). Benznidazole and posaconazole were included as reference compounds. For benznidazole, the number of parasites dropped to 100 in the first 48 h and stayed around 100 after washout at a drug concentration of $>40 \mu\text{M}$. For posaconazole, the number of parasites took much longer to drop below 100 and only remained below 100 after washout for treatments with the highest drug concentration of $>0.14 \mu\text{M}$. For waltherione F and G the number of parasites quickly dropped much below 100 in the first 24 h at high drug concentration of $>100 \mu\text{M}$ and $>200 \mu\text{M}$, respectively. However, regrowth after washout was observed even at the highest concentration of 302 and 271 μM , respectively. For all tested compounds, the dose-response-curve measured over the different time points remained very flat in the first 24 hours. Optimal dose-response curves for WF and WG appeared later at 96 hours. A minimum of 72 h were required for waltherione activity.

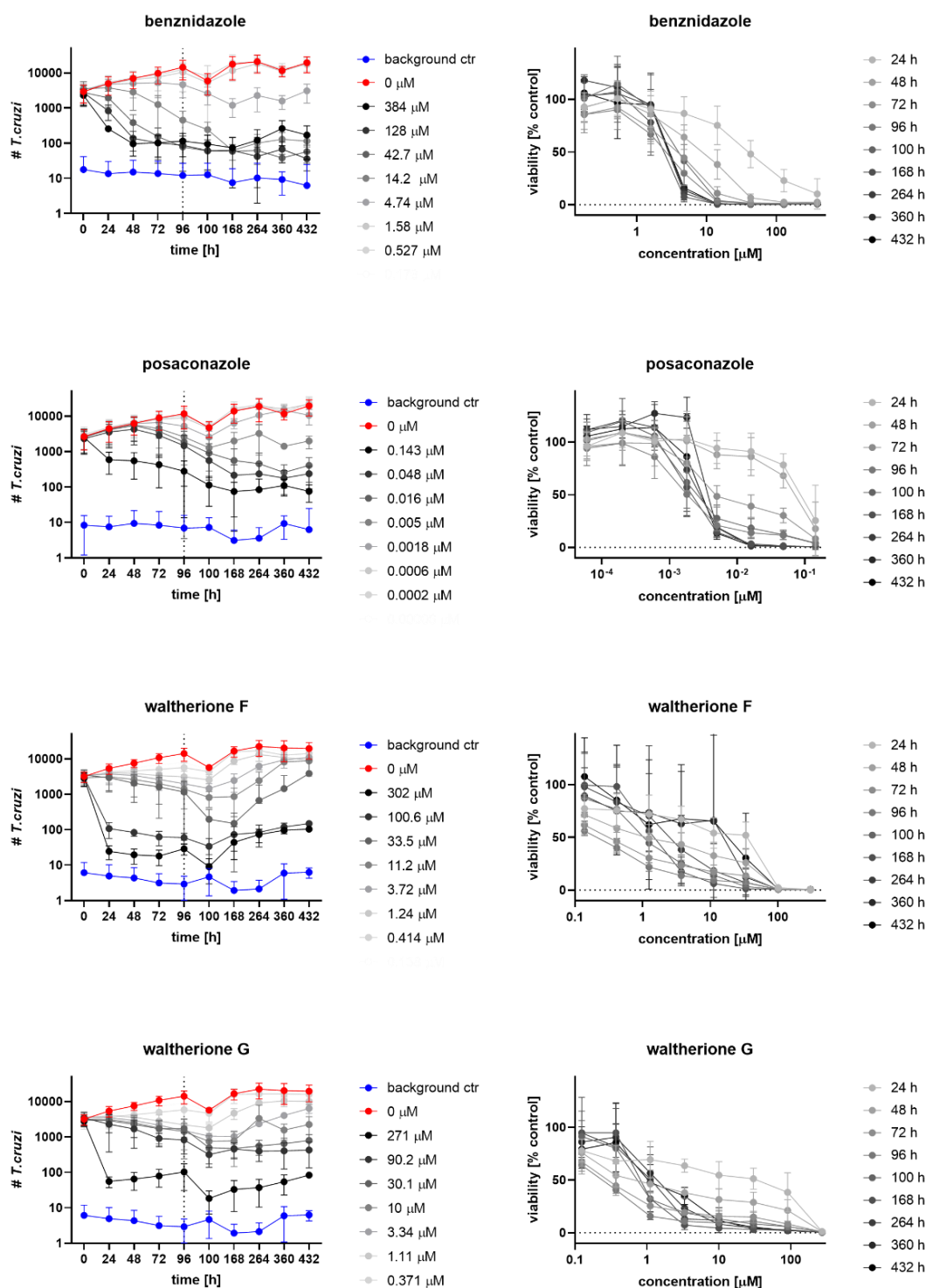


Figure 3. Amastigote time-laps/wash out assay. Time and concentration dependent representation of the same experiment ($n=4$). Number of amastigote *T. cruzi* detected by fluorescence over time shown on the left. Each curve shows one drug concentration. Background ctr represents the control of false positive *T. cruzi* detected in uninfected PMM (negative control). The dotted line at 96 h corresponds to the time point of washout. Dose-response curves shown on the right at different time points of the assay expressed by the viability in percentage of the normal amastigote growth (positive control).

4.4.5 *T. cruzi* selected with waltherione F are resistant towards waltheriones

Based on the findings above, we optimised the selection protocol as follows. Epimastigote *T. cruzi* STIB980 were continuously kept at a high density of 10^7 parasites in 10 mL medium and a high drug pressure of $10\times IC_{50}$, regularly providing 1 mL fresh medium with $10\times IC_{50}$ of drug. In the case of waltherione F, this led to the emergence of drug-resistant parasites after 40 days of selection (Figure 4A and B); no resistant parasites were obtained with waltherione G. The waltherione F selected epimastigote *T. cruzi* showed a significant increase in IC_{50} (adjusted p-value <0.0001 by One Way ANOVA with Tukey's multiple comparisons test) compared to the STIB980 wildtype. Not only did they become more than 10-fold resistant to the drug used for selection, but also more than 10-fold cross-resistant to waltherione G (adjusted p-value <0.0001 by One Way ANOVA with Tukey's multiple comparisons test) (Table 2). The obtained resistance was stable. Culturing the waltherione F selected and resistant epimastigote *T. cruzi* over one month in the absence of drug did not affect the resistance level (Figure 5).

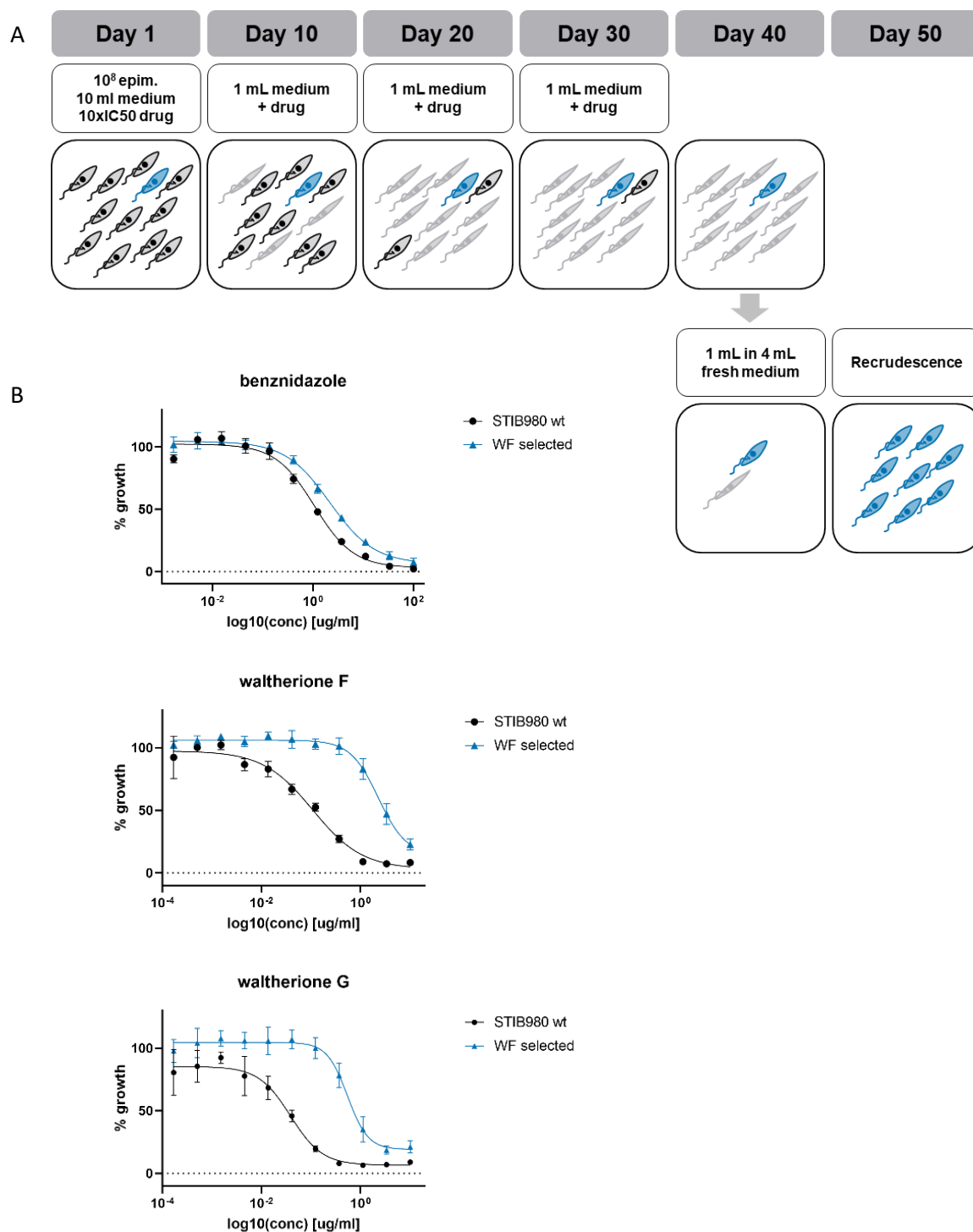


Figure 4. Drug resistance selection. (A) A total amount of 10⁸ epimastigote *T. cruzi* were kept in 10 mL medium under constant and high drug pressure with waltherione F or G at a concentration of 10× IC₅₀. Every ten days the parasites were supplied with a tenth of the original volume of fresh medium supplemented with the starting drug concentration to prevent death caused by starvation. (B) Dose-response curve of wildtype *T. cruzi* and *T. cruzi* selected with waltherione F (WF selected).

Table 2. Waltheronone F drug resistance selection. Epimastigote drug sensitivity of the parental STIB980_wt strain, the STIB980_ctr strain co-cultured as control, and the waltheronone F selected (WF selected) strain. The 50% inhibitory concentration is shown in $\mu\text{M} \pm$ standard deviation ($n \geq 3$). The WF selected strain is 20.7 times more resistant towards waltheronone F and 13.5 times more cross-resistant towards waltheronone G compared to the STIB980_wt.

	STIB980_wt		STIB980_ctr		WF selected	
Benznidazole	4.07	± 0.19	7.72	± 0.23	8.38	± 0.88
WF	0.33	± 0.09	0.63	± 0.18	6.89	± 1.02
WG	0.11	± 0.03	0.19	± 0.03	1.49	± 0.16

Stability of WF resistance over time

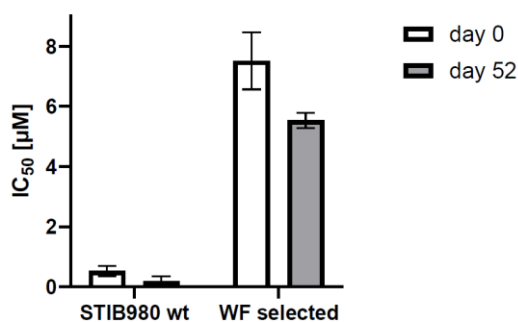


Figure 5. Stability of waltheronone F resistance over time. Between the first and the last drug sensitivity assay parasites were cultured for more than 50 d without any drug pressure. The 50% inhibitory concentration (IC_{50}) is shown in $\mu\text{M} \pm$ standard deviation ($n=3$). The parasites maintain more than 10-fold resistance compared to the wildtype which was assayed at the same time.

4.4.6 Transcriptomics reveals a single point mutation in the mitochondrial small subunit ribosomal protein

Transcriptomics was chosen as a preferred tool to investigate the molecular changes underlying the observed phenotype of waltheronone-resistance. It has the advantage to reveal qualitative mutations in coding regions and quantitative mutations in gene expression at the same time. Epimastigotes were grown in three independent cultures per cell line: parental STIB980 wildtype baseline control (STIB980_wt), STIB980 wildtype growth control (STIB980_ctr), which was cultured in parallel of the drug resistance selection but without drug, and the STIB980 waltheronone F selected (STIB980_WF) parasites. Resistant and sensitive parasites

were cultured for 10 to 15 days to reach the exponential phase. Total RNA was isolated and transcriptomics analysis was performed as described under methods.

Differential gene expression analysis did not show any significant change of any gene (Figure 6). The slightly outlying gene downregulated in the STIB980_WF compared to STIB980_ctr was the alpha-tubulin gene, C4B63_222g21. Very high expression in the co-cultured control sample but not in the baseline STIB980_wt and the WF-resistant samples points to an expression difference unrelated to the drug resistance phenotype. Mapping the reads from the two controls and the WF selected samples to the reference sequence of *T. cruzi* Dm28c 2018 yielded a total of 19,320 variants. These were filtered for i) variants showing a homozygous genotype towards the reference sequence in all the STIB980_wt and STIB980_ctr samples but a heterozygous or homozygous alternative genotype in STIB980_WF; ii) the impact “HIGH” and “MODERATE”, thus excluding synonymous variants. The filtering reduced the list to 13 candidate variants of single point mutations, which were manually inspected in the Integrative Genomics Viewer (version 2.5.0) (Thorvaldsdóttir et al., 2013). Variants in regions of low coverage, or having variants in the sensitive parental and control samples with low allele frequency, were counted as false positives and excluded. This revealed three non-synonymous single nucleotide mutations and one synonymous single nucleotide mutation which were unique to *T. cruzi* STIB980_WF (Table 3). Two of the non-synonymous mutations were present in more than 50% of the reads. The third non-synonymous mutation was present in only 9-25% of the reads which was confirmed with Sanger sequencing (Supplementary Figure 1). Therefore, the latter and the synonymous mutation were excluded from further analysis. The most promising mutation was a C to T transition at position 370 of the protein-coding sequence of the C4B63_2g442 gene, annotated in Dm28c 2018 as a mitochondrial small subunit protein, causing an amino acid substitution from proline to leucine. The other promising mutation was a G to A transition at position 459 of the protein coding sequence of the C4B63_52g56 gene, annotated in Dm28c 2018 as a conserved hypothetical protein, substituting tryptophan with a stop codon instead.

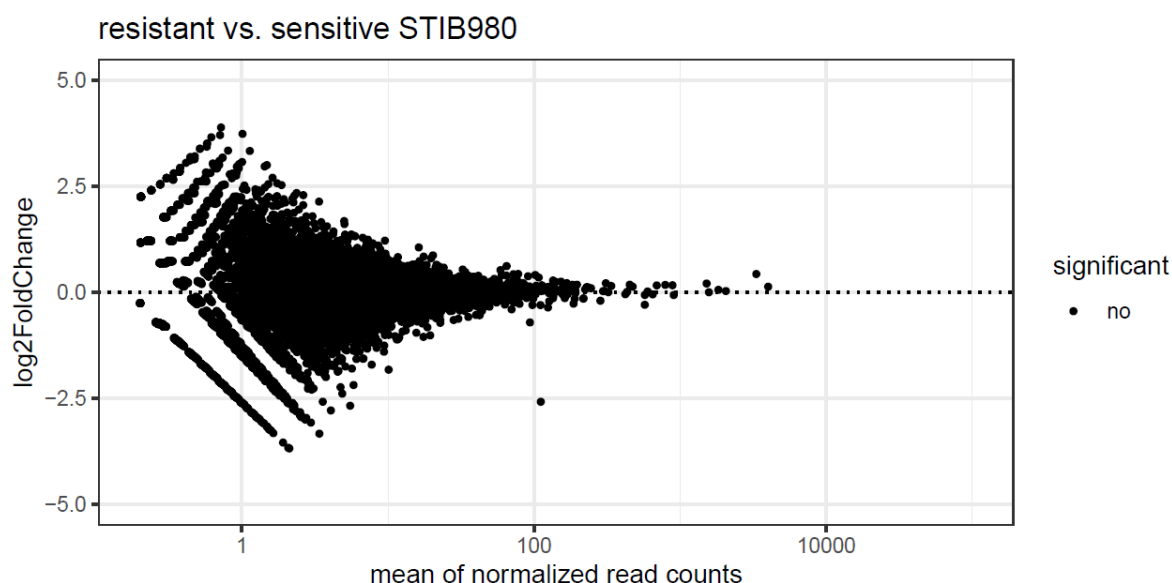


Figure 6. Differential gene expression. Analysis of waltherione F-resistant *T. cruzi* versus susceptible wildtype *T. cruzi* with DESeq2. The x-axis shows the mean of normalised read counts for all samples in the dataset giving the transcript abundance. The y-axis displays the logarithmic fold-change of transcript abundance. Included in the analysis were three resistant samples, three parent samples, and the control samples cultured in parallel. Overexpressed or underexpressed genes with a significantly different fold change would appear in a different colour. The outlier with a -2.5-fold change and a mean normalised read count of 100 corresponds to the alpha tubulin gene C4B63_222g21.

Table 3. Candidate resistance mutations. SNPs identified in the STIB980_WF samples during transcriptomic analysis. REF, reference allele; ALT, alternative allele; CHROME, chromosome; POS, position.

GENE ID	GENE	REF	ALT	MUTATION	CHROM	POS	COMMENT
C4B63_2g442	Mitochondrial small subunit ribosomal protein	C	T	Pro370Leu	PRFA01000002	1125697	53-56% reads contain SNP
C4B63_52g56	conserved hypothetical protein	G	A	Trp459*	PRFA01000052	205986	45-53% reads contain SNP
C4B63_4g435	protein kinase	G	A	Val to Val	PRFA01000004	321851	50-57% reads contain SNP
C4B63_16g95	conserved hypothetical protein	G	A	Arg22Gln	PRFA01000016	291927	9-25% reads contain SNP

4.4.7 Waltherione F-resistant epimastigote can be differentiated to amastigote *T. cruzi* without losing resistance and by keeping the candidate resistance mutation

T. cruzi STIB980 wildtype and three clones of STIB980_WF were differentiated from the epimastigote to the amastigote form, and subsequently tested for their drug sensitivity. Differentiating the WF-resistant parasites did not significantly affect their resistance to waltherione F (Table 4). The IC₅₀ value remained more than 4-fold higher than that of the STIB980 wildtype. The parasites also retained the cross-resistance to WG, however, it was not as pronounced as in the epimastigote form. Genomic DNA was isolated to perform Sanger sequencing on the PCR-amplified gene, C4B63_2g442. The mutations identified in the epimastigote WF-resistant *T. cruzi* were still present after differentiation to the amastigote form, with around 50% of the sequences showing the alternative base pair, indicating a heterozygous mutation (Supplementary Figure 2).

Table 4. Differentiation of resistant epimastigote to amastigote *T. cruzi*. The waltherione F selected and resistant *T. cruzi* epimastigotes were differentiated into the intracellular amastigote form. The 50% inhibitory concentration is shown in $\mu\text{M} \pm$ standard deviation (n=3). The parasites maintain a 4.2- to 5.0-fold resistance compared to the susceptible STIB980_wt. The cross-resistance to waltherione G is 2.3- to 2.7-fold compared to the susceptible STIB980_wt.

	STIB980_wt	STIB980_WF_ clone_14F	STIB980_WF_ clone_2E3	STIB980_WF_ clone_2G5
Benznidazole	5.65 \pm 0.42	4.96 \pm 0.88	5.26 \pm 0.92	5.07 \pm 0.35
WF	1.93 \pm 0.09	9.63 \pm 2.41	9.00 \pm 0.90	8.10 \pm 1.57
WG	0.76 \pm 0.08	1.76 \pm 0.43	2.00 \pm 0.27	1.84 \pm 0.30

4.4.8 The mitochondrial ribosomal small subunit protein is very conserved in the family of trypanosomatidae

We performed a phylogenetic analysis of the gene carrying one of the most promising candidate mutations, the mitochondrial small subunit ribosomal protein. As a first step, a search library was built manually. The mitochondrial small subunit ribosomal protein from *T. cruzi* (Trytryp Gene ID in Dm28c 2018: C4B63_2g442) was used as the starting sequence. A blastp search was performed against the non-redundant protein database from the NCBI. 88 hits were found in the class of kinetoplastea, of which 86 belonged to the trypanosomatidae. No hit outside the class of kinetoplastae was found. 18 sequences were selected based on their low

expectancy E-value and high percentage of coverage of the alignment. A neighbour-joining phylogenetic tree was constructed, which clearly showed the close relationship of *T. cruzi* to the non-pathogenic *Trypanosoma rangeli* and *T. brucei*, all in the same clade (Figure 7A and B). The overall mean distance of the phylogenetic tree was $p=0.42$. The multiple sequence alignment revealed that the proline to leucine mutation took place in a highly conserved region.

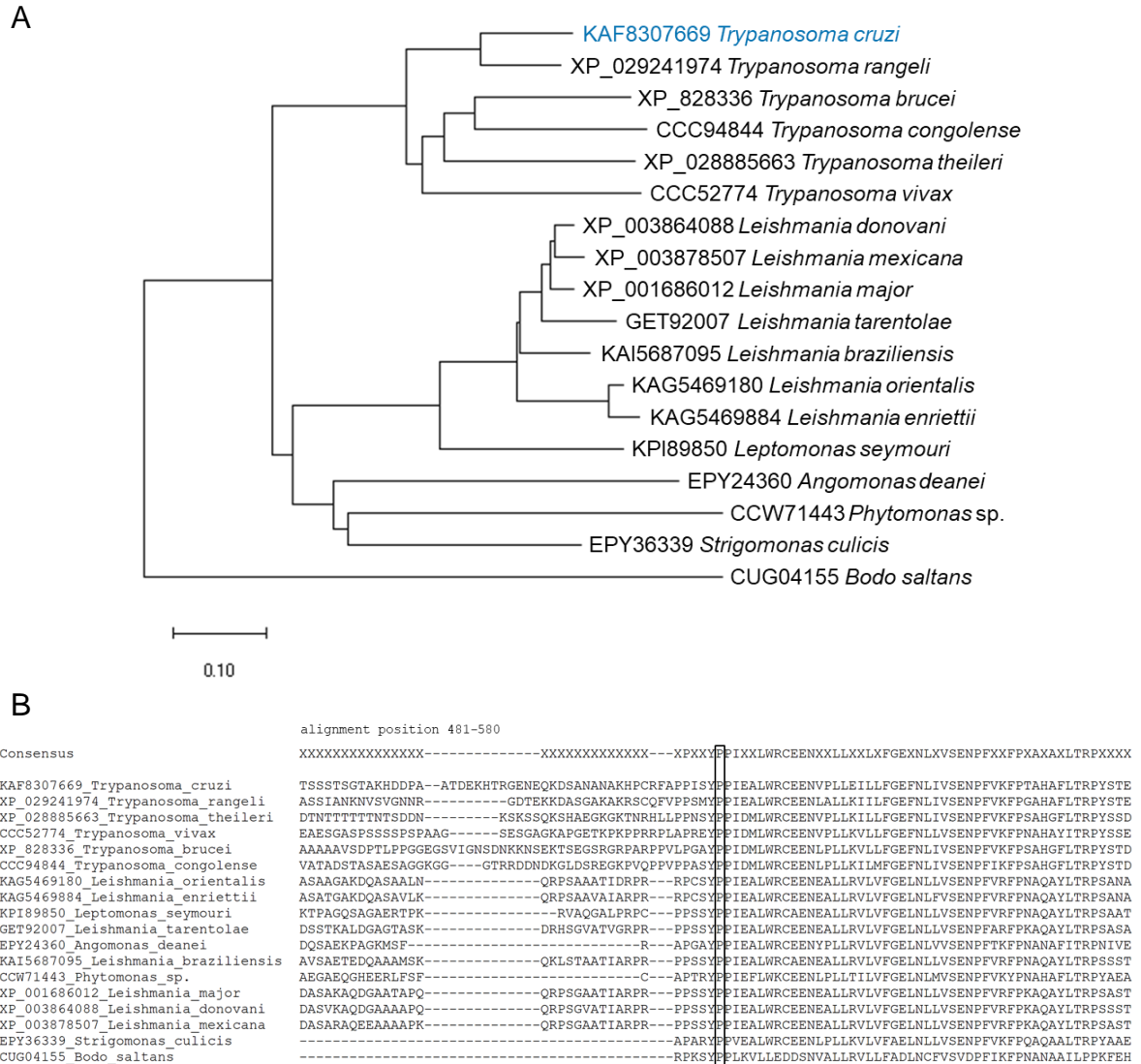


Figure 7. Phylogeny of the mitochondrial small subunit ribosomal protein in the class of kinetoplastida. (A) Phylogenetic tree built with the neighbour-joining method using *Bodo saltans* as outgroup. (B) Muscle alignment of the protein in different kinetoplastida. The region where the mutation in the transcriptome was observed appears to be conserved in amino acid sequence throughout this group of protozoans.

4.5 Discussion

Waltherione F and waltherione G are promising antichagasic molecules because of their high activity against *T. cruzi* and low toxicity towards mammalian cells. However, their mode of action remained completely obscure. The waltheriones are about 100-fold less active against *T. brucei* bloodstream forms than against *T. cruzi* amastigotes, which is unusual as the extracellular *T. brucei* are generally more sensitive than the intracellular *T. cruzi*. However, the procyclic, tsetse fly midgut-stage of *T. brucei* is more susceptible to waltheriones. This, again, is unusual since for reference drugs such as melarsoprol, the bloodstream forms are the more susceptible. The higher susceptibility of procyclic forms indicates the mitochondrion as a potential site of action, because the main metabolic difference between procyclic and bloodstream-form *T. brucei* is the active mitochondrion in the former. In *T. cruzi*, the waltheriones exhibit about the same activity against intracellular amastigotes and insect-stage, extracellular epimastigotes. This is convenient for further analysis of their mode of action, since the epimastigote forms are easier to investigate and to cultivate at high density.

The fact that they are cultivated axenically allows epimastigote *T. cruzi* to be investigated by isothermal microcalorimetry. This revealed that the waltheriones are special also in terms of their pharmacodynamics: they act immediately but slowly. The heat-flow curves of treated *T. cruzi* and non-treated control diverge right from the beginning of drug incubation. This prompt onset of drug action contrasts with other trypanocides, as described previously (Wenzler et al., 2012, Wiedemar et al., 2018). Epimastigote *T. cruzi* exposed to waltherione F and G still grow, even when the drug concentration is ten-fold higher than the IC_{50} , although with a decreased growth rate. This finding is confirmed by the time-laps/wash out assay performed on the disease relevant intracellular stage, in which drug action sets in immediately but slowly at lower drug concentrations, however, fast at higher drug concentrations. This can be seen from the time dependent representation where curves diverge from the beginning and concentration dependent representation where the growth response curves are shifted to the right in the first 96 hours. Only after 96 hours of drug exposure a good dose response curve can be observed (Figure 3). Optimisation of the molecules from this point of view is necessary and ongoing.

Selecting *T. cruzi* for drug resistance was very difficult with waltherione F and impossible with waltherione G. This further underscores the potential of these molecules. With the optimised selection procedure for *T. cruzi* using a shock-like waltherione drug exposure, it was still only possible to obtain about 10-fold waltherione F-resistant parasites. The selected *T. cruzi* culture required dilution with fresh medium to allow the resistant mutants to recover to a normal proliferating culture. Once obtained, the resistance was stable over at least 40 days of cultivation and it was maintained even after differentiation of the epimastigotes to the intracellular amastigote form.

Comparative transcriptomics of waltherione-resistant and -sensitive *T. cruzi* revealed no candidate genes of altered expression level as determined by comparing the numbers of mapped reads per gene. The alpha-tubulin gene (C4B63_222g21) was down-regulated in *T. cruzi* STIB980_WF as compared to the STIB980 growth control cultured in the absence of drug, but not when compared to the non-cultured STIB980 baseline control (demonstrating the added value of having both controls). Sequence comparison of the mapped reads identified four mutations that were present in the resistant trypanosomes but absent from both controls. One of the SNPs was synonymous and not further investigated. One out of three nonsynonymous SNPs was only present in about 9-25% reads and could not be confirmed with Sanger sequencing and was also excluded from further investigation. Two candidate mutations were heterozygous with about 50% of the reads carrying the alternative allele. This result is in line with the fact that *T. cruzi* is diploid and may be due to the short time of selection.

The most promising mutation is found at position 370 of the protein-coding sequence of the gene C4B63_2g442, mitochondrial small subunit ribosomal protein, resulting in a proline to leucine substitution. The mitochondrial small subunit protein is part of the mitochondrial ribosome, responsible for translation of the mitochondrial-encoded genes. The mutated leucine is located in a highly conserved region of a mitoribosomal protein specific for the class of kinetoplastae. Mitoribosomes were already suggested as promising drug targets in trypanosomatids because of their peculiar protein-based architecture differing from other eukaryotic cells (Sloof et al., 1985, Ramrath et al., 2018). This specific protein is located at the head of the small subunit of the mitoribosome. However, its function is unclear apart from playing a role in mitoribosomal small subunit assembly

(Ramrath et al., 2018, Scaltsoyiannes et al., 2022). The mitoribosomes of trypanosomatids are unique in that they possess more protein subunits, and fewer rRNA subunits, than those of other eukaryotes (Ramrath et al., 2018). The waltheriones might be the first examples to chemotherapeutically exploit this difference. However, proving that the waltheriones actually target trypanosomal mitoribosomes will be very difficult. As a next step, we will investigate the effect of the mutation in epimastigote *T. cruzi* by CRISPR-Cas9 mediated reverse genetics. In addition, knowing the procyclic *T. brucei* are susceptible to waltheriones and that the identified mutation is in a highly conserved region opens up possibilities for further research using *T. brucei* as a well-known model organism with well-established molecular biology tools.

4.6 Acknowledgment

We are grateful to Dr. Natalie Wiedemar for her support and helpful advice with transcriptomic analysis, to the Genomics Facility Basel of the ETH Zurich for Illumina library preparation and sequencing, to the scientific computing centre at University of Basel (sciCORE) for bioinformatics computation time, to the group of Prof. Dr. Muriel Cuendet from Université de Genève, School of Pharmaceutical Sciences for providing waltheriones, to Prof. Dr. J. Kelly and Dr. M. Taylor for providing the plasmid pTRIX2-Luc::Neon-HYG and pLEW-Cas9, to Dr. Anna Albisetti for support with molecular biology, and to Dr. Moritz Niemann for advice on mitoribosomes. This research was funded by the Swiss National Science Foundation, grant number CRSII5_183536.

4.7 Supplementary material

Supplementary Table 1. Primer list. Primers designed 300 bases upstream and downstream of to the candidate variant mutation.

Primer Name	Primer Sequence
13_16g95_SNP_PCR_sequencing_fw1	ATGGGGAAGACACCGTCATTTGAGT
14_16g95_SNP_PCR_sequencing_rv1	AGTGTGATGCAAAAGCCTTCATGCT
17_2g442_SNP_PCR_sequencing_fw2	CTGGAGGCCTACTACTACTT
18_2g442_SNP_PCR_sequencing_rv2	GCAGTAAGGTCTGAAAAGCTG
21_52g56_SNP_PCR_sequencing_fw2	ACTCGTGTTCGGTAACTGACT
22_52g56_SNP_PCR_sequencing_rv2	GCCAACAACGCCAACTGATT



Supplementary Figure 1. Electropherogram of Sanger sequencing. The presence of the three nonsynonymous candidate SNPs was confirmed with Sanger sequencing on PCR amplified epimastigote *T. cruzi* gDNA. Y, cytosine/thymidine (pyrimidine); R, guanine/adenine (purine).

5 *Trypanosoma cruzi* STIB980: a new assay strain for imaging and reverse genetics

Anna Fesser^{1,2,+}, Sabina Beilstein^{1,2}, Marcel Kaiser^{1,2}, Remo S. Schmidt^{1,2,#,*},
Pascal Mäser^{1,2*}

¹ Swiss Tropical and Public Health Institute, 4123 Allschwil, Switzerland

² University of Basel, 4001 Basel, Switzerland

⁺ Present address: Bundesamt für Gesundheit, 3097 Liebefeld, Switzerland

[#] Present address: Agroscope, 3097 Liebefeld, Switzerland

^{*} Contributed equally

2023

Working manuscript

I performed all experiments concerning the validation of CRISPR-Cas, including the transfection and analysis with flow cytometry. I assisted with transfection of the CRISPR-Cas9 and Luciferase Neogreen constructs and contributed drug sensitivity testing. Before publication of the manuscript, I will submit the sequencing data to the European Nucleotide Archive (ENA) and stocks of *T. cruzi* STIB980 wildtype and transgenic lines to the American Type Culture Collection (ATCC).

5.1 Abstract

Since the first published genome sequence of *Trypanosoma cruzi* in 2005, there has been tremendous technological advance in genomics, reverse genetics, and assay development for this elusive pathogen. However, there is still an unmet need for new and better drugs to treat Chagas disease. Here we introduce a *T. cruzi* assay strain that is useful for drug research as well as basic studies in host-pathogen interaction. *Trypanosoma cruzi* STIB980 is a strain of discrete typing unit TcI that grows well in culture as axenic epimastigotes or intracellular amastigotes. We have evaluated the optimal parameters for genetic transfection and constructed derivatives of *T. cruzi* STIB980 that express reporter genes for fluorescence- or bioluminescence-based drug efficacy testing, as well as a Cas9-expressing line for CRISPR/Cas9-mediated gene editing. The genome of *T. cruzi* STIB980 was sequenced by combining short-read Illumina with long-read Oxford Nanopore technologies. The latter served for the primary assembly, the former to correct mistakes. This resulted in a high-quality nuclear haplotype assembly of 28 Mb in 400 contigs, containing 10,043 open-reading frames with a median length of 1077 bp. We believe that *T. cruzi* STIB980 is a useful addition to the antichagasic toolbox, and that it can serve as a DTU TcI reference strain for antichagasic drug efficacy testing.

5.2 Introduction

Chagas disease is a neglected tropical disease and at the same time also a most elusive disease. Due to the chronic nature of Chagas disease, with an indeterminate phase that is asymptomatic and lasts for decades, the vast majority of the carriers do not know that they are infected. For the same reason, there are no solid data on the prevalence of Chagas disease. The epidemiology of Chagas disease is further complicated by (i) the large zoonotic reservoir of *Trypanosoma cruzi*, which infects all kinds of mammals provided they are preyed upon by the triatomine vectors; (ii) alternative transmission routes, including via the oral mucosa upon consumption of contaminated food, and transplacental to the unborn child; (iii) the genetic heterogeneity and genomic flexibility of *T. cruzi* with its (at least) seven different Discrete Typing Units (DTU) (Velásquez-Ortiz et al., 2022, Wang et al., 2021).

The parasites are elusive also in the human body. *Trypanosoma cruzi* can infect any type of nucleated cell, and the parasites will replicate intracellularly in the cytosol of the host cell. Infected macrophages distribute the parasites throughout the body. Thus, they can access different tissues and niches to hide in, including the heart and the intestinal tract, the typical sites of chronic pathology (Matsuda et al., 2009). Trypomastigote *T. cruzi* do not proliferate but persist extracellularly in the blood thanks to their elaborate immune evasion strategies (Ramírez-Tolosa and Ferreira, 2017). The intracellular amastigotes, too, can enter a non-replicative state of dormancy (Sanchez-Valdez et al., 2018). All this makes Chagas disease difficult to diagnose and even harder to cure, as became apparent in the clinical trials with new antichagasic drug candidates. In the laboratory, research on *T. cruzi* is hampered by the fact that the disease-relevant stages, the amastigotes, are strictly intracellular and require host cells for *in vitro* culture. The infectious nature of *T. cruzi* renders all experimental investigation resource-intensive in terms of biosafety measures, assay time, and overall cost.

On a positive note, there has been tremendous technological progress in genomics and reverse genetics with *T. cruzi*, which has boosted basic research as well as drug discovery. Classical genetic manipulation based on homologous recombination (Taylor et al., 2011, Docampo, 2011) is being replaced by CRISPR/Cas9-mediated gene editing (Lander and Chiurillo, 2019), which allows for functional genomics in spite of the fact that *T. cruzi* lacks the RNA interference

machinery (Kolev et al., 2011). Genetically engineered reporter strains of *T. cruzi* have enabled assay formats that better predict the potential of antichagasic molecules for irreversible and cidal action, both *in vitro* and *in vivo*. Here we present a new reference strain, *T. cruzi* STIB980, which is useful for all kinds of investigation including genomics, reverse genetics, and drug efficacy testing.

5.3 Results and discussion

5.3.1 Genotyping and cloning of *T. cruzi* STIB980

Trypanosoma cruzi STIB980, originally received in 1983 from Prof. Antonio Osuna, University of Granada, is one of the standard strains used for drug efficacy testing at the Parasite Chemotherapy Unit of the Swiss Tropical and Public Health Institute. Amastigote and epimastigote forms are readily cultured as described under Methods. A fresh clone of *T. cruzi* STIB980 was made with epimastigotes, employing the gilded paperclip method (Figure 1A). This clone was used for all further analyses. Genotyping based on restriction fragment length polymorphisms of three target loci (the large ribosomal RNA subunit, heat-shock protein 60, and glucose-6-phosphate isomerase) (Messenger and Miles, 2015) placed *T. cruzi* STIB980 in DTU TcI (Figure 1B to F). TcI is the DTU that circulates most broadly among humans, and is correlated mostly with cardiomyopathic symptoms (Zingales, 2018, Izeta-Alberdi et al., 2016). Therefore, a TcI strain is highly relevant as an assay strain.

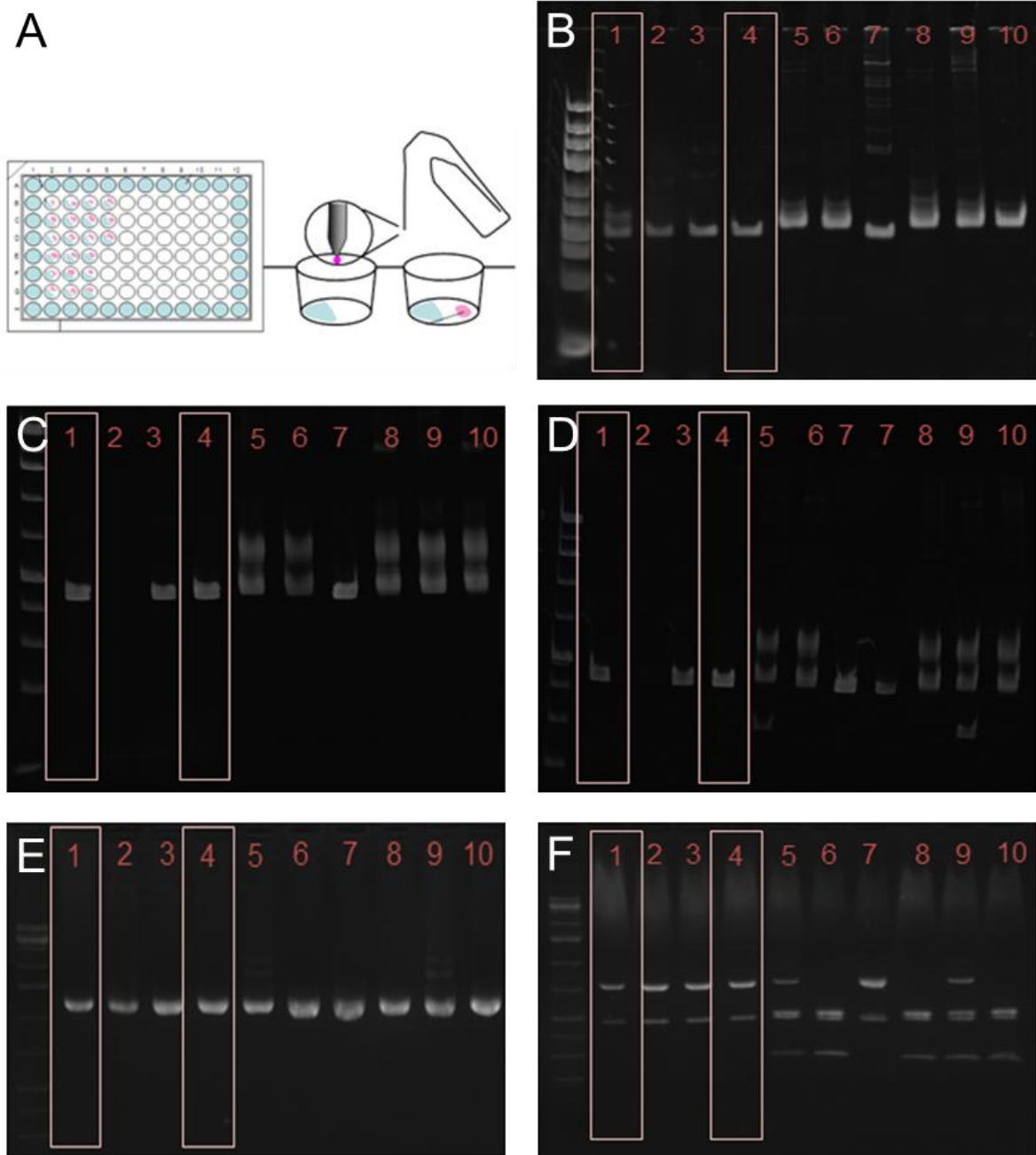


Figure 1. Establishing a *T. cruzi* STIB980 clonal line with the gilded paperclip method (A) and genotyping results. Agarose gels of the PCR products of the large ribosomal subunit (B), HSP60 before (C) and after (D) digestion with *EcoRV*, G6PI before (E) and after (F) digestion with *HhaI*. In all three reactions and subsequent digestions, STIB980 most closely resembled the DTU TcI strains. 1) Dm28c [TcI]; 2) Sylvio [TcI]; 3,4) STIB980; 5) Tulahuen [TcVI]; 6) Esmeraldo [TcII]; 7) Sylvio X10/4 [TcI]; 8) Y strain [TcII]; 9) CL Brener [TcVI]; 10) Y strain [TcII]. Genomic DNA kindly provided by Michael Lewis (LSHTM).

5.3.2 Genome sequence of *T. cruzi* STIB980

Genomic DNA of *T. cruzi* STIB980 was sequenced on the Illumina HiSeq 2500 and the Oxford Nanopore MinION platforms. Illumina sequencing was done with a 125-bp paired end protocol and yielded 67,187,531 reads that passed quality control. Assuming a diploid genome size of 53.3 Mb as reported for *T. cruzi* Dm28c (Berná et al., 2018), this corresponds to a coverage of 158-fold. With Nanopore sequencing we obtained 250,005 reads and a median length of 1.4 kb. The estimated coverage, again assuming a genome size of 53.3 Mb, was 12-fold. The reads were categorised according to their size and GC content (Figure 2) into nuclear genome, maxicircle (assembled to a single contig), minicircles, and sequences of unknown origin (Table 1). The best results for genome assembly (as judged by the mapping rate) was obtained by first assembling the long Nanopore reads (using Canu v1.7 (Koren et al., 2017)), followed by fixing errors with the short Illumina reads (using Pilon v1.22 (Walker et al., 2014)). This combination of Nanopore and Illumina reads led to drastic improvements compared to the assembly based on Illumina reads alone: the number of contigs was reduced 23-fold, the N50 increased 30-fold, and the numbers of gaps ($n=13,000$) and undetermined nucleotides (5 Mb) were reduced to zero. The total assembly amounted to 28.2 Mb in 492 contigs; the nuclear genome had a haploid size of 27.9 Mb in 397 contigs (Table 1).

Gene prediction was performed using GLIMMER (Salzberg et al., 1998) with the standard codon table. The genome of *T. cruzi* Dm28c (Berná et al., 2018) served as training set. This resulted in 10,043 open-reading frames (ORFs) with a median length of 1077 bp. The amino acid sequences were queried against UniProt KnowledgeBase (UniProt Consortium, 2023) using blastp (Altschul et al., 1990) with an expectancy (E-value) cut-off of 10^{-8} . This allowed the functional annotation of 3505 genes.

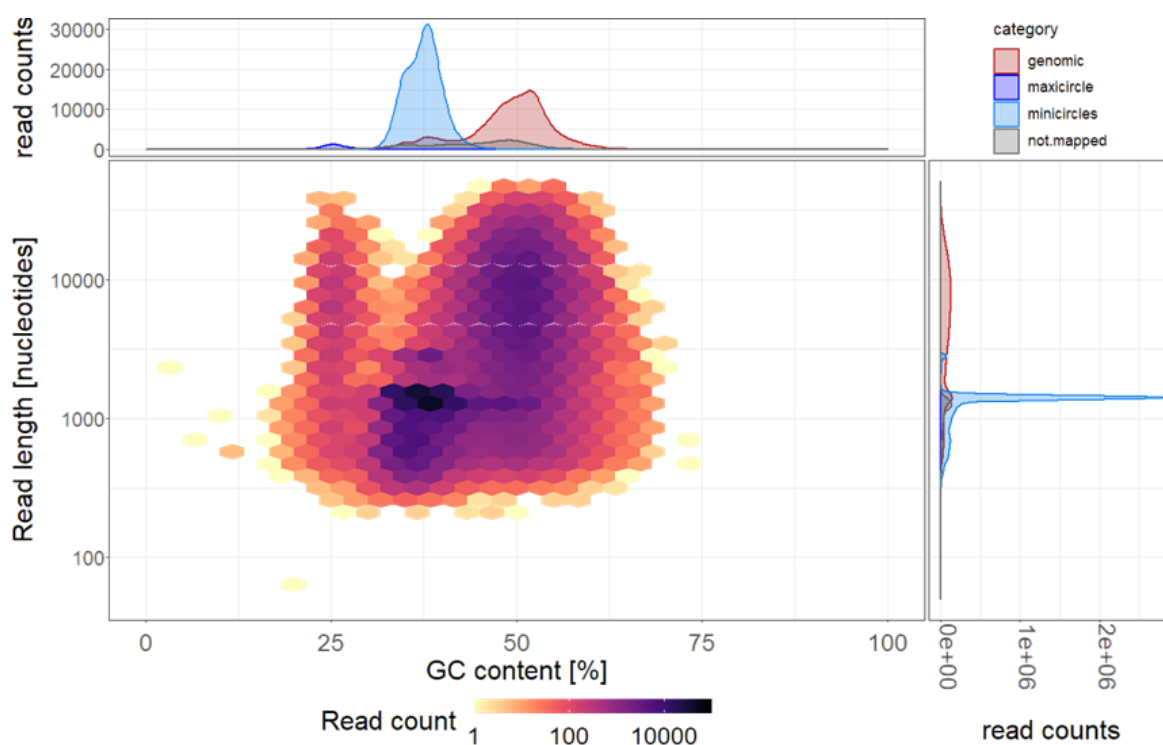


Figure 2. Distribution of the Nanopore reads ($n=250,005$) of *T. cruzi* STIB980 according to their GC content and length. This separates nuclear sequences from mitochondrial sequences. The majority of the reads were categorised as minicircles, with a GC content between 30% and 40% and a length of about 1.4 kb.

Table 1. Summary statistics of the separate genome assemblies for *T. cruzi* STIB980. n.a., not applicable.

	Total size (nt)	No. of contigs	N50 (nt)	longest contig (nt)	shortest contig (nt)
Nuclear	27,888,483	397	165,577	715,804	1,660
Minicircles	248,782	91	2,699	10,035	1,264
Maxicircle	68,708	1	n.a.	n.a.	n.a.
Unknown	14,070	3	3,090	9,979	1,001
Total	28,220,043	492	158,042	715,804	1,001

5.3.3 Antibiotic sensitivity profile of epimastigote *T. cruzi* STIB980

In order to determine the best selection markers for use in genetic manipulation, we tested the sensitivity of *T. cruzi* STIB980 epimastigotes to commonly used

antibiotics: blasticidin, G418, hygromycin, phleomycin, and puromycin. Benznidazole and nifurtimox were included as benchmark drugs, DMSO as the most commonly used solvent of test compounds. Drug sensitivity was tested for 72 h and 168 h of incubation. For the latter, we used two different inocula: a lower starting density (2×10^4 epimastigotes/mL) to assess the inhibition of proliferation, a higher density (10^5 epimastigotes/mL) to measure cidality. However, the obtained IC_{50} values were similar across all the tested conditions (Table 2). The STIB980 epimastigotes had comparably high IC_{50} values for G418, which is in agreement with the high concentrations (100 to 500 $\mu\text{g/mL}$) of G418 that are generally used for epimastigote *T. cruzi* (Olmo et al., 2018) and in stark contrast to the 1 to 5 $\mu\text{g/mL}$ used in the genetic manipulation of procyclic *T. brucei* (Burkard et al., 2007).

Table 2. Drug sensitivity profile of *T. cruzi* STIB980 epimastigotes. 95% CI is given in parentheses. Parasite inocula were $5 \times 10^5 \text{ mL}^{-1}$ (72 h), 10^5 mL^{-1} (168 h, high), and $2 \times 10^4 \text{ mL}^{-1}$ (168 h, low).

	IC_{50} 72 h [$\mu\text{g/mL}$]	IC_{50} 168 h [$\mu\text{g/mL}$] high inoculum	IC_{50} 168 h [$\mu\text{g/mL}$] low inoculum
Blasticidin	1.6 (1.2; 2.0)	0.37 (0.20; 0.54)	0.32 (0.29; 0.34)
Puromycin	1.3 (1.1; 1.4)	1.2 (1.1; 1.4)	0.56 (0.48; 0.64)
Hygromycin	41 (30; 52)	22 (13; 31)	37 (28; 46)
G418	46 (38; 54)	50 (42; 57)	31 (25; 37)
Phleomycin	89 (70; 110)	71 (60; 81)	27 (23; 32)
Benznidazole	1.9 (0.67; 3.1)	1.2 (0.90; 1.4)	0.66 (0.53; 0.79)
Nifurtimox	0.87 (0.58; 1.2)	0.41 (0.37; 0.46)	0.24 (0.20; 0.28)
DMSO	3.8 (3.2; 4.5)	3.2 (-1.1; 7.4)	1.2 (0.93; 1.4)

Besides the sensitivity of the untransfected trypanosomes, other factors will determine the optimal concentration of antibiotics to select positive transfectants. The expression level of the resistance gene will be affected by its copy number (especially in episomal transfections), and by the strength of the promoter, by the RNA polymerase (RNAPoIII usually resulting in a lower level of transcription than RNAPoII), and – in case of the ribosomal locus – the exact site of integration (Alsford et al., 2005). Overall, we recommend blasticidin or puromycin to select for *T. cruzi* STIB980 transfectants, rather than G418, hygromycin, or phleomycin.

5.3.4 Optimal transfection protocol for *T. cruzi* STIB980

The Lonza Nucleofector® 2b is a widely used electroporation device for genetic transfection. It provides excellent results also with trypanosomes but is a black box, as the provider does not disclose the characteristics of the electric discharge nor the composition of the buffers. Tests on Nucleofector® programs had already been published for *T. brucei* (Burkard et al., 2007) and *T. cruzi* (Pacheco-Lugo et al., 2017). We investigated which program is best suited for *T. cruzi* STIB980. Epimastigotes were transfected with a circular pTcRG plasmid, kindly provided by Santuza Teixeira (Federal University of Minas Gerais, Brazil), that contained the green fluorescent protein (GFP) gene plus the 3' UTR of the GAPDH gene, which confers constitutive expression. 4×10^7 epimastigotes in the exponential growth phase were transfected with 10 µg plasmid DNA using nine different Nucleofector® programs. Immediately after transfection, we counted the surviving parasites. Then, we incubated them for 24 h in 10 mL LIT medium at 27 °C. Finally, the proportion of GFP expressing parasites was quantified by flow cytometry (Burkard et al., 2007). The transfection efficiency was calculated as the product of cell survival and GFP positivity (Table 3). The programs U-033, X-001, and Z-001 had the best overall efficiencies. The lower survival rates with Z-001 and U-033 were compensated by higher fractions of GFP expression. For subsequent transfections, we have used the Nucleofector® programs U-033 or X-014.

Table 3. Efficiency of transient transfection of different Nucleofector® programs, expressed as the fraction of surviving cells multiplied with the fraction of GFP expressing cells.

Program	% Survival	% GFP expression	Efficiency
X-001	55.0	6.83	0.038
U-033	42.5	8.15	0.035
Z-001	32.5	7.80	0.025
X-014	58.8	4.16	0.024
X-013	57.5	4.23	0.024
X-024	65.0	3.56	0.023
Z-014	60.0	3.18	0.019
X-006	57.5	2.67	0.015
T-020	91.3	1.11	0.010

5.3.5 Transgenic *T. cruzi* STIB980 lines for drug testing and reverse genetics

The levels of cytosolic GFP obtained after transient transfection of pTcRG were too low for high-content fluorescence microscopy. Most of the parasite signal was below three times the background level (i.e. the autofluorescence of untransfected epimastigotes). For better use of *T. cruzi* STIB980 in drug efficacy testing and molecular genetics, we generated stable transgenic lines expressing a *LucNeon* reporter gene, *Cas9* nuclease gene, or both (Costa et al., 2018). *LucNeon* is a chimeric gene encoding a fusion protein of mNeonGreen, suitable for fluorescence-based *in vitro* imaging, plus a red-shifted luciferase that is suitable for bioluminescence-based *in vivo* imaging (Costa et al., 2018). The plasmids had been kindly provided by John Kelly (LSHTM). Epimastigotes were transfected as described in the Methods section. The three resulting transgenic lines all had similar growth rates with population doubling times around 20 h, slightly higher than the 17 h of the parental *T. cruzi* STIB980 (Figure 3). The sensitivity profiles to reference drugs (benznidazole and nifurtimox) and drug candidates (posaconazole, fexinidazole, and the oxaborole DNDi-6148) of parental *T. cruzi* STIB980 and STIB980-LucNeon were determined by high content imaging of intracellular amastigotes in expanded mouse peritoneal macrophages. The IC₅₀ values were calculated by two different methods, either based on the number of infected host cells or the total number of intracellular amastigotes (Table 4). The first method resulted in slightly higher IC₅₀ values, which was to be expected as the total number of parasites is reduced more readily than the host cells cured of the infection. Overall, the drug sensitivities of the parental STIB980 and transgenic derivative were very similar using either method (Table 4). The function of the *Cas9* nuclease was validated by CRISPR/Cas9-mediated deletion of the fluorescence reporter using specific guide RNAs for the *LucNeon* gene (Figure 4).

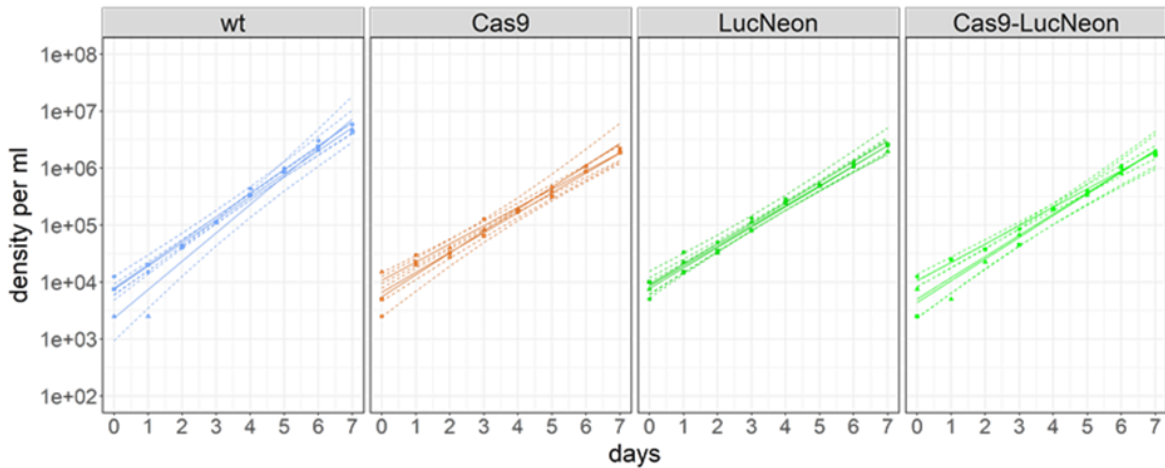


Figure 3. Growth curves of epimastigote *T. cruzi* STIB980 wildtype (wt) and transgenic derivatives expressing *Cas9* nuclease, *LucNeon* reporter gene, or both. The indicated population doubling times were calculated by linear regression to the log-transformed data.

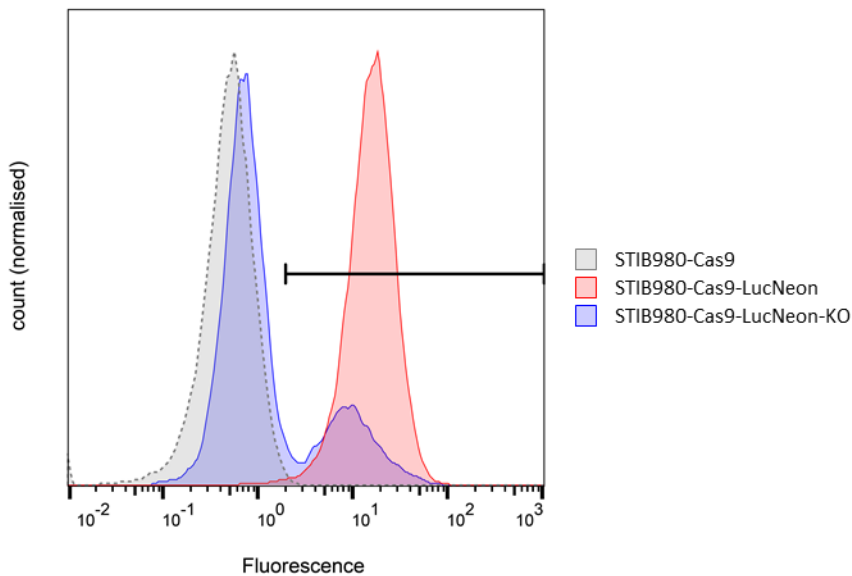


Figure 4. Validation of the *LucNeon* reporter and *Cas9* nuclease in *T. cruzi* STIB980-Cas9-LucNeon. The x-axis represents the fluorescence level measured in arbitrary units, with the green fluorescence channel (excitation 488 nm, emission 525/50 nm; bandwidth 50 nm); the y-axis the normalised cell counts. Only 23.7% of the cells still show a green fluorescence signal after CRISPR-Cas9 mediated knock-out of the *LucNeon* fusion gene.

Table 4. Drug sensitivity profiles of *T. cruzi* STIB980 wildtype (wt) and STIB980-LucNeon as determined by high content imaging of intracellular amastigotes. IC₅₀ values were calculated based on the number of infected host cells (Infection rate, left) or the total number of intracellular amastigotes (No. amastigotes, right).

	IC ₅₀ [ng/mL] Infection rate		IC ₅₀ [ng/mL] No. amastigotes	
	wt	LucNeon	wt	LucNeon
Benznidazole	750	840	550	600
Fexinidazole	3000	4500	2900	2300
DNDi-6148	110	110	100	70
Nifurtimox	580	700	<410	540
Posaconazole	0.85	0.72	0.51	0.69

5.4 Conclusion

Trypanosoma cruzi STIB980 is a useful new assay strain in the toolbox of antichagasic drug discovery. It is a DTU TcI strain that is readily cultured *in vitro* and amenable to genetic manipulation. We provide optimised electroporation conditions and the antibiotic sensitivity profile of epimastigotes to facilitate genetic transfection. The genome sequence of *T. cruzi* STIB980 was assembled by combining short reads generated by Illumina sequencing and long reads generated by Oxford Nanopore sequencing, demonstrating the power of combining both technologies, in particular for a genome with a high degree of repetitive regions like that of *T. cruzi*. We further provide *T. cruzi* STIB980 derivatives that express reporter genes (eGFP, LucNeon) for imaging *in vitro* and *in vivo*. The reporter genes are stable in the absence of selective pressure in epimastigotes but much less so in amastigotes, underlining the importance of frequently resorting to a new stabilate, e.g. when running drug testing campaigns against intracellular amastigotes. To facilitate CRISPR/Cas9-mediated gene editing, we have also constructed a line of *T. cruzi* STIB980-LucNeon with a stably integrated *Cas9* gene, and validated that line by knocking-out the *LucNeon* gene as a proof-of-principle. Thus *T. cruzi* STIB980 can serve not only as a reference strain for drug efficacy testing but also as a tool for molecular genetics.

5.5 Material and Methods

5.5.1 Cell cultivation

Trypanosoma cruzi epimastigotes were cultured at 27 °C in LIT medium supplemented with 2 µg/mL hemin and 10% heat-inactivated fetal calf serum (iFCS) (Fernandes and Castellani, 1966). The cultures were diluted weekly. Metacyclogenesis was stimulated by keeping the epimastigotes for 3 to 4 weeks in the same medium. Mouse embryonic fibroblasts (MEF) were cultured at 37 °C, 5% CO₂ in RPMI medium supplemented with 10% iFCS and >95% humidity. The MEF were subpassaged weekly at a ratio of 1:10 after 5 min treatment with trypsin. Peritoneal mouse macrophages (PMM) were obtained from female CD1 mice. A 2% starch solution in distilled water was injected *i.p.*, and the macrophages were harvested 24 h later by peritoneal lavage. The cells were washed and resuspended in RPMI medium containing 1× antibiotic cocktail (Mäser et al., 2002), 10% iFCS, and 15% medium conditioned by LADMAC cells (ATCC® CRL2420™), which secrete colony stimulating factor 1 (CSF-1). The macrophages were kept in this medium at 37 °C for 3 to 4 days and then detached with trypsin treatment and cell scrapers. The isolation of PMM from mice was conducted in accordance with the strict guidelines set out by the Swiss Federal Veterinary Office, under the ethical approval of license number #2374.

5.5.2 Cloning of *T. cruzi*

The gilded paper clip method was used for cloning (Figure 1A). An exponentially growing epimastigote culture was diluted to 5×10⁴ cells/mL. The outer wells of a 96-well plate were filled with 100 µL sterile water. 15 µL of conditioned LIT medium (LIT supplemented with 10% filtered post-culture medium and 20% iFCS) were placed at the edge of the other wells, so that some space of the well remained dry. Using a gold-plated paperclip, a micro-drop of approximately 0.1 µL was transferred from the diluted parasite suspension to the dry space of the well. Two people analysed the droplet under an inverted microscope. Wells that contained only one parasite were supplemented with 35 µL of conditioned LIT. The plates were incubated at 27 °C and assessed regularly for outgrowth of the clones.

5.5.3 Isolation of genomic DNA

Genomic DNA for genome sequencing was isolated from 10^8 epimastigotes. The cells were washed and resuspended in 500 μ L NTE, and lysed by addition of 25 μ L of 10% SDS. The lysate was treated with 50 μ L RNase A (10 mg/mL) and 25 μ L pronase (20 mg/mL), and incubated over night at 37 °C. The lysate was extracted sequentially with phenol and chloroform:isoamyl alcohol (24:1, v/v). The DNA was precipitated by the addition of 1 mL cold 100% ethanol. For Illumina sequencing, the DNA was pelleted by centrifugation; for Oxford Nanopore sequencing, the DNA was collected with a glass hook. The DNA was washed with 70% ethanol, air-dried, and resuspended in 80 μ L DNase-free water. For other purposes, genomic DNA was isolated with the QIAGEN DNeasy blood and tissue kit.

5.5.4 Genome sequencing and assembly

Library preparation and sequencing on the Illumina platform was performed at the Quantitative Genomics Facility Basel (GFB) of the ETH Zürich. Sequencing libraries were prepared using the PCR-free KAPA HyperPrep kit (Illumina). Paired-end sequencing of 125 nucleotides was done on an Illumina HiSeq 2500 sequencer. For Nanopore sequencing, the library was prepared using the Ligation Sequencing kit 108 (SQK-LSK108, Oxford Nanopore Technology) and sequenced using the MinION platform. Basecalling was carried out using Albacore. Quality control for all reads was done with FastQC (version 0.11.3) (Babraham Bioinformatics, 2022). Different assemblers were tested: Velvet (Zerbino and Birney, 2008) and SOAPdenovo (version 2.04) (Xie et al., 2014) for the Illumina reads (with a range of different kmer sizes from 17 to 73), Canu (version 1.7) (Koren et al., 2017) and Flye (release 2.3.3) (Kolmogorov et al., 2019) for the Nanopore reads. Illumina polishing of the Canu-assembled Nanopore reads was performed using Pilon (version 1.22) (Walker et al., 2014). The Flye assembly was done on the pore-chopped long reads, with an expected genome size of 53 Mb (Kolmogorov et al., 2019).

5.5.5 Optimisation of electroporation

10^7 epimastigotes from a dense culture were centrifuged and resuspended in 100 μ L TbBSF buffer (Burkard et al., 2007) containing 10 μ g of circular (for transient transfection) or linearized (for stable transfection) plasmid DNA. The cells were electroporated with a Nucleofector® device (Lonza) in a 0.2 mm cuvette (BioRad).

After electroporation, the cells were transferred to 10 mL LIT with a fine-tipped Pasteur pipette. The parasites transfected with circular plasmid were incubated for 24 h and then tested with flow cytometry for GFP expression. The parasites transfected with linearized plasmid were incubated for 24 h, diluted 1:10 in medium containing 100 µg/mL G418 (Gibco), and further distributed in a four-fold dilution series in a 48 well plate under antibiotic pressure. Outgrowing epimastigotes were cloned by limiting dilution and assessed for correct integration of the transgene by PCR and Southern blot.

5.5.6 Generation of transgenic lines

Exponentially growing *T. cruzi* epimastigotes were synchronised for 24 h with 20 mM of hydroxyurea (Sigma) (Olmo et al., 2018). Following hydroxyurea removal by washing twice with PBS, 10^7 epimastigotes were electroporated with 2.5 µg of pTRIX2-Luc::Neon-HYG plasmid linearized with *Ascl* and *Sacl* (New England Biolabs) or pLEW-Cas9 plasmid linearized with *NotI* (New England Biolabs). The pTRIX2-Luc::Neon-HYG plasmid had been derived from pTRIX-REh9 (Lewis et al., 2014). CRISPR-Cas9 mediated genetic knock-out was performed according to (Costa et al., 2018, Beneke et al., 2017). The resistance cassette was amplified by PCR from plasmid pPOTcruzi v1 blast-blast mNeonGreen with primers 5'-aacatcaagaagggaccagccccctctacggtagttaagagctcggaccac (forward) and 5'-acgagtgtctgggctcgggttccactatccaattgagagacctgtgc (reverse). sgRNA were amplified using a gene specific forward primer (5'-gaaattaatacgactcactatagggagtacttctacacagccatgttttagagctagaaatagc and 5'-gaaattaatacgactcactatagggcggctgtgccgctctccagggtttagagctagaaatagc) and the G00 (sgRNA scaffold) reverse primer. 24 h after transfection, the parasites were diluted 1:10 in medium containing 100 µg/mL G418 (Gibco).

5.5.7 Drug sensitivity assay with epimastigotes

In a 96-well microtiter plate, 100 µL epimastigotes at a starting density of 5×10^6 /mL, 10^5 /mL, or 2×10^4 /mL were incubated with test compound in three-fold serial dilution with 11 dilution steps. After 69 h or 165 h of incubation at 27 °C, 10 µL of resazurin (Sigma) solution (12.5 mg in 100 mL water) were added to each well. After another 3 h of incubation, the plates were read with a SpectraMAX GeminiXS fluorescence reader (Molecular Devices, San Jose, CA). 50% inhibitory values (IC₅₀) were

determined in R version 3.5.1 (R Core Team 2018) using the “drc” package (Ritz et al., 2015).

5.5.8 Flow cytometry

For flow cytometry, 10^5 epimastigotes were fixed with 10% formalin (Merck) for 15 min and then analysed for the green fluorescence levels (FL1) on a BD FACSCalibur (Becton Dickinson and Company, Franklin Lakes, NJ, USA). The threshold for GFP expression was set above the autofluorescence level of 99.6% of the untransfected control cells. The proportion of GFP expressing cells (Table 3) was therefore the proportion of cells exhibiting a higher level of fluorescence than the threshold.

5.5.9 High-content drug efficacy assay

Assays were performed with two technical and two biological replicates. For the standard assay, 10^4 PMM were seeded into the central wells of a black 96-well plate (Greiner, μ CLEAR®, black, REF 655090, Lot E1803364) in 100 μ L of RPMI medium containing 1% antibiotic mix (Mäser et al., 2002), 10% iFCS and 15% RPMI medium containing LADMAC growth factors per well. The border wells were filled with 100 μ L of water. After 48 hours, the PMM were infected with 10^4 trypomastigotes from either the wildtype or the transgenic STIB980 line. After 24 h, the remaining trypomastigotes were washed off twice with 200 μ L RPMI medium per well. The infected PMM were kept in 100 μ L RPMI medium containing 1% antibiotic mix and 10% iFCS. Drugs were added in three-fold serial dilution 24 h post-infection. 96 h after addition of drugs, the plates were fixed with 10% formalin for 15 min at room temperature. Subsequently, the plates were stained with 50 μ L of 5 μ M DRAQ5™ (Merck, Darmstadt, Germany) per well for 30 min at room temperature in the dark. The plates were stored at 4 °C for at least 24 h and then imaged using an ImageXpress Micro XLS microscope (Molecular Devices, San Jose, CA) with a 20 \times Zeiss objective with the Cy5 filter cube for 300 ms per image on 9 sites per well. Image analysis was performed with the MetaXpress 6 software. Statistical analysis and graphs were done in R version 3.5.1 (R Core Team 2018) using the packages “tidyverse” (Wickham, 2017) and “readxl” (Wickham, 2018).

5.6 Acknowledgments

We wish to thank Antonio Osuna for the kind provision of the original *T. cruzi* strain in 1984, Richard Neher and Nicholas Noll for all their help with Nanopore sequencing, Thomas Otto for advice on genome assembly, Santuza Teixeira for the plasmid pTcRG, John Kelly and Mark Taylor for the plasmid pTRIX2-RE9h, Michael Lewis for DNA of *T. cruzi* reference strains and recommendations concerning genotyping; and Monica Cal, Christina Kunz and Romina Rocchetti for expert technical assistance. Illumina sequencing was carried out on the University of Basel/ETHZ Genomics Platform, genome assembly was performed on sciCORE, the scientific computing cluster of the University of Basel. This work was financially supported by the Swiss National Science Foundation, the Nikolaus und Bertha Burckhardt-Bürgin-Stiftung, and the Freiwillige Akademische Gesellschaft Basel.

6 Waltheriones and *Trypanosoma cruzi* – general discussion

Waltherione F and G are natural molecules active on *Trypanosoma cruzi* in the submicromolar range. *In vitro* drug resistance selection was performed for subsequent target deconvolution by comparative transcriptomics analysis. Selecting *T. cruzi* for waltherione resistance was challenging and only possible for waltherione F. Untargeted metabolomics showed an accumulation of acylcarnitine in epimastigote *T. cruzi* upon exposure to waltherione G. Comparative transcriptomics of waltherione F-resistant and susceptible epimastigote *T. cruzi* revealed a candidate resistance mutation in a mitoribosomal protein. Additionally, waltheriones are also active on specific stages of other trypanosomatids including procyclic *T. brucei*. Together these findings suggest the mitochondrion as a potential site of drug action of waltheriones.

6.1 Waltheriones are hard-to-resist natural molecules

As reviewed in Chapter 2 (Beilstein et al., 2022) very different approaches can lead to successful drug resistance selection in trypanosomes. There is no general best procedure which guarantees finding resistant phenotypes. This is also underlined by the different outcome of selecting *T. cruzi* for waltherione F and G. Different approaches outlined in Chapter 4 were used to select extracellular epimastigote and intracellular amastigote *T. cruzi* resistant to waltheriones. Applying a sub-lethal drug concentration, parasites survived well, without showing any loss of sensitivity even after more than one year of selection. This procedure is the most commonly used and was previously successfully employed for selecting bloodstream form *T. brucei rhodesiense* for resistance against melarsoprol and pentamidine. However, the resistance arose only after 18-24 months of selective pressure and was then stable (Bernhard et al., 2007, Graf et al., 2016). In contrast, selecting *T. brucei* for suramin resistance with a presumably lethal drug concentration needed only one week until a 100-fold resistant parasite population recovered in the same medium. In comparison to the melarsoprol and pentamidine resistance, suramin resistance decreased after 80 days to a level of 10- to 50-fold (Wiedemar et al., 2018).

In the case of suramin, the resistance phenotype appeared during the selection process by the expression of a particular variant surface glycoprotein

(VSG). For melarsoprol-resistant parasites, the accumulation of spontaneous mutations during selection led to the loss of the *TbAT1* gene and consequently the P2 transporter, (Bernhard et al., 2007, Carter and Fairlamb, 1993, Mäser et al., 1999) and aquaglyceroporin 2 (Graf et al., 2016), causing decreased drug uptake.

During walterione resistance selection in *T. cruzi* a comparable phenomenon to melarsoprol and pentamidine or suramin could not exactly be observed. The parasites were finally successfully selected with a short but high drug pressure of $10\times IC_{50}$ and subsequently showed a stable resistance phenotype. For walterione G, no drug resistance arose with any applied selection method. This outcome speaks for the attractiveness of walteriones.

Two adaptations in the selection procedure were most critical for gaining walterione F-resistant *T. cruzi*. First, the parasites under drug pressure were supplied regularly with fresh medium. Second, the selection was started with a higher parasite number, increasing the genetic pool and the probability of including an already resistant mutant (Chapter 4). The advantage of the optimised selection procedure for walteriones lies in the comparably short experimental time until you get an answer whether some, potentially resistant cells have survived. Using a hypermutating strain, as it is often done with *Plasmodium falciparum*, might further shorten the time for *in vitro* resistance generation (Ding et al., 2012, Trotta et al., 2004, Rathod et al., 1997).

The microcalorimeter data showed that some parasites are able to endure very high drug pressure of up to $10\times IC_{50}$ over a long time (Chapter 4). Washout experiments confirmed that individual parasites persisted at very high walterione concentrations and regrew even at the highest tested drug concentration. A similar phenomenon had been observed for benznidazole in experiments in mice. Intracellular parasites were observed to resist the highly cytotoxic benznidazole over a long time, whereas the overall parasite number was rapidly reduced. Spontaneous dormant forms were also suggested for intracellular and extracellular *T. cruzi* (Sanchez-Valdez et al., 2018, Resende et al., 2020). Metabolically quiescent epimastigote forms might also still exist in our cultures, including the resistance selection, and be able to endure nutrient depletion better. For future research and development with walteriones, it should also be kept in mind that the drug acts instantly but slowly and a high dose is required for total parasite killing (Chapter 4). Testing walteriones in combination with other drugs might help to

improve the walterione action or even find a synergistic partner drug which might overcome the challenge to kill all parasites and to impede the emergence of drug resistance.

Considering fatty acid metabolism to be potentially involved in drug action (Chapter 3), the parasites might resist walteriones better at lower parasite density, when the nutrients are not yet scarce and fatty acid metabolism is not yet essential as they still can access other carbon sources, such as glucose, to gain energy (Souza et al., 2021). There would be no selective advantage to less sensitive mutants because the sensitive parasites would still have an alternative pathway to survive. Time-laps/washout experiments (Chapter 4) showed that the parasites become more sensitive when cell density increases and most probably nutrients are depleted. At a subcurative dosage, parasites would survive and proliferate well over a long time. Starting with a higher parasite number, the culture reaches the late exponential phase where drug action sets in much sooner, exerting a stronger selective force for walterione-resistant mutants.

6.2 Walteriones affect *T. cruzi* fatty acid catabolism

Acylcarnitines were upregulated in extracellular epimastigote *T. cruzi* exposed to 10× IC₅₀ of walterione G (Chapter 3). In eukaryotic cells, including trypanosomes, long-chain fatty acids are imported into the cells and coupled to Coenzyme A. At the mitochondrial outer membrane, carnitine palmitoyltransferase 1 (CPT1) shuttles acyl-CoA to the mitochondrial intermembrane space by transferring the acyl group to carnitine. Carnitine-acylcarnitine translocase (CACT) then shuttles acylcarnitine to the inner mitochondrial space where carnitine palmitoyltransferase 2 (CPT2), located at the inner membrane, transfers the acyl group to CoA again. An accumulation can thus occur after the enzymatic step of CPT1 in the inter-mitochondrial membrane space or before the enzymatic step of CPT2 in the mitochondrial matrix. (Kerner and Hoppel, 2000, Berg et al., 2013)

There are different hypothetical reasons for the observed accumulation of acylcarnitines. This might be an inhibition of the CACT or CPT2 involved in the carnitine dependent long-chain fatty acid shuttling into the mitochondrion. Acylcarnitines might then accumulate in the inter-mitochondrial membrane space or the mitochondrial matrix, respectively. It might also be a downregulation of enzymes

involved in β -oxidation, comprising acyl-CoA dehydrogenase, enoyl-CoA hydratase, 3-hydroxyacyl-CoA-dehydrogenase, or β -ketothiolase. In this case, acyl carnitines would not enter fatty acid catabolism and accumulate in the mitochondrial matrix.

Tracing palmitate uptake using uniformly ^{13}C -labelled palmitate (U- $^{13}\text{C}_{16}$ -palmitate) and its metabolism in treated compared to untreated *T. cruzi* did not provide evidence that β -oxidation or the TCA are affected by waltheriones. However, it also did not refute these hypotheses as inhibiting CPT1 and blocking the initiation of β -oxidation by etomoxir (ETO) also did not show the expected effect on acetate excretion and TCA metabolites (Chapter 3). In *T. cruzi*, it has been shown that 500 μM ETO only affects cells in the late exponential growth phase of parasites under starvation, where fatty acid oxidation gets essential for the epimastigote form (Souza et al., 2021). Effects of ETO were shown at very different concentrations in different organisms and cells (Agius et al., 1991, Kiorpes et al., 1984, Divakaruni et al., 2018). These findings therefore do not exclude that waltheriones might have an effect on fatty acid catabolism.

Instead of using the non-radioactive labelled U- $^{13}\text{C}_{16}$ -palmitate, radiolabelled U- $^{14}\text{C}_{16}$ -labelled palmitate would give a more global picture of metabolic effects caused by the compound. CO_2 as one of the TCA products and a sink for labelled carbon atoms from fatty acid metabolism could additionally be quantified by CO_2 trapping (Souza et al., 2021, Barisón et al., 2016, Girard et al., 2018). Glucose and triglyceride contents of the medium could be measured in parallel using a colorimetric enzymatic assay to estimate the level of glucose starvation (Souza et al., 2021). Experiments would thus be limited by access to the required instruments under appropriate biosafety conditions with *T. cruzi* as a biosafety level 3 parasite, which so far was the limiting factor for such approaches in the scope of this work.

At present, there are different possible explanations for parasite death caused by waltheriones and an accumulation of acylcarnitines. First, parasites might starve to death as soon as all other carbon sources such as glucose are used up and the fatty acid catabolism is blocked. Metabolically active parasites would have a disadvantage in survival. Second, the accumulation of acylcarnitine or a shortage in carnitine might intoxicate the parasite cells (Klein et al., 1982, Gilbert and Klein, 1984, Bringaud et al., 2006). From human diseases, including liver and kidney dysfunction, or endocrine imbalance, it is suggested that L-carnitine has a

detoxifying effect by its ability to bind fatty acids and a role in maintaining CoA balance in mitochondria (Kerner and Hoppel, 1998, Virmani and Cirulli, 2022). *T. brucei brucei* BSF possess a high activity of carnitine acetyltransferase (CAT) (Gilbert and Klein, 1982). CAT catalyses the transfer of the acetyl group from CoA to carnitine resulting in acetylcarnitine which then can be shuttled out of the mitochondrion and converted again to acetyl-CoA and used for lipid biosynthesis and the free carnitine can be recycled. Carnitine had been shown to stimulate acetyl-CoA hydrolysis by CAT (Klein et al., 1982, Gilbert and Klein, 1982). A shortage of carnitine might thus also affect CAT and have an influence on CoA balance in our walterione treated *T. cruzi* parasites. Providing parasites with L-carnitine as a detoxifying agent might reveal a rescuing effect.

6.3 A candidate walterione resistance mutation in mitoribosomes

The most likely candidate resistance mutation revealed by comparative transcriptomics lies in a mitochondrial ribosomal small subunit protein (Chapter 4). This observation is intriguing not only because trypanosomes feature a peculiar mitoribosome architecture but also because it further pinpoints the mitochondrion as the potential target site of walteriones. The individual function of many mitochondrial ribosomal proteins is hypothetical (Ramrath et al., 2018, Scaltsoyiannes et al., 2022). Looking at the homologue in *T. brucei*, the mutation lies in the sequence of the mS52 mitochondrial ribosomal protein which is unique to *Trypanosoma* and could be involved in the assembly of the small subunit (Scaltsoyiannes et al., 2022). Whether the identified mutation solely causes resistance, or together with the two other promising mutations in conserved hypothetical protein genes, needs further investigation.

Different options can be considered to confirm that the mutation confers walterione resistance to *T. cruzi*; i) insert the mutation into the wildtype gene by the use of an integrated CRISPR-Cas9 system (Costa et al., 2018, Beneke et al., 2017) (Chapter 5), ii) create a rescue construct by inserting the wildtype gene into the resistant cell line using homologous recombination (Barnes and McCulloch, 2007), or iii) co-transfect the rescue construct together with CRISPR-Cas9 directly as protein. The most promising approach would be i) as it is an already successfully established method in *T. cruzi*. Furthermore, the finding that walteriones are also

active on procyclic *T. brucei* provides now a well-established model organism to test our hypothesis (Alsford et al., 2012, Beneke et al., 2017). The mutation identified in the *T. cruzi* is conserved in the orthologue gene of *T. brucei*. The mutation could be introduced into *T. brucei*. To test whether the mutation confers resistance drug sensitivity would be assessed. The lower biosafety level of *T. brucei* will greatly facilitate the experimental procedure.

The mRNA to protein translation is the primary function of ribosomes, including the mitoribosomes. A mutation in one subunit might thus affect key translational processes. In human mitochondria, mutations in mitoribosomal proteins led to an effect on the assembly and an influence on mitochondrial protein synthesis, and subsequent respiratory chain deficiencies (Emdadul Haque et al., 2008). In bacteria, antibiotics often target ribosomes and thus interfere with translation (Yassin et al., 2005). Ribosomal and mitoribosomal translation as potential targets were also discussed for aminoglycosides in *Leishmania* and *Trypanosoma* as they were known to target ribosomes in bacteria (Carter et al., 2000). By producing bacterial recombinant ribosomes and mitoribosomes it then had been shown that the aminoglycoside paromomycin affects cytosolic translation in *Leishmania* and *Trypanosoma* (Hobbie et al., 2011). Investigating the effects on mitoribosomal assembly or mitoribosomal translation might be difficult as many subunits seem to have essential roles such as conferring rRNA stability as was researched in *T. brucei* (Lenarčič et al., 2022). We could hypothesise, that the waltheriones target the mitoribosomes decreasing the number of functional mitoribosomes in the cell and impairing translation. A compensatory mutation might prevent an interaction of the waltherione with the mitoribosomal protein without influencing its function in translation.

Confirming the mutations to be responsible for drug resistance is the first next step. Validation and providing direct proof of mitoribosomal proteins as a target will then be another much more challenging step.

6.4 The mitochondrion as a potential target site of waltheriones

Together, the results from untargeted metabolomics and comparative transcriptomics elicited the question of stage specificity of waltheriones in different protozoan parasites as energy acquisition and mitochondrial reliance differ between

life cycle stages. The difference in sensitivity between the bloodstream and procyclic *T. brucei rhodesiense* is a striking observation, as it is known that the bloodstream form *T. brucei* depends on glucose as carbon source (Bringaud et al., 2006).

Extracellular epimastigote *T. cruzi* preferentially use glucose as the primary carbon source *in vitro* (Barisón et al., 2017). However, under starvation, they switch to amino acids and fatty acid catabolism (Barisón et al., 2017, Souza et al., 2021). Intracellular amastigote *T. cruzi* preferentially use amino acids and fatty acids as the primary carbon source. Fatty acid oxidation is upregulated, and enzymes for the tricarboxylic acid cycle are abundant in this stage, which might also be dependent on gluconeogenesis (Atwood et al., 2005). Glucose uptake is downregulated in intracellular amastigote *T. cruzi* and proteome analysis additionally showed the absence of the hexose transporter in this parasite stage (Silber et al., 2009, Atwood et al., 2005). *In vitro*, procyclic *T. brucei* preferentially use glucose as the primary carbon source, similar to extracellular epimastigote *T. cruzi*. However, they switch to amino acids and fatty acid catabolism if no glucose is available, as it happens *in vivo* in the tsetse fly where glucose is scarce (Lamour et al., 2005). Bloodstream form *T. brucei*, on the contrary, depend on glucose for energy generation using glycolysis (Oppenheimer, 1987, Bakker et al., 1995, Bringaud et al., 2006). Their mitochondrion plays a minor role, although enzymes for oxidative phosphorylation, tricarboxylic acid cycle, and the respiratory chain enzymes are present (Bienen et al., 1981, Besteiro et al., 2005). *L. donovani* promastigotes mainly rely on glucose and amino acids as carbon sources, as was also confirmed by stage-specific transcriptomics analysis (Inbar et al., 2017). Upon differentiation to the intracellular amastigote form, *L. donovani* shows reduced glucose consumption and an increased β -oxidation as well as an upregulation of genes involved in the tricarboxylic acid cycle and oxidative phosphorylation (Rosenzweig et al., 2008, Saunders et al., 2014). Our results show that parasite stages relying less on the glycolytic pathway are more sensitive to waltheriones, confirming mitochondrial involvement in a potential mechanism of action.

To collect further evidence for this hypothesis we might evaluate the effects on mitochondrial membrane potential upon drug exposure, the differences in drug uptake by different parasite stages, or test for cross-resistance of waltherione F selected parasites towards drugs with known mechanisms of action. Especially

compounds aiming at mitochondrial targets would be first in focus. Oligomycin, a natural compound from streptomyces, targeting the F₀/F₁-ATP synthase could be one option. It was shown that procyclic *T. brucei* are only sensitive under glucose starvation (Coustou et al., 2003). This would contradict our finding from waltherione being active on procyclic *T. brucei*. Testing waltherione susceptibility on procyclic *T. brucei* grown with and without glucose might thus add valuable information. Rotenone, a natural compound from plants, would be another option. It was shown that at high concentration the NADH-fumarate reductase and mitochondrial respiratory chain are targeted (Hernandez and Turrens, 1998).

Next to antitrypanosomal activity, the antifungal activity of waltheriones was also assessed in different *Candida* species, thus displaying a broad activity spectrum and morphological changes in the plasma membrane and disorganisation of cytoplasmic content. This included the disintegration of mitochondrial structures after waltherione G treatment (Cretton et al., 2016). So far, no molecular target was found.

6.5 How can we test and confirm our findings?

The diverse repertoire of methods suitable for target deconvolution and target identification is especially powerful in a combined approach. With comparative transcriptomics analysis, we miss non-expressed genes and intergenic regions. Comparative genomic analysis as done for melarsoprol- and pentamidine-selected *T. brucei rhodesiense* can fill this gap (Graf et al., 2016).

Affinity-based chemical proteomics is another tool to investigate the interaction between the compound and candidate targets. However, this requires knowledge about the chemical synthesis of the phytochemical molecule and its structure-activity relationship to add modifications such as biotin or immobilise the molecule in a matrix without impairing activity or specificity (Wright and Sieber, 2016). Waltherione F can be chemically synthesised, which is so far not the case for the chiral waltherione G (Zdorichenko et al., 2019). Two positions of the core structure of waltherione F have been in focus to add modifications useful for medicinal chemistry. After affinity purification, interaction partners are identified by mass spectrometry analysis. This method was already successfully applied in *T.*

cruzi and revealed an aldo-keto reductase (TcAKR) among interaction partners of immobilised benzimidazole (Trochine et al., 2014a).

Drug Affinity Responsive Target Stability (DARTS) and cellular thermal shift assay (CETSA) are two label-free methods to assess protein interaction and target engagement. These methods would evade the dependency of a functional group. DARTS is based on the increased proteolytic stability of the target protein conferred by interaction with an inhibitor (Pai et al., 2015, Lomenick et al., 2011, Hwang et al., 2020). CETSA relies on drug-induced thermal stabilisation of a target protein. For instance, the purine nucleoside phosphorylase was identified as a target of the quinoline drug quinine in *Plasmodium falciparum* using CETSA (Dziekan et al., 2019). Applying these methods in *T. cruzi* on walteriones as quinoline related molecules, might reveal candidate target proteins in a straight forward way without requiring any drug modifications. This approach would be new to *T. cruzi*, where prior optimisation will be required especially regarding cell lysis and protein digestion.

Structural biology with crystal structure formation or prediction by AlphaFold (Jumper et al., 2021), combined with modelling of molecular dynamics and docking contributes valuable information in an advanced stage of finding and evaluating a candidate target. Especially mitoribosomes as a potential target might be interesting to investigate. Here we might profit from the research which was performed around mitoribosomal architecture and assembly in *T. brucei* and the knowledge on protein structures in this peculiar trypanosomal complex (Ramrath et al., 2018).

7 Waltheriones and *T. cruzi* – final conclusion

In this study, the investigation of waltherione drug action and drug resistance selection in *T. cruzi* coupled with transcriptomic analysis brought mitochondria into the focus, suggesting fatty acid metabolism to be involved in drug action and the mitoribosome as a potential target. The waltheriones are very attractive molecules because i) they are selective against *T. cruzi*, ii) they are more active on *T. cruzi* than the standard drug benznidazole, iii) they are not prone to resistance *in vitro*, iv) they might guide antitrypanosomal drug research to a new druggable target of *T. cruzi*, and v) they are being further developed as candidate antichagasic molecules by DNDi (INNOSUISSE, 2022). Finding the mechanism of action and possible targets of waltheriones in *T. cruzi* will be a valuable contribution to antichagasic drug discovery and development.

References

- ACOSTA, H., BURCHMORE, R., NAULA, C., GUALDRÓN-LÓPEZ, M., QUINTERO-TROCONIS, E., CÁCERES, A. J., MICHELS, P. A. M., CONCEPCIÓN, J. L. & QUIÑONES, W. 2019. Proteomic analysis of glycosomes from *Trypanosoma cruzi* epimastigotes. *Mol Biochem Parasitol*, 229, 62-74.
- AGIUS, L., PEAK, M. & SHERRATT, S. A. 1991. Differences between human, rat and guinea pig hepatocyte cultures. A comparative study of their rates of beta-oxidation and esterification of palmitate and their sensitivity to R-etomoxir. *Biochem Pharmacol*, 42, 1711-5.
- ALDASORO, E., POSADA, E., REQUENA-MÉNDEZ, A., CALVO-CANO, A., SERRET, N., CASELLAS, A., SANZ, S., SOY, D., PINAZO, M. J. & GASCON, J. 2018. What to expect and when: benznidazole toxicity in chronic Chagas' disease treatment. *J Antimicrob Chemother*, 73, 1060-1067.
- ALI, J. A., CREEK, D. J., BURGESS, K., ALLISON, H. C., FIELD, M. C., MASER, P. & DE KONING, H. P. 2013a. Pyrimidine salvage in *Trypanosoma brucei* bloodstream forms and the trypanocidal action of halogenated pyrimidines. *Mol Pharmacol*, 83, 439-53.
- ALI, J. A., CREEK, D. J., BURGESS, K., ALLISON, H. C., FIELD, M. C., MÄSER, P. & DE KONING, H. P. 2013b. Pyrimidine salvage in *Trypanosoma brucei* bloodstream forms and the trypanocidal action of halogenated pyrimidines. *Mol Pharmacol*, 83, 439-53.
- ALKHALDI, A. A., CREEK, D. J., IBRAHIM, H., KIM, D. H., QUASHIE, N. B., BURGESS, K. E., CHANGTAM, C., BARRETT, M. P., SUKSAMRARN, A. & DE KONING, H. P. 2015. Potent trypanocidal curcumin analogs bearing a monoenone linker motif act on *trypanosoma brucei* by forming an adduct with trypanothione. *Mol Pharmacol*, 87, 451-64.
- ALSFORD, S., ECKERT, S., BAKER, N., GLOVER, L., SANCHEZ-FLORES, A., LEUNG, K. F., TURNER, D. J., FIELD, M. C., BERRIMAN, M. & HORN, D. 2012. High-throughput decoding of antitrypanosomal drug efficacy and resistance. *Nature*, 482, 232-6.
- ALSFORD, S., KAWAHARA, T., GLOVER, L. & HORN, D. 2005. Tagging a *T. brucei* RRNA locus improves stable transfection efficiency and circumvents inducible expression position effects. *Mol Biochem Parasitol*, 144, 142-8.
- ALSFORD, S., TURNER, D. J., OBADO, S. O., SANCHEZ-FLORES, A., GLOVER, L., BERRIMAN, M., HERTZ-FOWLER, C. & HORN, D. 2011. High-throughput phenotyping using parallel sequencing of RNA interference targets in the African trypanosome. *Genome Res*, 21, 915-24.
- ALTSCHUL, S. F., GISH, W., MILLER, W., MYERS, E. W. & LIPMAN, D. J. 1990. Basic local alignment search tool. *J Mol Biol*, 215, 403-10.
- ALZAHIRANI, K. J. H., ALI, J. A. M., EZE, A. A., LOOI, W. L., TAGOE, D. N. A., CREEK, D. J., BARRETT, M. P. & DE KONING, H. P. 2017. Functional and genetic evidence that nucleoside transport is highly conserved in *Leishmania* species: Implications for pyrimidine-based chemotherapy. *Int J Parasitol Drugs Drug Resist*, 7, 206-226.
- ANDERS, S., PYL, P. T. & HUBER, W. 2015. HTSeq--a Python framework to work with high-throughput sequencing data. *Bioinformatics*, 31, 166-9.

- APHASIZHEVA, I., MASLOV, D. A. & APHASIZHEV, R. 2013. Kinetoplast DNA-encoded ribosomal protein S12: a possible functional link between mitochondrial RNA editing and translation in *Trypanosoma brucei*. *RNA Biol*, 10, 1679-88.
- ATWOOD, J. A., 3RD, WEATHERLY, D. B., MINNING, T. A., BUNDY, B., CAVOLA, C., OPPERDOES, F. R., ORLANDO, R. & TARLETON, R. L. 2005. The *Trypanosoma cruzi* proteome. *Science*, 309, 473-6.
- BABRAHAM BIOINFORMATICS. 2022. FastQC A Quality Control tool for High Throughput Sequence Data [Online]. Available: <https://www.bioinformatics.babraham.ac.uk/projects/fastqc/> [Accessed 12.05.2022 2022].
- BAHIA, M. T., DE ANDRADE, I. M., MARTINS, T. A., DO NASCIMENTO Á, F., DINIZ LDE, F., CALDAS, I. S., TALVANI, A., TRUNZ, B. B., TORREELE, E. & RIBEIRO, I. 2012. Fexinidazole: a potential new drug candidate for Chagas disease. *PLoS Negl Trop Dis*, 6, e1870.
- BAKER, N., ALSFORD, S. & HORN, D. 2011. Genome-wide RNAi screens in African trypanosomes identify the nifurtimox activator NTR and the eflornithine transporter AAT6. *Mol Biochem Parasitol*, 176, 55-7.
- BAKKER, B. M., WESTERHOFF, H. V. & MICHELS, P. A. 1995. Regulation and control of compartmentalized glycolysis in bloodstream form *Trypanosoma brucei*. *J Bioenerg Biomembr*, 27, 513-25.
- BALA, A., ADAMU, T., ABUBAKAR, U., LADAN, M. & ABUBAKAR, M. 2010. Studies on the In Vitro Trypanocidal Effect of the Extracts of Some Selected Medicinal Plants in Sokoto State, Nigeria. *Nigerian Journal of Basic and Applied Sciences*, 17.
- BALANCO, J. M., PRAL, E. M., DA SILVA, S., BIJOVSKY, A. T., MORTARA, R. A. & ALFIERI, S. C. 1998. Axenic cultivation and partial characterization of *Leishmania braziliensis* amastigote-like stages. *Parasitology*, 116 (Pt 2), 103-13.
- BALTZ, T., BALTZ, D., GIROUD, C. & CROCKETT, J. 1985. Cultivation in a semi-defined medium of animal infective forms of *Trypanosoma brucei*, *T. equiperdum*, *T. evansi*, *T. rhodesiense* and *T. gambiense*. *EMBO J*, 4, 1273-1277.
- BARISÓN, M. J., DAMASCENO, F. S., MANTILLA, B. S. & SILBER, A. M. 2016. The active transport of histidine and its role in ATP production in *Trypanosoma cruzi*. *J Bioenerg Biomembr*, 48, 437-49.
- BARISÓN, M. J., RAPADO, L. N., MERINO, E. F., FURUSHO PRAL, E. M., MANTILLA, B. S., MARCHESE, L., NOWICKI, C., SILBER, A. M. & CASSERA, M. B. 2017. Metabolomic profiling reveals a finely tuned, starvation-induced metabolic switch in *Trypanosoma cruzi* epimastigotes. *J Biol Chem*, 292, 8964-8977.
- BARNES, R. L. & MCCULLOCH, R. 2007. *Trypanosoma brucei* homologous recombination is dependent on substrate length and homology, though displays a differential dependence on mismatch repair as substrate length decreases. *Nucleic Acids Res*, 35, 3478-93.
- BARNES, R. L., SHI, H., KOLEV, N. G., TSCHUDI, C. & ULLU, E. 2012. Comparative genomics reveals two novel RNAi factors in *Trypanosoma brucei* and provides insight into the core machinery. *PLoS Pathog*, 8, e1002678.

- BARRETT, F. M. & FRIEND, W. G. 1975. Differences in the concentration of free amino acids in the haemolymph of adult male and female *Rhodnius prolixus*. *Comp Biochem Physiol B*, 52, 427-31.
- BATISTA, T. M. & MARQUES, J. T. 2011. RNAi pathways in parasitic protists and worms. *J Proteomics*, 74, 1504-14.
- BEILSTEIN, S., EL PHIL, R., SAHRAOUI, S. S., SCAPOZZA, L., KAISER, M. & MÄSER, P. 2022. Laboratory Selection of Trypanosomatid Pathogens for Drug Resistance. *Pharmaceuticals (Basel)*, 15.
- BELLIARD, A. M., LEROY, C., BANIDE, H., FARINOTTI, R. & LACOUR, B. 2003. Decrease of intestinal P-glycoprotein activity by 2n-propylquinoline, a new oral treatment for visceral leishmaniasis. *Exp Parasitol*, 103, 51-6.
- BENEKE, T. & GLUENZ, E. 2020. Bar-seq strategies for the LeishGEedit toolbox. *Mol Biochem Parasitol*, 239, 111295.
- BENEKE, T., MADDEN, R., MAKIN, L., VALLI, J., SUNTER, J. & GLUENZ, E. 2017. A CRISPR Cas9 high-throughput genome editing toolkit for kinetoplastids. *R Soc Open Sci*, 4, 170095.
- BERENS, R. L., BRUN, R. & KRASSNER, S. M. 1976. A simple monophasic medium for axenic culture of hemoflagellates. *J Parasitol*, 62, 360-5.
- BERENS, R. L., MARR, J. J., LAFON, S. W. & NELSON, D. J. 1981. Purine metabolism in *Trypanosoma cruzi*. *Mol Biochem Parasitol*, 3, 187-96.
- BERG, J. M., TYMOCZKO, J. L. & STRYER, L. 2013. *Biochemie*. Springer Spektrum, 7. Auflage.
- BERGER, B. J., CARTER, N. S. & FAIRLAMB, A. H. 1993. Polyamine and pentamidine metabolism in African trypanosomes. *Acta Trop*, 54, 215-24.
- BERN, C. & MONTGOMERY, S. P. 2009. An estimate of the burden of Chagas disease in the United States. *Clin Infect Dis*, 49, e52-4.
- BERNÁ, L., RODRIGUEZ, M., CHIRIBAO, M. L., PARODI-TALICE, A., PITA, S., RIJO, G., ALVAREZ-VALIN, F. & ROBELLO, C. 2018. Expanding an expanded genome: long-read sequencing of *Trypanosoma cruzi*. *Microb Genom*, 4.
- BERNHARD, S. C., NERIMA, B., MÄSER, P. & BRUN, R. 2007. Melarsoprol- and pentamidine-resistant *Trypanosoma brucei rhodesiense* populations and their cross-resistance. *Int J Parasitol*, 37, 1443-8.
- BERRIMAN, M., GHEDIN, E., HERTZ-FOWLER, C., BLANDIN, G., RENAULD, H., BARTHOLOMEU, D. C., LENNARD, N. J., CALER, E., HAMLIN, N. E., HAAS, B., BÖHME, U., HANNICK, L., ASLETT, M. A., SHALLOM, J., MARCELLO, L., HOU, L., WICKSTEAD, B., ALSMARK, U. C., ARROWSMITH, C., ATKIN, R. J., BARRON, A. J., BRINGAUD, F., BROOKS, K., CARRINGTON, M., CHEREVACH, I., CHILLINGWORTH, T. J., CHURCHER, C., CLARK, L. N., CORTON, C. H., CRONIN, A., DAVIES, R. M., DOGGETT, J., DJIKENG, A., FELDBLYUM, T., FIELD, M. C., FRASER, A., GOODHEAD, I., HANCE, Z., HARPER, D., HARRIS, B. R., HAUSER, H., HOSTETLER, J., IVENS, A., JAGELS, K., JOHNSON, D., JOHNSON, J., JONES, K., KERHORNOU, A. X., KOO, H., LARKE, N., LANDFEAR, S., LARKIN, C., LEECH, V., LINE, A., LORD, A., MACLEOD, A., MOONEY, P. J., MOULE, S., MARTIN, D. M., MORGAN, G. W., MUNGALL, K., NORBERTCZAK, H., ORMOND, D., PAI, G., PEACOCK, C. S., PETERSON, J., QUAIL, M. A., RABBINOWITSCH, E., RAJANDREAM, M. A., REITTER, C., SALZBERG, S. L., SANDERS, M., SCHOBEL, S., SHARP, S., SIMMONDS, M., SIMPSON, A. J., TALLON, L., TURNER, C.

- M., TAIT, A., TIVEY, A. R., VAN AKEN, S., WALKER, D., WANLESS, D., WANG, S., WHITE, B., WHITE, O., WHITEHEAD, S., WOODWARD, J., WORTMAN, J., ADAMS, M. D., EMBLEY, T. M., GULL, K., ULLU, E., BARRY, J. D., FAIRLAMB, A. H., OPPERDOES, F., BARRELL, B. G., DONELSON, J. E., HALL, N., FRASER, C. M., et al. 2005. The genome of the African trypanosome *Trypanosoma brucei*. *Science*, 309, 416-22.
- BESTEIRO, S., BARRETT, M. P., RIVIÈRE, L. & BRINGAUD, F. 2005. Energy generation in insect stages of *Trypanosoma brucei*: metabolism in flux. *Trends Parasitol*, 21, 185-91.
- BEVERLEY, S. M., CODERRE, J. A., SANTI, D. V. & SCHIMKE, R. T. 1984. Unstable DNA amplifications in methotrexate-resistant *Leishmania* consist of extrachromosomal circles which relocalize during stabilization. *Cell*, 38, 431-439.
- BHATTACHARYA, A., LEPROHON, P., BIGOT, S., PADMANABHAN, P. K., MUKHERJEE, A., ROY, G., GINGRAS, H., MESTDAGH, A., PAPADOPOULOU, B. & OUELLETTE, M. 2019. Coupling chemical mutagenesis to next generation sequencing for the identification of drug resistance mutations in *Leishmania*. *Nat Commun*, 10, 5627.
- BIENEN, E. J., HAMMADI, E. & HILL, G. C. 1981. *Trypanosoma brucei*: biochemical and morphological changes during in vitro transformation of bloodstream- to procyclic-trypomastigotes. *Exp Parasitol*, 51, 408-17.
- BRIDGES, D. J., GOULD, M. K., NERIMA, B., MÄSER, P., BURCHMORE, R. J. & DE KONING, H. P. 2007. Loss of the high-affinity pentamidine transporter is responsible for high levels of cross-resistance between arsenical and diamidine drugs in African trypanosomes. *Mol Pharmacol*, 71, 1098-108.
- BRINGAUD, F., RIVIÈRE, L. & COUSTOU, V. 2006. Energy metabolism of trypanosomatids: adaptation to available carbon sources. *Mol Biochem Parasitol*, 149, 1-9.
- BROAD INSTITUTE. 2022. Picard Tools [Online]. Available: <https://broadinstitute.github.io/picard/> [Accessed 18.05.2022].
- BROOK, K., BENNETT, J. & DESAI, S. P. 2017. The Chemical History of Morphine: An 8000-year Journey, from Resin to de-novo Synthesis. *J Anesth Hist*, 3, 50-55.
- BRUN, R. & SCHÖNENBERGER, M. 1979. Cultivation and in vivo cloning of procyclic culture forms of *Trypanosoma brucei* in a semi-defined medium. *Acta Trop.*, 36, 289-292.
- BUCKNER, F. S., WILSON, A. J., WHITE, T. C. & VAN VOORHIS, W. C. 1998. Induction of resistance to azole drugs in *Trypanosoma cruzi*. *Antimicrob Agents Chemother*, 42, 3245-50.
- BURKARD, G., FRAGOSO, C. M. & RODITI, I. 2007. Highly efficient stable transformation of bloodstream forms of *Trypanosoma brucei*. *Mol Biochem Parasitol*, 153, 220-3.
- CALLEJAS-HERNÁNDEZ, F., HERREROS-CABELLO, A., DEL MORAL-SALMORAL, J., FRESNO, M. & GIRONÈS, N. 2021. The Complete Mitochondrial DNA of *Trypanosoma cruzi*: Maxicircles and Minicircles. *Front Cell Infect Microbiol*, 11, 672448.
- CAMPOS, M. C., CASTRO-PINTO, D. B., RIBEIRO, G. A., BERREDO-PINHO, M. M., GOMES, L. H., DA SILVA BELLINENY, M. S., GOULART, C. M., ECHEVARRIA, A. & LEON, L. L. 2013. P-glycoprotein efflux pump plays an

- important role in *Trypanosoma cruzi* drug resistance. *Parasitol Res*, 112, 2341-51.
- CAMPOS, M. C., LEON, L. L., TAYLOR, M. C. & KELLY, J. M. 2014. Benznidazole-resistance in *Trypanosoma cruzi*: evidence that distinct mechanisms can act in concert. *Mol Biochem Parasitol*, 193, 17-9.
- CAMPOS, M. C., PHELAN, J., FRANCISCO, A. F., TAYLOR, M. C., LEWIS, M. D., PAIN, A., CLARK, T. G. & KELLY, J. M. 2017. Genome-wide mutagenesis and multi-drug resistance in American trypanosomes induced by the front-line drug benznidazole. *Sci Rep*, 7, 14407.
- CARTER, A. P., CLEMONS, W. M., BRODERSEN, D. E., MORGAN-WARREN, R. J., WIMBERLY, B. T. & RAMAKRISHNAN, V. 2000. Functional insights from the structure of the 30S ribosomal subunit and its interactions with antibiotics. *Nature*, 407, 340-8.
- CARTER, N. S. & FAIRLAMB, A. H. 1993. Arsenical-resistant trypanosomes lack an unusual adenosine transporter. *Nature*, 361, 173-6.
- CDC. 2021. Parasites - American Trypanosomiasis (also known as Chagas Disease), Antiparasitic Treatment [Online]. Available: https://www.cdc.gov/parasites/chagas/health_professionals/tx.html [Accessed 18.04.2023].
- CDC. 2022. Neglected Tropical Diseases, Diseases [Online]. Available: <https://www.cdc.gov/globalhealth/ntd/diseases/index.html> [Accessed 10.05.2023].
- CHAMBERS, M. C., MACLEAN, B., BURKE, R., AMODEI, D., RUDERMAN, D. L., NEUMANN, S., GATTO, L., FISCHER, B., PRATT, B., EGERTSON, J., HOFF, K., KESSNER, D., TASMAN, N., SHULMAN, N., FREWEN, B., BAKER, T. A., BRUSNIAK, M. Y., PAULSE, C., CREASY, D., FLASHNER, L., KANI, K., MOULDING, C., SEYMOUR, S. L., NUWAYSIR, L. M., LEFEBVRE, B., KUHLMANN, F., ROARK, J., RAINER, P., DETLEV, S., HEMENWAY, T., HUHMER, A., LANGRIDGE, J., CONNOLLY, B., CHADICK, T., HOLLY, K., ECKELS, J., DEUTSCH, E. W., MORITZ, R. L., KATZ, J. E., AGUS, D. B., MACCOSS, M., TABB, D. L. & MALLICK, P. 2012. A cross-platform toolkit for mass spectrometry and proteomics. *Nature Biotechnology*, 30, 918-920.
- CHATELAIN, E. 2015. Chagas Disease Drug Discovery: Toward a New Era. 20, 22-35.
- CHATELAIN, E. & IOSET, J. R. 2018. Phenotypic screening approaches for Chagas disease drug discovery. *Expert Opin Drug Discov*, 13, 141-153.
- CHIDLEY, C., HARUKI, H., PEDERSEN, M. G., MULLER, E. & JOHANSSON, K. 2011. A yeast-based screen reveals that sulfasalazine inhibits tetrahydrobiopterin biosynthesis. *Nat Chem Biol*, 7, 375-83.
- CHIQUERO, M. J., PÉREZ-VICTORIA, J. M., O'VALLE, F., GONZÁLEZ-ROS, J. M., DEL MORAL, R. G., FERRAGUT, J. A., CASTANYS, S. & GAMARRO, F. 1998. Altered drug membrane permeability in a multidrug-resistant *Leishmania tropica* line. *Biochem Pharmacol*, 55, 131-9.
- CHUGH, M., SCHEURER, C., SAX, S., BILSLAND, E., VAN SCHALKWYK, D. A., WICHT, K. J., HOFMANN, N., SHARMA, A., BASHYAM, S., SINGH, S., OLIVER, S. G., EGAN, T. J., MALHOTRA, P., SUTHERLAND, C. J., BECK, H. P., WITTLIN, S., SPANGENBERG, T. & DING, X. C. 2015. Identification and deconvolution of cross-resistance signals from antimalarial compounds

- using multidrug-resistant *Plasmodium falciparum* strains. *Antimicrob Agents Chemother*, 59, 1110-8.
- CINGOLANI, P., PLATTS, A., WANG LE, L., COON, M., NGUYEN, T., WANG, L., LAND, S. J., LU, X. & RUDEN, D. M. 2012. A program for annotating and predicting the effects of single nucleotide polymorphisms, SnpEff: SNPs in the genome of *Drosophila melanogaster* strain w1118; iso-2; iso-3. *Fly (Austin)*, 6, 80-92.
- CONTRERAS, V. T., MOREL, C. M. & GOLDENBERG, S. 1985. Stage specific gene expression precedes morphological changes during *Trypanosoma cruzi* metacyclogenesis. *Mol Biochem Parasitol*, 14, 83-96.
- COSTA, F. C., FRANCISCO, A. F., JAYAWARDHANA, S., CALDERANO, S. G., LEWIS, M. D., OLMO, F., BENEKE, T., GLUENZ, E., SUNTER, J., DEAN, S., KELLY, J. M. & TAYLOR, M. C. 2018. Expanding the toolbox for *Trypanosoma cruzi*: A parasite line incorporating a bioluminescence-fluorescence dual reporter and streamlined CRISPR/Cas9 functionality for rapid in vivo localisation and phenotyping. *PLoS Negl Trop Dis*, 12, e0006388.
- COUSTOU, V., BESTEIRO, S., BIRAN, M., DIOLEZ, P., BOUCHAUD, V., VOISIN, P., MICHELS, P. A., CANIONI, P., BALTZ, T. & BRINGAUD, F. 2003. ATP generation in the *Trypanosoma brucei* procyclic form: cytosolic substrate level is essential, but not oxidative phosphorylation. *J Biol Chem*, 278, 49625-35.
- CREEK, D. J., CHUA, H. H., COBBOLD, S. A., NIJAGAL, B., MACRAE, J. I., DICKERMAN, B. K., GILSON, P. R., RALPH, S. A. & MCCONVILLE, M. J. 2016. Metabolomics-Based Screening of the Malaria Box Reveals both Novel and Established Mechanisms of Action. *Antimicrob Agents Chemother*, 60, 6650-6663.
- CREEK, D. J., JANKEVICS, A., BREITLING, R., WATSON, D. G., BARRETT, M. P. & BURGESS, K. E. 2011. Toward global metabolomics analysis with hydrophilic interaction liquid chromatography-mass spectrometry: improved metabolite identification by retention time prediction. *Anal Chem*, 83, 8703-10.
- CRETTON, S., BREANT, L., POURREZ, L., AMBUEHL, C., MARCOURT, L., EBRAHIMI, S. N., HAMBURGER, M., PEROZZO, R., KARIMOU, S., KAISER, M., CUENDET, M. & CHRISTEN, P. 2014. Antitrypanosomal Quinoline Alkaloids from the Roots of *Waltheria indica*. *Journal of Natural Products*, 77, 2304-2311.
- CRETTON, S., BREANT, L., POURREZ, L., AMBUEHL, C., PEROZZO, R., MARCOURT, L., KAISER, M., CUENDET, M. & CHRISTEN, P. 2015. Chemical constituents from *Waltheria indica* exert in vitro activity against *Trypanosoma brucei* and *T. cruzi*. *Fitoterapia*, 105, 55-60.
- CRETTON, S., DORSAZ, S., AZZOLLINI, A., FAVRE-GODAL, Q., MARCOURT, L., EBRAHIMI, S. N., VOINESCO, F., MICHELLOD, E., SANGLARD, D., GINDRO, K., WOLFENDER, J.-L., CUENDET, M. & CHRISTEN, P. 2016. Antifungal Quinoline Alkaloids from *Waltheria indica*. *Journal of Natural Products*, 79, 300-307.
- DATTANI, A., DRAMMEH, I., MAHMOOD, A., RAHMAN, M., SZULAR, J. & WILKINSON, S. R. 2021. Unraveling the antitrypanosomal mechanism of benzimidazole and related 2-nitroimidazoles: From prodrug activation to DNA damage. *Mol Microbiol*, 116, 674-689.

- DAWIDOWSKI, M., EMMANOUILIDIS, L., KALEL, V. C., TRIPSANES, K., SCHORPP, K., HADIAN, K., KAISER, M., MASER, P., KOLONKO, M., TANGHE, S., RODRIGUEZ, A., SCHLIEBS, W., ERDMANN, R., SATTLER, M. & POPOWICZ, G. M. 2017. Inhibitors of PEX14 disrupt protein import into glycosomes and kill Trypanosoma parasites. *Science*, 355, 1416-1420.
- DE KONING, H. 2001. Uptake of pentamidine in Trypanosoma brucei is mediated by three distinct transporters: implications for cross-resistance with arsenicals. *Mol Pharmacol*, 59, 586-592.
- DE SOUZA, W., DE CARVALHO, T. M. & BARRIAS, E. S. 2010. Review on Trypanosoma cruzi: Host Cell Interaction. *Int J Cell Biol*, 2010.
- DEAN, S., GOULD, M. K., DEWAR, C. E. & SCHNAUFER, A. C. 2013. Single point mutations in ATP synthase compensate for mitochondrial genome loss in trypanosomes. *Proc Natl Acad Sci U S A*, 110, 14741-6.
- DETKE, S., KATAKURA, K. & CHANG, K. P. 1989. DNA amplification in arsenite-resistant Leishmania. *Exp Cell Res*, 180, 161-70.
- DIETERLE, F., ROSS, A., SCHLOTTERBECK, G. & SENN, H. 2006. Probabilistic quotient normalization as robust method to account for dilution of complex biological mixtures. Application in 1H NMR metabonomics. *Anal Chem*, 78, 4281-90.
- DING, X. C., UBBEN, D. & WELLS, T. N. 2012. A framework for assessing the risk of resistance for anti-malarials in development. *Malar J*, 11, 292.
- DIVAKARUNI, A. S., HSIEH, W. Y., MINARRIETA, L., DUONG, T. N., KIM, K. K. O., DESOUSA, B. R., ANDREYEV, A. Y., BOWMAN, C. E., CARADONNA, K., DRANKA, B. P., FERRICK, D. A., LIESA, M., STILES, L., ROGERS, G. W., BRAAS, D., CIARALDI, T. P., WOLFGANG, M. J., SPARWASSER, T., BEROD, L., BENSINGER, S. J. & MURPHY, A. N. 2018. Etomoxir Inhibits Macrophage Polarization by Disrupting CoA Homeostasis. *Cell Metab*, 28, 490-503.e7.
- DOCAMPO, R. 2011. Molecular parasitology in the 21st century. *Essays Biochem*, 51, 1-13.
- DOS SANTOS, F. M., CALDAS, S., DE ASSIS CÁU, S. B., CREPALDE, G. P., DE LANA, M., MACHADO-COELHO, G. L., VELOSO, V. M. & BAHIA, M. T. 2008. Trypanosoma cruzi: Induction of benznidazole resistance in vivo and its modulation by in vitro culturing and mice infection. *Exp Parasitol*, 120, 385-90.
- DOWNING, T., IMAMURA, H., DECUYPERE, S., CLARK, T. G., COOMBS, G. H., COTTON, J. A., HILLEY, J. D., DE DONCKER, S., MAES, I., MOTTRAM, J. C., QUAIL, M. A., RIJAL, S., SANDERS, M., SCHÖNIAN, G., STARK, O., SUNDAR, S., VANAERSCHOT, M., HERTZ-FOWLER, C., DUJARDIN, J. C. & BERRIMAN, M. 2011. Whole genome sequencing of multiple Leishmania donovani clinical isolates provides insights into population structure and mechanisms of drug resistance. *Genome Res*, 21, 2143-56.
- DÜHRKOP, K., FLEISCHAUER, M., LUDWIG, M., AKSENOV, A. A., MELNIK, A. V., MEUSEL, M., DORRESTEIN, P. C., ROUSU, J. & BÖCKER, S. 2019. SIRIUS 4: a rapid tool for turning tandem mass spectra into metabolite structure information. *Nat Methods*, 16, 299-302.
- DÜHRKOP, K., NOTHIAS, L. F., FLEISCHAUER, M., REHER, R., LUDWIG, M., HOFFMANN, M. A., PETRAS, D., GERWICK, W. H., ROUSU, J., DORRESTEIN, P. C. & BÖCKER, S. 2021. Systematic classification of

- unknown metabolites using high-resolution fragmentation mass spectra. *Nat Biotechnol*, 39, 462-471.
- DÜHRKOP, K., SHEN, H., MEUSEL, M., ROUSU, J. & BÖCKER, S. 2015. Searching molecular structure databases with tandem mass spectra using CSI:FingerID. *Proc Natl Acad Sci U S A*, 112, 12580-5.
- DUMOULIN, P. C. & BURLEIGH, B. A. 2018. Stress-Induced Proliferation and Cell Cycle Plasticity of Intracellular *Trypanosoma cruzi* Amastigotes. *MBio*, 9.
- DUNN, W. B., BROADHURST, D., BEGLEY, P., ZELENA, E., FRANCIS-MCINTYRE, S., ANDERSON, N., BROWN, M., KNOWLES, J. D., HALSALL, A., HASELDEN, J. N., NICHOLLS, A. W., WILSON, I. D., KELL, D. B. & GOODACRE, R. 2011. Procedures for large-scale metabolic profiling of serum and plasma using gas chromatography and liquid chromatography coupled to mass spectrometry. *Nat Protoc*, 6, 1060-83.
- DVORAK, J. A. & HYDE, T. P. 1973. *Trypanosoma cruzi*: Interaction with vertebrate cells in vitro. 34, 268-283.
- DZIEKAN, J. M., YU, H., CHEN, D., DAI, L., WIRJANATA, G., LARSSON, A., PRABHU, N., SOBOTA, R. M., BOZDECH, Z. & NORDLUND, P. 2019. Identifying purine nucleoside phosphorylase as the target of quinine using cellular thermal shift assay. *Sci Transl Med*, 11.
- EDDY, S. R. 2009. A new generation of homology search tools based on probabilistic inference. *Genome Inform*, 23, 205-11.
- EDWARDS, D. I. 1993. Nitroimidazole drugs--action and resistance mechanisms. I. Mechanisms of action. *J Antimicrob Chemother*, 31, 9-20.
- EHRlich, P. 1907. Chemotherapeutische Trypanosomen-Studien. *Berliner klinische Wochenschrift*, 11, 310-314.
- EHRlich, P. 1908. Partial cell functions. Nobel Lecture.
- EL-SAYED, N. M., MYLER, P. J., BARTHOLOMEU, D. C., NILSSON, D., AGGARWAL, G., TRAN, A. N., GHEDIN, E., WORTHEY, E. A., DELCHER, A. L., BLANDIN, G., WESTENBERGER, S. J., CALER, E., CERQUEIRA, G. C., BRANCHE, C., HAAS, B., ANUPAMA, A., ARNER, E., ASLUND, L., ATTIPOE, P., BONTEMPI, E., BRINGAUD, F., BURTON, P., CADAG, E., CAMPBELL, D. A., CARRINGTON, M., CRABTREE, J., DARBAN, H., DA SILVEIRA, J. F., DE JONG, P., EDWARDS, K., ENGLUND, P. T., FAZELINA, G., FELDBLYUM, T., FERELLA, M., FRASCH, A. C., GULL, K., HORN, D., HOU, L., HUANG, Y., KINDLUND, E., KLINGBEIL, M., KLUGE, S., KOO, H., LACERDA, D., LEVIN, M. J., LORENZI, H., LOUIE, T., MACHADO, C. R., MCCULLOCH, R., MCKENNA, A., MIZUNO, Y., MOTTRAM, J. C., NELSON, S., OCHAYA, S., OSOEGAWA, K., PAI, G., PARSONS, M., PENTONY, M., PETTERSSON, U., POP, M., RAMIREZ, J. L., RINTA, J., ROBERTSON, L., SALZBERG, S. L., SANCHEZ, D. O., SEYLER, A., SHARMA, R., SHETTY, J., SIMPSON, A. J., SISK, E., TAMMI, M. T., TARLETON, R., TEIXEIRA, S., VAN AKEN, S., VOGT, C., WARD, P. N., WICKSTEAD, B., WORTMAN, J., WHITE, O., FRASER, C. M., STUART, K. D. & ANDERSSON, B. 2005. The genome sequence of *Trypanosoma cruzi*, etiologic agent of Chagas disease. *Science*, 309, 409-15.
- EL GHOUZZI, M. H., BOIRET, E., WIND, F., BROCHARD, C., FITTERE, S., PARIS, L., MAZIER, D., SANSONETTI, N. & BIERLING, P. 2010. Testing blood donors for Chagas disease in the Paris area, France: first results after 18 months of screening. *Transfusion*, 50, 575-83.

- ELLENBERGER, T. E. & BEVERLEY, S. M. 1989. Multiple drug resistance and conservative amplification of the H region in *Leishmania major*. *J. Biol. Chem.*, 264, 15094-15103.
- EMDADUL HAQUE, M., GRASSO, D., MILLER, C., SPREMULLI, L. L. & SAADA, A. 2008. The effect of mutated mitochondrial ribosomal proteins S16 and S22 on the assembly of the small and large ribosomal subunits in human mitochondria. *Mitochondrion*, 8, 254-61.
- ENGEL, J. C. & DVORAK, J. A. 1988. *Trypanosoma cruzi*: cell biological behavior of epimastigote and amastigote forms in axenic culture. *J Protozool*, 35, 513-8.
- FAIRLAMB, A. H., CARTER, N. S., CUNNINGHAM, M. & SMITH, K. 1992. Characterisation of melarsen-resistant *Trypanosoma brucei brucei* with respect to cross-resistance to other drugs and trypanothione metabolism. *Mol. Biochem. Parasitol.*, 53, 213-222.
- FERNANDES, J. F. & CASTELLANI, O. 1966. Growth Characteristics and Chemical Composition of *Trypanosoma cruzi*. *Experimental Parasitology*, 18,(2), 195-202.
- FERNANDEZ-PRADA, C., SHARMA, M., PLOURDE, M., BRESSON, E., ROY, G., LEPROHON, P. & OUELLETTE, M. 2018. High-throughput Cos-Seq screen with intracellular *Leishmania infantum* for the discovery of novel drug-resistance mechanisms. *Int J Parasitol Drugs Drug Resist*, 8, 165-173.
- FESSER, A. F. 2021. Every parasite counts?! Improving in vitro assay design for Chagas' disease drug discovery. Ph. D. University of Basel.
- FESSER, A. F., BRAISSANT, O., OLMO, F., KELLY, J. M., MÄSER, P. & KAISER, M. 2020. Non-invasive monitoring of drug action: A new live in vitro assay design for Chagas' disease drug discovery. *PLoS Negl Trop Dis*, 14, e0008487.
- FIDALGO, L. M. & GILLE, L. 2011. Mitochondria and Trypanosomatids: Targets and Drugs. *Pharmaceutical Research*, 28, 2758-2770.
- FILLET, M. & FREDERICH, M. 2015. The emergence of metabolomics as a key discipline in the drug discovery process. *Drug Discov Today Technol*, 13, 19-24.
- FLEMING, A. 1945. Penicillin. Nobel Lecture.
- FOLEY, M. & TILLEY, L. 1997. Quinoline antimalarials: mechanisms of action and resistance. *Int J Parasitol*, 27, 231-40.
- FOURNET, A., BARRIOS, A. A., MUÑOZ, V., HOCQUEMILLER, R., CAVÉ, A. & BRUNETON, J. 1993. 2-substituted quinoline alkaloids as potential antileishmanial drugs. *Antimicrob Agents Chemother*, 37, 859-63.
- FROMMEL, T. O. & BALBER, A. E. 1987. Flow cytofluorimetric analysis of drug accumulation by multidrug-resistant *Trypanosoma brucei brucei* and *T. b. rhodesiense*. *Mol. Biochem. Parasitol.*, 26, 183-192.
- FULTON, J. D. & YORKE, W. 1942. Further Observations on the Stability of Drug-Resistance in Trypanosomes. *Ann. Trop. Med. Parasitol.*, 35, 221-227.
- FUSTER, V. & SWEENEY, J. M. 2011. Aspirin: a historical and contemporary therapeutic overview. *Circulation*, 123, 768-78.
- GARCÍA-HERNÁNDEZ, R., MANZANO, J. I., CASTANYS, S. & GAMARRO, F. 2012. *Leishmania donovani* develops resistance to drug combinations. *PLoS Negl Trop Dis*, 6, e1974.
- GARCIA, M. N., AGUILAR, D., GORCHAKOV, R., ROSSMANN, S. N., MONTGOMERY, S. P., RIVERA, H., WOC-COLBURN, L., HOTEZ, P. J. &

- MURRAY, K. O. 2015. Evidence of autochthonous Chagas disease in southeastern Texas. *Am J Trop Med Hyg*, 92, 325-30.
- GARCIA SILVA, M. R., TOSAR, J. P., FRUGIER, M., PANTANO, S., BONILLA, B., ESTEBAN, L., SERRA, E., ROVIRA, C., ROBELLO, C. & CAYOTA, A. 2010. Cloning, characterization and subcellular localization of a *Trypanosoma cruzi* argonaute protein defining a new subfamily distinctive of trypanosomatids. *Gene*, 466, 26-35.
- GARVEY, E. P., CODERRE, J. A. & SANTI, D. V. 1985. Selection and properties of *Leishmania tropica* resistant to 10-propargyl-5,8-dideazafolate, an inhibitor of thymidylate synthetase. *Mol Biochem Parasitol*, 17, 79-91.
- GAZANION, É., FERNÁNDEZ-PRADA, C., PAPADOPOULOU, B., LEPROHON, P. & OUELLETTE, M. 2016. Cos-Seq for high-throughput identification of drug target and resistance mechanisms in the protozoan parasite *Leishmania*. *Proc Natl Acad Sci U S A*, 113, E3012-21.
- GILBERT, R. & KLEIN, R. A. 1982. Carnitine stimulates ATP synthesis in *Trypanosoma brucei brucei*. *FEBS Lett*, 141, 271-4.
- GILBERT, R. J. & KLEIN, R. A. 1984. Pyruvate kinase: a carnitine-regulated site of ATP production in *Trypanosoma brucei brucei*. *Comp Biochem Physiol B*, 78, 595-9.
- GIRARD, R., CRISPIM, M., ALENCAR, M. B. & SILBER, A. M. 2018. Uptake of L-Alanine and Its Distinct Roles in the Bioenergetics of *Trypanosoma cruzi*. *mSphere*, 3.
- GLOCKZIN, K., KOSTOMIRIS, D., MINNOW, Y. V. T., SUTHAGAR, K., CLINCH, K., GAI, S., BUCKLER, J. N., SCHRAMM, V. L., TYLER, P. C., MEEK, T. D. & KATZFUSS, A. 2022. Kinetic Characterization and Inhibition of *Trypanosoma cruzi* Hypoxanthine-Guanine Phosphoribosyltransferases. *Biochemistry*, 61, 2088-2105.
- GRAF, F. E., LUDIN, P., ARQUINT, C., SCHMIDT, R. S., SCHAUB, N., KUNZ RENGGLI, C., MUNDAY, J. C., KREZDORN, J., BAKER, N., HORN, D., BALMER, O., CACCONE, A., DE KONING, H. P. & MASER, P. 2016. Comparative genomics of drug resistance in *Trypanosoma brucei rhodesiense*. *Cell Mol Life Sci*, 73, 3387-400.
- GRAY, E. B., LA HOZ, R. M., GREEN, J. S., VIKRAM, H. R., BENEDICT, T., RIVERA, H. & MONTGOMERY, S. P. 2018. Reactivation of Chagas disease among heart transplant recipients in the United States, 2012-2016. *Transpl Infect Dis*, 20, e12996.
- GÜTHER, M. L., URBANIAK, M. D., TAVENDALE, A., PRESCOTT, A. & FERGUSON, M. A. 2014. High-confidence glycosome proteome for procyclic form *Trypanosoma brucei* by epitope-tag organelle enrichment and SILAC proteomics. *J Proteome Res*, 13, 2796-806.
- GYSIN, M., BRAISSANT, O., GILLINGWATER, K., BRUN, R., MÄSER, P. & WENZLER, T. 2018. Isothermal microcalorimetry - A quantitative method to monitor *Trypanosoma congolense* growth and growth inhibition by trypanocidal drugs in real time. *Int J Parasitol Drugs Drug Resist*, 8, 159-164.
- HALL, B. S., BOT, C. & WILKINSON, S. R. 2011. Nifurtimox activation by trypanosomal type I nitroreductases generates cytotoxic nitrile metabolites. *J Biol Chem*, 286, 13088-95.
- HAWKING, F. & WALKER, P. J. 1966. Analysis of the development of arsenical resistance in trypanosomes in vitro. *Exp Parasitol*, 18, 63-86.

- HELLEMOND, J. J., BAKKER, B. M. & TIELENS, A. G. 2005. Energy metabolism and its compartmentation in *Trypanosoma brucei*. *Adv Microb Physiol*, 50, 199-226.
- HENDRICKX, S., MONDELAERS, A., EBERHARDT, E., DELPUTTE, P., COS, P. & MAES, L. 2015. In Vivo Selection of Paromomycin and Miltefosine Resistance in *Leishmania donovani* and *L. infantum* in a Syrian Hamster Model. *Antimicrob Agents Chemother*, 59, 4714-8.
- HERNANDEZ, F. R. & TURRENS, J. F. 1998. Rotenone at high concentrations inhibits NADH-fumarate reductase and the mitochondrial respiratory chain of *Trypanosoma brucei* and *T. cruzi*. *Mol Biochem Parasitol*, 93, 135-7.
- HITZ, E., WIEDEMAR, N., PASSECKER, A., GRAÇA, B. A. S., SCHEURER, C., WITTLIN, S., BRANCUCCI, N. M. B., VAKONAKIS, I., MÄSER, P. & VOSS, T. S. 2021. The 3-phosphoinositide-dependent protein kinase 1 is an essential upstream activator of protein kinase A in malaria parasites. *PLoS Biol*, 19, e3001483.
- HOBBIE, S. N., KAISER, M., SCHMIDT, S., SHCHERBAKOV, D., JANUSIC, T., BRUN, R. & BÖTTGER, E. C. 2011. Genetic reconstruction of protozoan rRNA decoding sites provides a rationale for paromomycin activity against *Leishmania* and *Trypanosoma*. *PLoS Negl Trop Dis*, 5, e1161.
- HORAI, H., ARITA, M., KANAYA, S., NIHEI, Y., IKEDA, T., SUWA, K., OJIMA, Y., TANAKA, K., TANAKA, S., AOSHIMA, K., ODA, Y., KAKAZU, Y., KUSANO, M., TOHGE, T., MATSUDA, F., SAWADA, Y., HIRAI, M. Y., NAKANISHI, H., IKEDA, K., AKIMOTO, N., MAOKA, T., TAKAHASHI, H., ARA, T., SAKURAI, N., SUZUKI, H., SHIBATA, D., NEUMANN, S., IIDA, T., TANAKA, K., FUNATSU, K., MATSUURA, F., SOGA, T., TAGUCHI, R., SAITO, K. & NISHIOKA, T. 2010. MassBank: a public repository for sharing mass spectral data for life sciences. *J Mass Spectrom*, 45, 703-14.
- HOTEZ, P. J., DUMONTEIL, E., HEFFERNAN, M. J. & BOTTAZZI, M. E. 2013. Innovation for the 'bottom 100 million': eliminating neglected tropical diseases in the Americas. *Adv Exp Med Biol*, 764, 1-12.
- HOWARD, E. J., XIONG, X., CARLIER, Y., SOSA-ESTANI, S. & BUEKENS, P. 2014. Frequency of the congenital transmission of *Trypanosoma cruzi*: a systematic review and meta-analysis. *Bjog*, 121, 22-33.
- HUYNH, F. K., GREEN, M. F., KOVES, T. R. & HIRSCHEY, M. D. 2014. Measurement of Fatty Acid Oxidation Rates in Animal Tissues and Cell Lines. Elsevier.
- HWANG, H. Y., KIM, T. Y., SZÁSZ, M. A., DOME, B., MALM, J., MARKO-VARGA, G. & KWON, H. J. 2020. Profiling the Protein Targets of Unmodified Bio-Active Molecules with Drug Affinity Responsive Target Stability and Liquid Chromatography/Tandem Mass Spectrometry. *PROTEOMICS*, 20, 1900325.
- IGOILLO-ESTEVE, M., MAZET, M., DEUMER, G., WALLEMACQ, P. & MICHELS, P. A. 2011. Glycosomal ABC transporters of *Trypanosoma brucei*: characterisation of their expression, topology and substrate specificity. *Int J Parasitol*, 41, 429-38.
- INBAR, E., HUGHITT, V. K., DILLON, L. A., GHOSH, K., EL-SAYED, N. M. & SACKS, D. L. 2017. The Transcriptome of *Leishmania major* Developmental Stages in Their Natural Sand Fly Vector. *mBio*, 8.
- INNOSUISSE. 2022. Development of waltherione F-based chemical entities for Chagas disease [Online]. Available:

- <https://www.aramis.admin.ch/Texte/?ProjectID=43232> [Accessed 15.05.2023].
- IOVANNISCI, D. M. & BEVERLEY, S. M. 1989. Structural alterations of chromosome 2 in *Leishmania major* as evidence for diploidy, including spontaneous amplification of the mini-exon array. *Mol Biochem Parasitol*, 34, 177-88.
- IZETA-ALBERDI, A., IBARRA-CERDENA, C. N., MOO-LLANES, D. A. & RAMSEY, J. M. 2016. Geographical, landscape and host associations of *Trypanosoma cruzi* DTUs and lineages. *Parasit Vectors*, 9, 631.
- JANSEN, O., ANGENOT, L., TITS, M., NICOLAS, J. P., DE MOL, P., NIKIÉMA, J. B. & FRÉDÉRICH, M. 2010. Evaluation of 13 selected medicinal plants from Burkina Faso for their antiplasmodial properties. *Journal of Ethnopharmacology*, 130, 143-150.
- JHINGRAN, A., CHAWLA, B., SAXENA, S., BARRETT, M. P. & MADHUBALA, R. 2009. Paromomycin: uptake and resistance in *Leishmania donovani*. *Mol Biochem Parasitol*, 164, 111-7.
- JUMPER, J., EVANS, R., PRITZEL, A., GREEN, T., FIGURNOV, M., RONNEBERGER, O., TUNYASUVUNAKOOL, K., BATES, R., ŽÍDEK, A., POTAPENKO, A., BRIDGLAND, A., MEYER, C., KOHL, S. A. A., BALLARD, A. J., COWIE, A., ROMERA-PAREDES, B., NIKOLOV, S., JAIN, R., ADLER, J., BACK, T., PETERSEN, S., REIMAN, D., CLANCY, E., ZIELINSKI, M., STEINEGGER, M., PACHOLSKA, M., BERGHAMMER, T., BODENSTEIN, S., SILVER, D., VINYALS, O., SENIOR, A. W., KAVUKCUOGLU, K., KOHLI, P. & HASSABIS, D. 2021. Highly accurate protein structure prediction with AlphaFold. *Nature*, 596, 583-589.
- KAMINSKY, R. & MÄSER, P. 2000. Drug resistance in African trypanosomes. *Curr Opin Anti-Inf Inv Drugs*, 2, 76-82.
- KAUR, K., COONS, T., EMMETT, K. & ULLMAN, B. 1988. Methotrexate-resistant *Leishmania donovani* genetically deficient in the folate-methotrexate transporter. *J. Biol. Chem.*, 263, 7020-7028.
- KEISER, J., ERICSSON, O. & BURRI, C. 2000. Investigations of the metabolites of the trypanocidal drug melarsoprol. *Clin Pharmacol Ther*, 67, 478-88.
- KERNER, J. & HOPPEL, C. 1998. Genetic disorders of carnitine metabolism and their nutritional management. *Annu Rev Nutr*, 18, 179-206.
- KERNER, J. & HOPPEL, C. 2000. Fatty acid import into mitochondria. *Biochim Biophys Acta*, 1486, 1-17.
- KHARE, S., ROACH, S. L., BARNES, S. W., HOEPFNER, D., WALKER, J. R., CHATTERJEE, A. K., NEITZ, R. J., ARKIN, M. R., MCNAMARA, C. W., BALLARD, J., LAI, Y., FU, Y., MOLTENI, V., YEH, V., MCKERROW, J. H., GLYNNE, R. J. & SUPEK, F. 2015. Utilizing Chemical Genomics to Identify Cytochrome b as a Novel Drug Target for Chagas Disease. *PLoS Pathog*, 11, e1005058.
- KIORPES, T. C., HOERR, D., HO, W., WEANER, L. E., INMAN, M. G. & TUTWILER, G. F. 1984. Identification of 2-tetradecylglycidyl coenzyme A as the active form of methyl 2-tetradecylglycidate (methyl palmoxirate) and its characterization as an irreversible, active site-directed inhibitor of carnitine palmitoyltransferase A in isolated rat liver mitochondria. *J Biol Chem*, 259, 9750-5.
- KLEIN, R. A., ANGUS, J. M. & WATERHOUSE, A. E. 1982. Carnitine in *Trypanosoma brucei brucei*. *Mol Biochem Parasitol*, 6, 93-110.

- KOLEV, N. G., TSCHUDI, C. & ULLU, E. 2011. RNA interference in protozoan parasites: achievements and challenges. *Eukaryot Cell*, 10, 1156-63.
- KOLMOGOROV, M., YUAN, J., LIN, Y. & PEVZNER, P. A. 2019. Assembly of long, error-prone reads using repeat graphs. *Nat Biotechnol*, 37, 540-546.
- KOREN, S., WALENZ, B. P., BERLIN, K., MILLER, J. R., BERGMAN, N. H. & PHILLIPPY, A. M. 2017. Canu: scalable and accurate long-read assembly via adaptive k-mer weighting and repeat separation. *Genome Res*, 27, 722-736.
- KRASSNER, S. M. & FLORY, B. 1972. Proline metabolism in *Leishmania donovani* promastigotes. *J Protozool*, 19, 682-5.
- KRISHNAN, A., KLOEHN, J., LUNGHI, M., CHIAPPINO-PEPE, A., WALDMAN, B. S., NICOLAS, D., VARESI, E., HEHL, A., LOURIDO, S., HATZIMANIKATIS, V. & SOLDATI-FAVRE, D. 2020. Functional and Computational Genomics Reveal Unprecedented Flexibility in Stage-Specific *Toxoplasma* Metabolism. *Cell Host Microbe*, 27, 290-306.e11.
- KUBOTA, K., FUNABASHI, M. & OGURA, Y. 2019. Target deconvolution from phenotype-based drug discovery by using chemical proteomics approaches. *Biochim Biophys Acta Proteins Proteom*, 1867, 22-27.
- KUETTEL, S., GREENWALD, J., KOSTREWA, D., AHMED, S., SCAPOZZA, L. & PEROZZO, R. 2011. Crystal structures of *T. b. rhodesiense* adenosine kinase complexed with inhibitor and activator: implications for catalysis and hyperactivation. *PLoS Negl Trop Dis*, 5, e1164.
- KUETTEL, S., MOSIMANN, M., MASER, P., KAISER, M., BRUN, R., SCAPOZZA, L. & PEROZZO, R. 2009. Adenosine Kinase of *T. b. Rhodesiense* identified as the putative target of 4-[5-(4-phenoxyphenyl)-2H-pyrazol-3-yl]morpholine using chemical proteomics. *PLoS Negl Trop Dis*, 3, e506.
- LAMOUR, N., RIVIÈRE, L., COUSTOU, V., COOMBS, G. H., BARRETT, M. P. & BRINGAUD, F. 2005. Proline metabolism in procyclic *Trypanosoma brucei* is down-regulated in the presence of glucose. *J Biol Chem*, 280, 11902-10.
- LANDER, N. & CHIURILLO, M. A. 2019. State-of-the-art CRISPR/Cas9 Technology for Genome Editing in Trypanosomatids. *J Eukaryot Microbiol*.
- LANDER, N., LI, Z. H., NIYOGI, S. & DOCAMPO, R. 2015. CRISPR/Cas9-Induced Disruption of Paraflagellar Rod Protein 1 and 2 Genes in *Trypanosoma cruzi* Reveals Their Role in Flagellar Attachment. *MBio*, 6, e01012.
- LANTERI, C. A., STEWART, M. L., BROCK, J. M., ALIBU, V. P., MESHNICK, S. R., TIDWELL, R. R. & BARRETT, M. P. 2006. Roles for the *Trypanosoma brucei* P2 transporter in DB75 uptake and resistance. *Mol Pharmacol*, 70, 1585-92.
- LEE, B. Y., BACON, K. M., BOTTAZZI, M. E. & HOTEZ, P. J. 2013. Global economic burden of Chagas disease: a computational simulation model. *The Lancet Infectious Diseases*, 13, 342-348.
- LENARČIČ, T., NIEMANN, M., RAMRATH, D. J. F., CALDERARO, S., FLÜGEL, T., SAURER, M., LEIBUNDGUT, M., BOEHRINGER, D., PRANGE, C., HORN, E. K., SCHNEIDER, A. & BAN, N. 2022. Mitoribosomal small subunit maturation involves formation of initiation-like complexes. *Proc Natl Acad Sci U S A*, 119.
- LEPESHEVA, G. I., ZAITSEVA, N. G., NES, W. D., ZHOU, W., ARASE, M., LIU, J., HILL, G. C. & WATERMAN, M. R. 2006. CYP51 from *Trypanosoma cruzi*: a phyla-specific residue in the B' helix defines substrate preferences of sterol 14alpha-demethylase. *J Biol Chem*, 281, 3577-85.

- LEPROHON, P., FERNANDEZ-PRADA, C., GAZANION, E., MONTE-NETO, R. & OUELLETTE, M. 2015. Drug resistance analysis by next generation sequencing in *Leishmania*. *Int J Parasitol Drugs Drug Resist*, 5, 26-35.
- LEWIS, M. D., FORTES FRANCISCO, A., TAYLOR, M. C., BURRELL-SAWARD, H., MCLATCHIE, A. P., MILES, M. A. & KELLY, J. M. 2014. Bioluminescence imaging of chronic *Trypanosoma cruzi* infections reveals tissue-specific parasite dynamics and heart disease in the absence of locally persistent infection. *Cell Microbiol*, 16, 1285-300.
- LI, H. & DURBIN, R. 2009. Fast and accurate short read alignment with Burrows-Wheeler transform. *Bioinformatics*, 25, 1754-60.
- LIPINSKI, C. A. 2004. Lead- and drug-like compounds: the rule-of-five revolution. *Drug Discov Today Technol*, 1, 337-41.
- LIPINSKI, C. A., LOMBARDO, F., DOMINY, B. W. & FEENEY, P. J. 2001. Experimental and computational approaches to estimate solubility and permeability in drug discovery and development settings. *Adv Drug Deliv Rev*, 46, 3-26.
- LOMENICK, B., JUNG, G., WOHLSCHEGEL, J. A. & HUANG, J. 2011. Target identification using drug affinity responsive target stability (DARTS). *Curr Protoc Chem Biol*, 3, 163-180.
- LOPASCHUK, G. D., WALL, S. R., OLLEY, P. M. & DAVIES, N. J. 1988. Etomoxir, a carnitine palmitoyltransferase I inhibitor, protects hearts from fatty acid-induced ischemic injury independent of changes in long chain acylcarnitine. *Circ Res*, 63, 1036-43.
- LOURIE, E. M. & YORKE, W. 1938. The Preparation of Strains of Trypanosomes Resistant to Synthalin and Undecane Diamidine, and an Analysis of Their Characters. *Ann. Trop. Med. Parasitol.*, 201-213.
- LOVE, M. I., HUBER, W. & ANDERS, S. 2014. Moderated estimation of fold change and dispersion for RNA-seq data with DESeq2. *Genome Biol*, 15, 550.
- LUCENA, A. C. R., AMORIM, J. C., DE PAULA LIMA, C. V., BATISTA, M., KRIEGER, M. A., DE GODOY, L. M. F. & MARCHINI, F. K. 2019. Quantitative phosphoproteome and proteome analyses emphasize the influence of phosphorylation events during the nutritional stress of *Trypanosoma cruzi*: the initial moments of in vitro metacyclogenesis. *Cell Stress Chaperones*.
- LYE, L. F., OWENS, K., SHI, H., MURTA, S. M., VIEIRA, A. C., TURCO, S. J., TSCHUDI, C., ULLU, E. & BEVERLEY, S. M. 2010. Retention and loss of RNA interference pathways in trypanosomatid protozoans. *PLoS Pathog*, 6, e1001161.
- MAHMOUD, A. B., MÄSER, P., KAISER, M., HAMBURGER, M. & KHALID, S. 2020. Mining Sudanese Medicinal Plants for Antiprotozoal Agents. *Front Pharmacol*, 11, 865.
- MARQUIS, N., GOUBAL, B., ROSEN, B. P., MUKHOPADHYAY, R. & OUELLETTE, M. 2005. Modulation in aquaglyceroporin AQP1 gene transcript levels in drug-resistant *Leishmania*. *Mol Microbiol*, 57, 1690-9.
- MÄSER, P., GREYER-BÜHLER, Y., KAMINSKY, R. & BRUN, R. 2002. An anti-contamination cocktail for the in vitro isolation and cultivation of parasitic protozoa. *Parasitol Res*, 88, 172-4.
- MÄSER, P., SÜTTERLIN, C., KRALLI, A. & KAMINSKY, R. 1999. A nucleoside transporter from *Trypanosoma brucei* involved in drug resistance. *Science*, 285, 242-4.

- MATOVU, E., STEWART, M. L., GEISER, F., BRUN, R., MÄSER, P., WALLACE, L. J., BURCHMORE, R. J., ENYARU, J. C., BARRETT, M. P., KAMINSKY, R., SEEBECK, T. & DE KONING, H. P. 2003. Mechanisms of arsenical and diamidine uptake and resistance in *Trypanosoma brucei*. *Euk Cell*, 2, 1003-8.
- MATSUDA, N. M., MILLER, S. M. & EVORA, P. R. 2009. The chronic gastrointestinal manifestations of Chagas disease. *Clinics (Sao Paulo)*, 64, 1219-24.
- MATVEYEV, A. V., ALVES, J. M., SERRANO, M. G., LEE, V., LARA, A. M., BARTON, W. A., COSTA-MARTINS, A. G., BEVERLEY, S. M., CAMARGO, E. P., TEIXEIRA, M. M. & BUCK, G. A. 2017. The Evolutionary Loss of RNAi Key Determinants in Kinetoplastids as a Multiple Sporadic Phenomenon. *J Mol Evol*, 84, 104-115.
- MCKENNA, A., HANNA, M., BANKS, E., SIVACHENKO, A., CIBULSKIS, K., KERNYTSKY, A., GARIMELLA, K., ALTSHULER, D., GABRIEL, S., DALY, M. & DEPRISTO, M. A. 2010. The Genome Analysis Toolkit: a MapReduce framework for analyzing next-generation DNA sequencing data. *Genome Res*, 20, 1297-303.
- MEJIA, A. M., HALL, B. S., TAYLOR, M. C., GOMEZ-PALACIO, A., WILKINSON, S. R., TRIANA-CHAVEZ, O. & KELLY, J. M. 2012. Benznidazole-resistance in *Trypanosoma cruzi* is a readily acquired trait that can arise independently in a single population. *J Infect Dis*, 206, 220-8.
- MERCER, L., BOWLING, T., PERALES, J., FREEMAN, J., NGUYEN, T., BACCHI, C., YARLETT, N., DON, R., JACOBS, R. & NARE, B. 2011. 2,4-Diaminopyrimidines as potent inhibitors of *Trypanosoma brucei* and identification of molecular targets by a chemical proteomics approach. *PLoS Negl Trop Dis*, 5, e956.
- MESENTER, L. A. & MILES, M. A. 2015. Evidence and importance of genetic exchange among field populations of *Trypanosoma cruzi*. *Acta Trop*, 151, 150-5.
- MOLINA, I., GOMEZ I PRAT, J., SALVADOR, F., TREVINO, B., SULLEIRO, E., SERRE, N., POU, D., ROURE, S., CABEZOS, J., VALERIO, L., BLANCO-GRAU, A., SANCHEZ-MONTALVA, A., VIDAL, X. & PAHISSA, A. 2014. Randomized trial of posaconazole and benznidazole for chronic Chagas' disease. *N Engl J Med*, 370, 1899-908.
- MOLINA, I., SALVADOR, F., SÁNCHEZ-MONTALVÁ, A., TREVIÑO, B., SERRE, N., SAO AVILÉS, A. & ALMIRANTE, B. 2015. Toxic Profile of Benznidazole in Patients with Chronic Chagas Disease: Risk Factors and Comparison of the Product from Two Different Manufacturers. *Antimicrob Agents Chemother*, 59, 6125-31.
- MURRAY, C. J. L. & LOPEZ, A. D. 2017. Measuring global health: motivation and evolution of the Global Burden of Disease Study. *Lancet*, 390, 1460-1464.
- MURTA, S. M. & ROMANHA, A. J. 1998. In vivo selection of a population of *Trypanosoma cruzi* and clones resistant to benznidazole. *Parasitology*, 116 (Pt 2), 165-71.
- MUSCAT, S., GRASSO, G., SCAPOZZA, L. & DANANI, A. 2023. In silico investigation of cytochrome bc1 molecular inhibition mechanism against *Trypanosoma cruzi*. *PLoS Negl Trop Dis*, 17, e0010545.

- NIRDE, P., LARROQUE, C. & BARNABE, C. 1995. Drug-resistant epimastigotes of *Trypanosoma cruzi* and persistence of this phenotype after differentiation into amastigotes. *C R Acad Sci III*, 318, 1239-44.
- NOGUEIRA, F. B., KRIEGER, M. A., NIRDE, P., GOLDENBERG, S., ROMANHA, A. J. & MURTA, S. M. 2006. Increased expression of iron-containing superoxide dismutase-A (TcFeSOD-A) enzyme in *Trypanosoma cruzi* population with in vitro-induced resistance to benznidazole. *Acta Trop*, 100, 119-32.
- NOZAKI, T. & DVORAK, J. A. 1993. Molecular biology studies of tubercidin resistance in *Trypanosoma cruzi*. *Parasitol. Res.*, 79, 451-455.
- NOZAKI, T., ENGEL, J. C. & DVORAK, J. A. 1996. Cellular and molecular biological analyses of nifurtimox resistance in *Trypanosoma cruzi*. *Am J Trop Med Hyg*, 55, 111-7.
- NYEKO, J. H., GOLDBERGER, T. K. & OTIENO, L. H. 1988. Selection for drug resistance in *Trypanosoma congolense* during cyclic transmissions through *Glossina morsitans morsitans* and drug treated rabbits. *Acta Trop*, 45, 21-6.
- OLMO, F., COSTA, F. C., MANN, G. S., TAYLOR, M. C. & KELLY, J. M. 2018. Optimising genetic transformation of *Trypanosoma cruzi* using hydroxyurea-induced cell-cycle synchronisation. *Molecular and Biochemical Parasitology*, 226, 34-36.
- OPPERDOES, F. R. 1987. Compartmentation of carbohydrate metabolism in trypanosomes. *Annu Rev Microbiol*, 41, 127-51.
- OPPERDOES, F. R., BAUDHUIN, P., COPPENS, I., DE ROE, C., EDWARDS, S. W., WEIJERS, P. J. & MISSET, O. 1984. Purification, morphometric analysis, and characterization of the glycosomes (microbodies) of the protozoan hemoflagellate *Trypanosoma brucei*. *J Cell Biol*, 98, 1178-84.
- OPPERDOES, F. R. & BORST, P. 1977. Localization of nine glycolytic enzymes in a microbody-like organelle in *Trypanosoma brucei*: the glycosome. *FEBS Lett*, 80, 360-4.
- PACHECO-LUGO, L., DÍAZ-OLMOS, Y., SÁENZ-GARCÍA, J., PROBST, C. M. & DAROCHA, W. D. 2017. Effective gene delivery to *Trypanosoma cruzi* epimastigotes through nucleofection. *Parasitol Int*, 66, 236-239.
- PAI, M. Y., LOMENICK, B., HWANG, H., SCHIESTL, R., MCBRIDE, W., LOO, J. A. & HUANG, J. 2015. Drug Affinity Responsive Target Stability (DARTS) for Small-Molecule Target Identification. Springer New York.
- PATRICK, K. L., SHI, H., KOLEV, N. G., ERSFELD, K., TSCHUDI, C. & ULLU, E. 2009. Distinct and overlapping roles for two Dicer-like proteins in the RNA interference pathways of the ancient eukaryote *Trypanosoma brucei*. *Proc Natl Acad Sci U S A*, 106, 17933-8.
- PENG, D., KURUP, S. P., YAO, P. Y., MINNING, T. A. & TARLETON, R. L. 2014. CRISPR-Cas9-mediated single-gene and gene family disruption in *Trypanosoma cruzi*. *MBio*, 6, e02097-14.
- PEREIRA, M. G., VISBAL, G., COSTA, T. F. R., FRASES, S., DE SOUZA, W., ATELLA, G. & CUNHA, E. S. N. 2018. *Trypanosoma cruzi* epimastigotes store cholesteryl esters in lipid droplets after cholesterol endocytosis. *Mol Biochem Parasitol*, 224, 6-16.
- PÉREZ-MOLINA, J. A., CRESPILO-ANDÚJAR, C., BOSCH-NICOLAU, P. & MOLINA, I. 2021. Trypanocidal treatment of Chagas disease. *Enferm Infecc Microbiol Clin (Engl Ed)*, 39, 458-470.

- PÉREZ-MOLINA, J. A. & MOLINA, I. 2018. Chagas disease. *The Lancet*, 391, 82-94.
- PERRY, M. R., WYLLIE, S., RAAB, A., FELDMANN, J. & FAIRLAMB, A. H. 2013. Chronic exposure to arsenic in drinking water can lead to resistance to antimonial drugs in a mouse model of visceral leishmaniasis. *Proc Natl Acad Sci U S A*, 110, 19932-7.
- PETIT, C., BUJARD, A., SKALICKA-WOŹNIAK, K., CRETTON, S., HOURIET, J., CHRISTEN, P., CARRUPT, P. A. & WOLFENDER, J. L. 2016. Prediction of the Passive Intestinal Absorption of Medicinal Plant Extract Constituents with the Parallel Artificial Membrane Permeability Assay (PAMPA). *Planta Med*, 82, 424-31.
- PINAZO, M. J., MIRANDA, B., RODRÍGUEZ-VILLAR, C., ALTCLAS, J., BRUNET SERRA, M., GARCÍA-OTERO, E. C., DE ALMEIDA, E. A., DE LA MATA GARCÍA, M., GASCON, J., GARCÍA RODRÍGUEZ, M., MANITO, N., MORENO CAMACHO, A., OPPENHEIMER, F., PUENTE PUENTE, S., RIASTE, A., SALAS CORONAS, J., SALAVERT LLETÍ, M., SANZ, G. F., TORRICO, F., TORRÚS TENDERO, D., USSETTI, P. & SHIKANAI-YASUDA, M. A. 2011. Recommendations for management of Chagas disease in organ and hematopoietic tissue transplantation programs in nonendemic areas. *Transplant Rev (Orlando)*, 25, 91-101.
- PLUSKAL, T., CASTILLO, S., VILLAR-BRIONES, A. & OREAIC, M. 2010. MZmine 2: Modular framework for processing, visualizing, and analyzing mass spectrometry-based molecular profile data. *BMC Bioinformatics*, 11, 1-11.
- POSPICHAL, H., BRUN, R., KAMINSKY, R. & JENNI, L. 1994. Induction of resistance to melarsenoxide cysteamine (Mel Cy) in *Trypanosoma brucei*. *Acta Trop.*, 58, 187-197.
- QUIÑONES, W., ACOSTA, H., GONÇALVES, C. S., MOTTA, M. C. M., GUALDRÓN-LÓPEZ, M. & MICHELS, P. A. M. 2020. Structure, Properties, and Function of Glycosomes in *Trypanosoma cruzi*. *Front Cell Infect Microbiol*, 10, 25.
- RAJÃO, M. A., FURTADO, C., ALVES, C. L., PASSOS-SILVA, D. G., DE MOURA, M. B., SCHAMBER-REIS, B. L., KUNRATH-LIMA, M., ZUMA, A. A., VIEIRA-DA-ROCHA, J. P., GARCIA, J. B., MENDES, I. C., PENA, S. D., MACEDO, A. M., FRANCO, G. R., DE SOUZA-PINTO, N. C., DE MEDEIROS, M. H., CRUZ, A. K., MOTTA, M. C., TEIXEIRA, S. M. & MACHADO, C. R. 2014. Unveiling benznidazole's mechanism of action through overexpression of DNA repair proteins in *Trypanosoma cruzi*. *Environ Mol Mutagen*, 55, 309-21.
- RAJU, T. N. M. 1998. The Nobel Chronicles. 1908: Elie Metchnikoff (1845–1916) and Paul Ehrlich (1854–1915). *Lancet*, 352, 661.
- RAMÍREZ-TOLOZA, G. & FERREIRA, A. 2017. *Trypanosoma cruzi* Evades the Complement System as an Efficient Strategy to Survive in the Mammalian Host: The Specific Roles of Host/Parasite Molecules and *Trypanosoma cruzi* Calreticulin. *Front Microbiol*, 8, 1667.
- RAMRATH, D. J. F., NIEMANN, M., LEIBUNDGUT, M., BIERI, P., PRANGE, C., HORN, E. K., LEITNER, A., BOEHRINGER, D., SCHNEIDER, A. & BAN, N. 2018. Evolutionary shift toward protein-based architecture in trypanosomal mitochondrial ribosomes. *Science*, 362.
- RANADE, R. M., GILLESPIE, J. R., SHIBATA, S., VERLINDE, C. L., FAN, E., HOL, W. G. & BUCKNER, F. S. 2013. Induced resistance to methionyl-tRNA

- synthetase inhibitors in *Trypanosoma brucei* is due to overexpression of the target. *Antimicrob Agents Chemother*, 57, 3021-8.
- RASSI, A., RASSI, A. & MARIN-NETO, J. A. 2010. Chagas disease. *The Lancet*, 375, 1388-1402.
- RATHOD, P. K., MCERLEAN, T. & LEE, P. C. 1997. Variations in frequencies of drug resistance in *Plasmodium falciparum*. *Proc Natl Acad Sci U S A*, 94, 9389-93.
- REQUENA-MÉNDEZ, A., ALDASORO, E., DE LAZZARI, E., SICURI, E., BROWN, M., MOORE, D. A. J., GASCON, J. & MUÑOZ, J. 2015. Prevalence of Chagas Disease in Latin-American Migrants Living in Europe: A Systematic Review and Meta-analysis. *PLOS Neglected Tropical Diseases*, 9, e0003540.
- RESENDE, B. C., OLIVEIRA, A. C. S., GUAÑABENS, A. C. P., REPOLÊS, B. M., SANTANA, V., HIRAIWA, P. M., PENA, S. D. J., FRANCO, G. R., MACEDO, A. M., TAHARA, E. B., FRAGOSO, S. P., ANDRADE, L. O. & MACHADO, C. R. 2020. The Influence of Recombinational Processes to Induce Dormancy in *Trypanosoma cruzi*. *Front Cell Infect Microbiol*, 10, 5.
- REVOLLO, S., OURY, B., VELA, A., TIBAYRENC, M. & SERENO, D. 2019. In Vitro Benzimidazole and Nifurtimox Susceptibility Profile of *Trypanosoma cruzi* Strains Belonging to Discrete Typing Units TcI, TcII, and TcV. *Pathogens*, 8.
- RICO, E., JEACOCK, L., KOVÁŘOVÁ, J. & HORN, D. 2018. Inducible high-efficiency CRISPR-Cas9-targeted gene editing and precision base editing in African trypanosomes. *Sci Rep*, 8, 7960.
- RITZ, C., BATY, F., STREIBIG, J. C. & GERHARD, D. 2015. Dose-Response Analysis Using R. *PLoS One*, 10, e0146021.
- ROLLO, I. M. & WILLIAMSON, J. 1951. Acquired resistance to 'melarsen', tryparsamide and amidines in pathogenic trypanosomes after treatment with 'melarsen' alone. *Nature*, 167, 147-148.
- ROSENZWEIG, D., SMITH, D., OPPERDOES, F., STERN, S., OLAFSON, R. W. & ZILBERSTEIN, D. 2008. Retooling *Leishmania* metabolism: from sand fly gut to human macrophage. *Faseb j*, 22, 590-602.
- SALZBERG, S. L., DELCHER, A. L., KASIF, S. & WHITE, O. 1998. Microbial gene identification using interpolated Markov models. *Nucleic Acids Res*, 26, 544-8.
- SANCHEZ-VALDEZ, F. J., PADILLA, A., WANG, W., ORR, D. & TARLETON, R. L. 2018. Spontaneous dormancy protects *Trypanosoma cruzi* during extended drug exposure. *Elife*, 7.
- SANGSTER, N. C., SONG, J. & DEMELER, J. 2005. Resistance as a tool for discovering and understanding targets in parasite neuromusculature. *Parasitology*, 131 Suppl, S179-90.
- SARKAR, M., HAMILTON, C. J. & FAIRLAMB, A. H. 2003. Properties of phosphoenolpyruvate mutase, the first enzyme in the aminoethylphosphonate biosynthetic pathway in *Trypanosoma cruzi*. *J Biol Chem*, 278, 22703-8.
- SAUNDERS, E. C., NG, W. W., CHAMBERS, J. M., NG, M., NADERER, T., KRÖMER, J. O., LIKIC, V. A. & MCCONVILLE, M. J. 2011. Isotopomer profiling of *Leishmania mexicana* promastigotes reveals important roles for succinate fermentation and aspartate uptake in tricarboxylic acid cycle (TCA) anaplerosis, glutamate synthesis, and growth. *J Biol Chem*, 286, 27706-17.

- SAUNDERS, E. C., NG, W. W., KLOEHN, J., CHAMBERS, J. M., NG, M. & MCCONVILLE, M. J. 2014. Induction of a stringent metabolic response in intracellular stages of *Leishmania mexicana* leads to increased dependence on mitochondrial metabolism. *PLoS Pathog*, 10, e1003888.
- SCALTSOYIANNES, V., CORRE, N., WALTZ, F. & GIEGÉ, P. 2022. Types and Functions of Mitoribosome-Specific Ribosomal Proteins across Eukaryotes. *Int J Mol Sci*, 23.
- SCHMIDT, T. J., KHALID, S. A., ROMANHA, A. J., ALVES, T. M., BIAVATTI, M. W., BRUN, R., DA COSTA, F. B., DE CASTRO, S. L., FERREIRA, V. F., DE LACERDA, M. V., LAGO, J. H., LEON, L. L., LOPES, N. P., DAS NEVES AMORIM, R. C., NIEHUES, M., OGUNGBE, I. V., POHLIT, A. M., SCOTTI, M. T., SETZER, W. N., DE, N. C. S. M., STEINDEL, M. & TEMPONE, A. G. 2012. The potential of secondary metabolites from plants as drugs or leads against protozoan neglected diseases - part I. *Curr Med Chem*, 19, 2128-75.
- SCHNAUFER, A., CLARK-WALKER, G. D., STEINBERG, A. G. & STUART, K. 2005. The F1-ATP synthase complex in bloodstream stage trypanosomes has an unusual and essential function. *Embo j*, 24, 4029-40.
- SCHUMANN BURKARD, G., JUTZI, P. & RODITI, I. 2011. Genome-wide RNAi screens in bloodstream form trypanosomes identify drug transporters. *Mol Biochem Parasitol*, 175, 91-4.
- SCOTT, A. G., TAIT, A. & TURNER, C. M. R. 1997. *Trypanosoma brucei*: lack of cross-resistance to melarsoprol in vitro by cymelarsan-resistant parasites. *Exp. Parasitol.*, 86, 181-190.
- SCOTT, A. G., TAIT, A. & TURNER, M. R. 1996. Characterisation of cloned lines of *Trypanosoma brucei* expressing stable resistance to MelCy and Suramin. *Acta Trop*, 60, 251-262.
- SEIFERT, K., MATU, S., JAVIER PÉREZ-VICTORIA, F., CASTANYS, S., GAMARRO, F. & CROFT, S. L. 2003. Characterisation of *Leishmania donovani* promastigotes resistant to hexadecylphosphocholine (miltefosine). *Int J Antimicrob Agents*, 22, 380-7.
- SHANG, X. F., MORRIS-NATSCHKE, S. L., LIU, Y. Q., LI, X. H., ZHANG, J. Y. & LEE, K. H. 2022. Biology of quinoline and quinazoline alkaloids. *Alkaloids Chem Biol*, 88, 1-47.
- SHAW, S., KNÜSEL, S., HOENNER, S. & RODITI, I. 2020. A transient CRISPR/Cas9 expression system for genome editing in *Trypanosoma brucei*. *BMC Res Notes*, 13, 268.
- SHIKANAI-YASUDA, M. A. & CARVALHO, N. B. 2012. Oral transmission of Chagas disease. *Clin Infect Dis*, 54, 845-52.
- SIGNORELL, A., GLUENZ, E., RETTIG, J., SCHNEIDER, A., SHAW, M. K., GULL, K. & BÜTIKOFER, P. 2009. Perturbation of phosphatidylethanolamine synthesis affects mitochondrial morphology and cell-cycle progression in procyclic-form *Trypanosoma brucei*. *Mol Microbiol*, 72, 1068-79.
- SILBER, A. M., TONELLI, R. R., LOPES, C. G., CUNHA-E-SILVA, N., TORRECILHAS, A. C., SCHUMACHER, R. I., COLLI, W. & ALVES, M. J. 2009. Glucose uptake in the mammalian stages of *Trypanosoma cruzi*. *Mol Biochem Parasitol*, 168, 102-8.
- SLOUD, M. 2007. Main approaches to target discovery and validation. *Methods Mol Biol*, 360, 1-12.
- SLOOF, P., VAN DEN BURG, J., VOOGD, A., BENNE, R., AGOSTINELLI, M., BORST, P., GUTELL, R. & NOLLER, H. 1985. Further characterization of the

- extremely small mitochondrial ribosomal RNAs from trypanosomes: a detailed comparison of the 9S and 12S RNAs from *Crithidia fasciculata* and *Trypanosoma brucei* with rRNAs from other organisms. *Nucleic Acids Res*, 13, 4171-90.
- SOARES MEDEIROS, L. C., SOUTH, L., PENG, D., BUSTAMANTE, J. M., WANG, W., BUNKOFSKE, M., PERUMAL, N., SANCHEZ-VALDEZ, F. & TARLETON, R. L. 2017. Rapid, Selection-Free, High-Efficiency Genome Editing in Protozoan Parasites Using CRISPR-Cas9 Ribonucleoproteins. *mBio*, 8.
- SOKOLOVA, A. Y., WYLLIE, S., PATTERSON, S., OZA, S. L., READ, K. D. & FAIRLAMB, A. H. 2010. Cross-resistance to nitro drugs and implications for treatment of human African trypanosomiasis. *Antimicrob Agents Chemother*, 54, 2893-900.
- SOLLELIS, L., GHORBAL, M., MACPHERSON, C. R., MARTINS, R. M., KUK, N., CROBU, L., BASTIEN, P., SCHERF, A., LOPEZ-RUBIO, J. J. & STERKERS, Y. 2015. First efficient CRISPR-Cas9-mediated genome editing in *Leishmania* parasites. *Cell Microbiol*, 17, 1405-12.
- SOUZA, R. O. O., DAMASCENO, F. S., MARSICCOBETRE, S., BIRAN, M., MURATA, G., CURI, R., BRINGAUD, F. & SILBER, A. M. 2021. Fatty acid oxidation participates in resistance to nutrient-depleted environments in the insect stages of *Trypanosoma cruzi*. *PLoS Pathog*, 17, e1009495.
- SYKES, M. L., KENNEDY, E. K. & AVERY, V. M. 2023. Impact of Laboratory-Adapted Intracellular *Trypanosoma cruzi* Strains on the Activity Profiles of Compounds with Anti-T. *cruzi* Activity. *Microorganisms*, 11.
- TAYLOR, M. C., HUANG, H. & KELLY, J. M. 2011. Genetic techniques in *Trypanosoma cruzi*. *Adv Parasitol*, 75, 231-50.
- TAYLOR, M. C., WARD, A., OLMO, F., JAYAWARDHANA, S., FRANCISCO, A. F., LEWIS, M. D. & KELLY, J. M. 2020. Intracellular DNA replication and differentiation of *Trypanosoma cruzi* is asynchronous within individual host cells in vivo at all stages of infection. *PLoS Negl Trop Dis*, 14, e0008007.
- TEKA, I. A., KAZIBWE, A. J., EL-SABBAGH, N., AL-SALABI, M. I., WARD, C. P., EZE, A. A., MUNDAY, J. C., MÄSER, P., MATOVU, E., BARRETT, M. P. & DE KONING, H. P. 2011. The diamidine diminazene aceturate is a substrate for the high-affinity pentamidine transporter: implications for the development of high resistance levels in trypanosomes. *Mol Pharmacol*, 80, 110-6.
- TERSTAPPEN, G. C., SCHLÜPEN, C., RAGGIASCHI, R. & GAVIRAGHI, G. 2007. Target deconvolution strategies in drug discovery. *Nat Rev Drug Discov*, 6, 891-903.
- THORVALDSDÓTTIR, H., ROBINSON, J. T. & MESIROV, J. P. 2013. Integrative Genomics Viewer (IGV): high-performance genomics data visualization and exploration. *Brief Bioinform*, 14, 178-92.
- TORRICO, F., GASCÓN, J., ORTIZ, L., PINTO, J., ROJAS, G., PALACIOS, A., BARREIRA, F., BLUM, B., SCHIJMAN, A. G., VAILLANT, M., STRUB-WOURGAFT, N., PINAZO, M. J., BILBE, G. & RIBEIRO, I. 2023. A Phase 2, Randomized, Multicenter, Placebo-Controlled, Proof-of-Concept Trial of Oral Fexinidazole in Adults With Chronic Indeterminate Chagas Disease. *Clin Infect Dis*, 76, e1186-e1194.
- TROCHINE, A., ALVAREZ, G., CORRE, S., FARAL-TELLO, P., DURÁN, R., BATTHYANY, C. I., CERECETTO, H., GONZÁLEZ, M. & ROBELLO, C.

- 2014a. *Trypanosoma cruzi* chemical proteomics using immobilized benzimidazole. *Exp Parasitol*, 140, 33-8.
- TROCHINE, A., CREEK, D. J., FARAL-TELLO, P., BARRETT, M. P. & ROBELLO, C. 2014b. Benzimidazole biotransformation and multiple targets in *Trypanosoma cruzi* revealed by metabolomics. *PLoS Negl Trop Dis*, 8, e2844.
- TROTTA, R. F., BROWN, M. L., TERRELL, J. C. & GEYER, J. A. 2004. Defective DNA repair as a potential mechanism for the rapid development of drug resistance in *Plasmodium falciparum*. *Biochemistry*, 43, 4885-91.
- TU, Y. 2016. Artemisinin-A Gift from Traditional Chinese Medicine to the World (Nobel Lecture). *Angew Chem Int Ed Engl*, 55, 10210-26.
- ULLMAN, B., CARRERO-VALENZUELA, E. & COONS, T. 1989. *Leishmania donovani*: isolation and characterization of sodium stibogluconate (Pentostam)-resistant cell lines. *Exp Parasitol*, 69, 157-63.
- UNIPROT CONSORTIUM 2023. UniProt: the Universal Protein Knowledgebase in 2023. *Nucleic Acids Res*, 51, D523-d531.
- URBINA, J. A. & DOCAMPO, R. 2003. Specific chemotherapy of Chagas disease: controversies and advances. *Trends Parasitol*, 19, 495-501.
- URBINA, J. A., PAYARES, G., CONTRERAS, L. M., LIENDO, A., SANOJA, C., MOLINA, J., PIRAS, M., PIRAS, R., PEREZ, N., WINCKER, P. & LOEBENBERG, D. 1998. Antiproliferative effects and mechanism of action of SCH 56592 against *Trypanosoma* (*Schizotrypanum*) *cruzi*: in vitro and in vivo studies. *Antimicrob Agents Chemother*, 42, 1771-7.
- VELÁSQUEZ-ORTIZ, N., HERRERA, G., HERNÁNDEZ, C., MUÑOZ, M. & RAMÍREZ, J. D. 2022. Discrete typing units of *Trypanosoma cruzi*: Geographical and biological distribution in the Americas. *Sci Data*, 9, 360.
- VINCENT, I. M., CREEK, D., WATSON, D. G., KAMLEH, M. A., WOODS, D. J., WONG, P. E., BURCHMORE, R. J. & BARRETT, M. P. 2010. A molecular mechanism for eflornithine resistance in African trypanosomes. *PLoS Pathog*, 6, e1001204.
- VIRMANI, M. A. & CIRULLI, M. 2022. The Role of L-Carnitine in Mitochondria, Prevention of Metabolic Inflexibility and Disease Initiation. *Int J Mol Sci*, 23.
- WALKER, B. J., ABEEL, T., SHEA, T., PRIEST, M., ABOUELLIEL, A., SAKTHIKUMAR, S., CUOMO, C. A., ZENG, Q., WORTMAN, J., YOUNG, S. K. & EARL, A. M. 2014. Pilon: an integrated tool for comprehensive microbial variant detection and genome assembly improvement. *PLoS One*, 9, e112963.
- WALL, R. J., CARVALHO, S., MILNE, R., BUEREN-CALABUIG, J. A., MONIZ, S., CANTIZANI-PEREZ, J., MACLEAN, L., KESSLER, A., COTILLO, I., SASTRY, L., MANTHRI, S., PATTERSON, S., ZUCCOTTO, F., THOMPSON, S., MARTIN, J. J., MARCO, M., MILES, T. J., DE RYCKER, M., THOMAS, M., FAIRLAMB, A. H., GILBERT, I. H. & WYLLIE, S. 2020. The Qi site of cytochrome b is a promiscuous drug target in *Trypanosoma cruzi* and *Leishmania donovani*. *ACS Infect Dis*.
- WALL, R. J., RICO, E., LUKAC, I., ZUCCOTTO, F., ELG, S., GILBERT, I. H., FREUND, Y., ALLEY, M. R. K., FIELD, M. C., WYLLIE, S. & HORN, D. 2018. Clinical and veterinary trypanocidal benzoxaboroles target CPSF3. *Proc Natl Acad Sci U S A*, 115, 9616-9621.

- WANG, W., PENG, D., BAPTISTA, R. P., LI, Y., KISSINGER, J. C. & TARLETON, R. L. 2021. Strain-specific genome evolution in *Trypanosoma cruzi*, the agent of Chagas disease. *PLoS Pathog*, 17, e1009254.
- WANI, M. C., TAYLOR, H. L., WALL, M. E., COGGON, P. & MCPHAIL, A. T. 1971. Plant antitumor agents. VI. The isolation and structure of taxol, a novel antileukemic and antitumor agent from *Taxus brevifolia*. *J Am Chem Soc*, 93, 2325-7.
- WENZLER, T., STEINHUBER, A., WITTLIN, S., SCHEURER, C., BRUN, R. & TRAMPUZ, A. 2012. Isothermal microcalorimetry, a new tool to monitor drug action against *Trypanosoma brucei* and *Plasmodium falciparum*. *PLoS Negl Trop Dis*, 6, e1668.
- WERBOVETZ, K. A. 2000. Target-based drug discovery for malaria, leishmaniasis, and trypanosomiasis. *Curr Med Chem*, 7, 835-60.
- WHEELER, R. J., GULL, K. & GLUENZ, E. 2012. Detailed interrogation of trypanosome cell biology via differential organelle staining and automated image analysis. *BMC Biol*, 10, 1.
- WHO. 2002. Control of Chagas disease : second report of the WHO expert committee [Online]. Available: <https://apps.who.int/iris/handle/10665/42443> [Accessed 10.05.2023].
- WHO. 2023. Neglected tropical diseases [Online]. Available: <https://www.who.int/news-room/questions-and-answers/item/neglected-tropical-diseases> [Accessed 10.05.2023].
- WICKHAM, H. 2017. tidyverse: Easily Install and Load the 'Tidyverse' [Online]. Available: <https://CRAN.R-project.org/package=tidyverse> [Accessed 2018-2020].
- WICKHAM, H., & BRYAN, J. 2018. readxl: Read Excel Files [Online]. Available: <https://CRAN.R-project.org/package=readxl> [Accessed 2018-2020].
- WIEDEMAR, N., GRAF, F. E., ZWYER, M., NDOMBA, E., KUNZ RENGGLI, C., CAL, M., SCHMIDT, R. S., WENZLER, T. & MASER, P. 2018. Beyond immune escape: a variant surface glycoprotein causes suramin resistance in *Trypanosoma brucei*. *Mol Microbiol*, 107, 57-67.
- WILKINSON, S. R., TAYLOR, M. C., HORN, D., KELLY, J. M. & CHEESEMAN, I. 2008. A mechanism for cross-resistance to nifurtimox and benznidazole in trypanosomes. *Proc Natl Acad Sci U S A*, 105, 5022-7.
- WILSON, K., BERENS, R. L., SIFRI, C. D. & ULLMAN, B. 1994. Amplification of the inosinate dehydrogenase gene in *Trypanosoma brucei gambiense* due to an increase in chromosome copy number. *J. Biol. Chem.*, 269, 28979-28987.
- WRIGHT, M. H. & SIEBER, S. A. 2016. Chemical proteomics approaches for identifying the cellular targets of natural products. *Nat Prod Rep*, 33, 681-708.
- XIE, Y., WU, G., TANG, J., LUO, R., PATTERSON, J., LIU, S., HUANG, W., HE, G., GU, S., LI, S., ZHOU, X., LAM, T. W., LI, Y., XU, X., WONG, G. K. & WANG, J. 2014. SOAPdenovo-Trans: de novo transcriptome assembly with short RNA-Seq reads. *Bioinformatics*, 30, 1660-6.
- XUE, J., LAI, Y., LIU, C. W. & RU, H. 2019. Towards Mass Spectrometry-Based Chemical Exposome: Current Approaches, Challenges, and Future Directions. *Toxics*, 7.
- YAGOUBAT, A., CORRALES, R. M., BASTIEN, P., LÉVÊQUE, M. F. & STERKERS, Y. 2020. Gene Editing in Trypanosomatids: Tips and Tricks in the CRISPR-Cas9 Era. *Trends Parasitol.*

- YANG, P. Y., WANG, M., HE, C. Y. & YAO, S. Q. 2012a. Proteomic profiling and potential cellular target identification of K11777, a clinical cysteine protease inhibitor, in *Trypanosoma brucei*. *Chem Commun (Camb)*, 48, 835-7.
- YANG, P. Y., WANG, M., LIU, K., NGAI, M. H., SHERIFF, O., LEAR, M. J., SZE, S. K., HE, C. Y. & YAO, S. Q. 2012b. Parasite-based screening and proteome profiling reveal orlistat, an FDA-approved drug, as a potential anti *Trypanosoma brucei* agent. *Chemistry*, 18, 8403-13.
- YASSIN, A., FREDRICK, K. & MANKIN, A. S. 2005. Deleterious mutations in small subunit ribosomal RNA identify functional sites and potential targets for antibiotics. *Proc Natl Acad Sci U S A*, 102, 16620-5.
- YASUR-LANDAU, D., JAFFE, C. L., DORON-FAIGENBOIM, A., DAVID, L. & BANETH, G. 2017. Induction of allopurinol resistance in *Leishmania infantum* isolated from dogs. *PLoS Negl Trop Dis*, 11, e0005910.
- YORKE, W. & MURGATROYD, F. 1930. The action in vitro of certain arsenical and antimonial compounds on *T. rhodesiense* and on atoxyl- and acriflavine-resistant strains of this parasite. *Ann. Trop. Med. Parasitol.*, 449-476.
- YORKE, W., MURGATROYD, F. & HAWKING, F. 1931. Preliminary contribution on the nature of drug resistance. *Ann. Trop. Med. Parasitol.*, 25, 351-358.
- YORKE, W., MURGATROYD, F. & HAWKING, F. 1933. Comparison of Strains of *T. rhodesiense* Made Resistant to Various Arsenicals and Antimonials, to Bayer 205, and to Acriflavine, Respectively. *Ann. Trop. Med. Parasitol.*, 577-586.
- ZAMBONI, N., FENDT, S. M., RÜHL, M. & SAUER, U. 2009. (13)C-based metabolic flux analysis. *Nat Protoc*, 4, 878-92.
- ZDORICHENKO, V., PAUMIER, R., WHITMARSH-EVERISS, T., ROE, M. & COX, B. 2019. The Synthesis of Waltherione F and Its Analogues with Modifications at the 2- and 3-Positions as Potential Antitrypanosomal Agents. *Chemistry*, 25, 1286-1292.
- ZERBINO, D. R. & BIRNEY, E. 2008. Velvet: algorithms for de novo short read assembly using de Bruijn graphs. *Genome Res*, 18, 821-9.
- ZHANG, W. W. & MATLASHEWSKI, G. 2015. CRISPR-Cas9-Mediated Genome Editing in *Leishmania donovani*. *mBio*, 6, e00861.
- ZIEGELBAUER, K. & OVERATH, P. 1992. Identification of invariant surface glycoproteins in the bloodstream stage of *Trypanosoma brucei*. *J Biol Chem*, 267, 10791-6.
- ZINGALES, B. 2018. *Trypanosoma cruzi* genetic diversity: Something new for something known about Chagas disease manifestations, serodiagnosis and drug sensitivity. *Acta Tropica*, 184, 38-52.
- ZINGALES, B., MILES, M. A., CAMPBELL, D. A., TIBAYRENC, M., MACEDO, A. M., TEIXEIRA, M. M. G., SCHIJMAN, A. G., LLEWELLYN, M. S., LAGES-SILVA, E., MACHADO, C. R., ANDRADE, S. G. & STURM, N. R. 2012. The revised *Trypanosoma cruzi* subspecific nomenclature: Rationale, epidemiological relevance and research applications. *Infection, Genetics and Evolution*, 12, 240-253.
- ZINGALES, B., PEREIRA, M. E., OLIVEIRA, R. P., ALMEIDA, K. A., UMEZAWA, E. S., SOUTO, R. P., VARGAS, N., CANO, M. I., DA SILVEIRA, J. F., NEHME, N. S., MOREL, C. M., BRENER, Z. & MACEDO, A. 1997. *Trypanosoma cruzi* genome project: biological characteristics and molecular typing of clone CL Brener. *Acta Trop*, 68, 159-73.

References

- ZONGO, F., RIBUOT, C., BOUMENDJEL, A. & GUISSOU, I. 2013. Botany, traditional uses, phytochemistry and pharmacology of *Waltheria indica* L. (syn. *Waltheria americana*): a review. *J Ethnopharmacol*, 148, 14-26.

Acknowledgment

I wish to thank my two first supervisors Pascal Mäser and Marcel Kaiser for giving me the opportunity to work with such a freedom on my project. I want to thank my second supervisor Till Voss for supporting me during my project and taking the time to discuss the progress. My thanks also go to Jürg Gertsch for reviewing my work as external expert.

My gratitude also goes to all the members of the parasite chemotherapy unit. Exceptional thanks go to Monica Cal, Romina Rocchetti and Sonja Keller-Märki. Thank you for all the work you did for me and do for us all. Very special thanks go to Anna Albisetti for all her support. Thank you for discussing science with me and understanding my emotional highs and lows. Big thanks go to my Ph. D. colleagues Patricia Bravo, Dennis Hauser, and Lore Baert, you made a huge difference in my Ph. D. life. I also want to express my appreciation to the whole BSL3 team. It was a great experience to work in such a lab together with an amazing team. Warmest thanks also goes to so many other dear colleagues and some very close friends from Swiss TPH. Thank you all for your support and friendship, it was an unforgettable journey.

I further wish to thank Natalie Wiedemar for taking her precious time to show me bioinformatics and supporting me later during analysis. Very special thanks also go to Anna Fesser who introduced me to *T. cruzi* in the first place, trusting that I would be competent enough to take over her work. I also want to thank Remo Schmidt for answering all the *T. cruzi* specific questions at the beginning of the project.

Many thanks go to all my collaborators who made this work possible. I especially also wish to thank all the members of the Sinergia consortium, particularly Ozlem Sevik Kilicaslan and Sylvian Cretton and equally to Julien Boccard who supported us with data analysis. Many thanks also go to Frédéric Bringaud for his uncomplicated and fast metabolomics support, and Joachim Kloehn who analysed my precious samples incredibly fast.

I am deeply grateful to my dear friends, Carina, Monika, Elisabeth, and Manuel, my singing teacher Heike, my cousin Andreas, and my dear sister for supporting me and carrying me through all the highs and lows. My deepest gratitude goes to my parents. I cannot imagine getting more support from anyone else than you gave me. You are always there for me. Thank you so much.